NIOBIUM SILICIDES FOR HIGH TEMPERATURE APPLICATIONS

FINAL REPORT

8/1/89 - 12/31/92

PROF. JOHN J. LEWANDOWSKI

JANUARY 25, 1993

U.S. AIR FORCE OFFICE OF SCIENTIFIC RESEARCH

AFOSR-89-0508

THE CASE SCHOOL OF ENGINEERING
CASE WESTERN RESERVE UNIVERSITY
DEPT. MATERIALS SCIENCE AND ENGINEERING
CLEVELAND, OHIO 44106

APPROVED FOR PUBLIC RELEASE;

DISTRIBUTION UNLIMITED

REPORT DOCUMENTATION PAGE

Form Approved
OMB No. 0704-0188

1. AGENCY USE ONLY (Leave blank)	2. REPORT DATE	3. REPORT TYPE AND DATES COVERED
	January 27, 1993	FINAL TECHNICAL - 8/1/89 - 12/31/92

4. TITLE AND SUBTITLE
NIOBIUM SILICIDES FOR HIGH TEMPERATURE APPLICATIONS

5. FUNDING NUMBERS
61102F
2306/A1

6. AUTHOR(S)
PROFESSOR JOHN J. LEWANDOWSKI

7. PERFORMING ORGANIZATION NAME(S) AND ADDRESS(ES)
PROFESSOR JOHN J. LEWANDOWSKI
DEPT. MATL'S SCI. AND ENGINEERING
CASE WESTERN RESERVE UNIVERSITY
CLEVELAND, OHIO 44106

8. PERFORMING ORGANIZATION REPORT NUMBER

9. SPONSORING/MONITORING AGENCY NAME(S) AND ADDRESS(ES)
DEPARTMENT OF THE AIR FORCE
AIR FORCE OFFICE OF SCIENTIFIC RESEARCH
BOLLING AIR FORCE BASE, DC 20332-6448
NE

10. SPONSORING/MONITORING AGENCY REPORT NUMBER
AFOSR-89-0508

11. SUPPLEMENTARY NOTES
THE VIEW, OPINIONS AND/OR FINDINGS CONTAINED IN THIS REPORT ARE THOSE OF THE AUTHOR AND SHOULD NOT BE CONSTRUED AS AN OFFICIAL DEPARTMENT OF AIR FORCE POSITION, POLICY, OR DECISION, UNLESS SO DESIGNATED ELSEWHERE.

12a. DISTRIBUTION/AVAILABILITY STATEMENT
APPROVED FOR PUBLIC RELEASE; DISTRIBUTION UNLIMITED.

12b. DISTRIBUTION CODE

13. ABSTRACT (Maximum 200 words)

The processing and properties of advanced intermetallics based on aluminide and silicide matrices have been investigated. Vacuum hot press techniques were utilized to produce both monolithic and composite Ni_3Al, NiAl, and Nb_5Si_3. The effects of 10 volume percent TiB_2 particulates on the fracture toughness of Ni_3Al and NiAl were determined while in-situ monitoring of the fracture toughness tests was conducted with the aid of a deformation stage mounted inside a scanning electron microscope. The Nb_5Si_3 powders were produced via reaction synthesis followed by hot press consolidation and evaluation of fracture toughness on both the monolithic silicide as well as in-situ Nb_5Si_3/Nb composites. The Nb particles imparted significant toughening while both crack bridging and ductile phase toughening were observed in the in-situ fracture studies. Significant effects of loading rate on the resulting toughness was observed.

14. SUBJECT TERMS	15. NUMBER OF PAGES
SILICIDES, INTERMETALLICS, COMPOSITES, PROCESSING, DUCTILE PHASE TOUGHENING, R-CURVE BEHAVIOR, IN-SITU	55
	16. PRICE CODE

17. SECURITY CLASSIFICATION OF REPORT	18. SECURITY CLASSIFICATION OF THIS PAGE	19. SECURITY CLASSIFICATION OF ABSTRACT	20. LIMITATION OF ABSTRACT
UNCLASSIFIED	UNCLASSIFIED	UNCLASSIFIED	UNLIMITED

NSN 7540-01-280-5500

Standard Form 298 (Rev. 2-89)
Prescribed by ANSI Std. 239.18
298-102

53-85

TABLE OF CONTENTS

A. INTRODUCTION

While many advanced intermetallic systems possess desirable properties such as high temperature strength and stiffness, these systems typically do not exhibit adequate ductility and toughness at low temperatures. In addition, there is a need for the development of advanced processing techniques in order to provide materials in adequate quantities for subsequent use. The successful utilization of these desirable material properties also requires the development of techniques to impart higher toughness without sacrificing strength.

A variety of toughening mechanisms may be utilized to impart toughness in such systems. In brittle matrix systems, toughening may be acheived via the introduction of particles which are either brittle or ductile. In the former case, toughening may occur via crack bowing, Figure 1, and/or crack deflection as shown in Figures 2a and 2b. The introduction of ductile particles may induce ductile phase toughening, as shown in Figure 3a. The introduction of the reinforcement imparts some damage tolerance, the details of which are affected by the volume fraction of reinforcement, reinforcement/matrix interface characteristics, and the strength/ductility of the reinforcement. In both cases, it is possible to produce brittle matrix materials which exhibit some degree of damage tolerance. This is reflected in the stress-strain curve of specimens tested under displacement control, as shown in Figure 3b. The monolithic material exhibits catastrophic failure at low stress and strain, while the "toughened" material exhibits a significantly non-linear stress-strain curve. In the composite case, the material actually becomes tougher with an increase in crack length, a phenomena known as R-curve behavior.

The AFOSR Program at Case Western Reserve University, AFOSR 89-0508, has focused on key issues in the processing and properties of advanced intermetallic composite systems. The period 8/1/89 - 12/31/92 was devoted to the following:

1. Processing of Monolithic and Composite Intermetallics

The matrices of interest included Nb_5Si_3, Ni_3Al, and NiAl. The concept of ductile phase toughening via incorporation of Nb was explored for the former, while additions of TiB_2 were utilized in the latter two systems. Processing of both the matrix as well as the composites were accomplished via reaction synthesis and vacuum hot pressing at Case Western Reserve University. Vacuum arc-cast and extruded Nb-Si composites were additionally obtained via collaboration with researchers at Wright Patterson Air Force Base.

2. Fracture Toughness Testing of Monolithic and Composite Intermetallics

Fracture mechanics-type tests were conducted to determine the fracture toughness of the monolithic intermetallics as well as the composites. Little information regarding the fracture toughness of the monolithic matrices was available in the literature. In-situ video monitoring of the deformation and fracture experiments was conducted with the aid of a deformation stage mounted inside a scanning electron microscope. This provided direct evidence of the mechanisms contributing to the toughness of the systems under study.

In addition, laminated Nb_5Si_3/Nb composites were manufactured to contain various interfaces (e.g. weak, strong) in order to examine the effects of interface strength on the resulting behavior of the Nb and the subsequent toughness.

3. Effects of Loading Rate on the Toughness of Nb_5Si_3/Nb In-situ Composites

While the studies outlined in Section 2 above provide information on the fracture toughness obtained under static test conditions, the fracture properties of ductile-phase toughened systems may be highly rate-dependent because of the rate dependence of the "ductile" phase. In such systems, the "ductile" constituent may undergo a ductile-to-brittle transition which could affect the resulting toughness. The effects of loading rate on the resulting toughness was studied using identically notched specimens subjected to loading rates which varied by over four orders of magnitude.

The results of the works described above have been both orally presented and published in the journals and conference proceedings listed in Sections D and E. Highlights of the results are presented in the order described above, while selected relevant publications are enclosed in the **Appendix** for completeness. Additional detailed information may be obtained by consulting the other published references.

B. RESULTS OF EXPERIMENTAL PROGRAM

1. Processing of Monolithic and Composite Intermetallics

a) Ni_3Al and NiAl Systems

Figure 4 shows the processing route utilized for the monolithic aluminides as well as the aluminide composites, while Table I details the processing parameters. Included are the details of the matrix powders as well as the TiB_2 reinforcement characteristics, while Table II lists the resulting microstructural characteristics for the composites. Included in Table II are the matrix grain size for both the monolithic and composite materials as well as the contiguity ratio (C_t) which provides a quantitative measure of the degree of reinforcement clustering. Values for C_t can vary from 0 to 1, that is, from completely dispersed second phase particles (i.e. no touching of reinforcement) to an entirely contiguous phase (i.e. fully agglomerated). It is clear from the values in Table II that the range of powder sizes utilized provided a significant variation in the level of clustering (as measured by C_t) between systems. SEM, TEM, and Auger analyses were additionally utilized to characterize the degree of reaction between matrix and reinforcement. Copies of two published journal papers are included in the **Appendix** to provide more details. They are as follows:

Paper 1. J.D. Rigney and J.J. Lewandowski, "Fracture Toughness of Monolithic Aluminides", Materials Science and Engineering, A149, 1992, pp. 143-151.

Paper 2. J.D. Rigney and J.J. Lewandowski, "Fracture Toughness of Composite Nickel Aluminides", Materials Science and Engineering, A158, 1992, pp. 31-45.

b) Nb_5Si_3 System

The silicide system was successfully processed via reaction synthesis of elemental powders using a high energy ball mill operated at room temperature. Elemental Si and Nb powders were obtained with a particle size of -325 mesh (< 44 um) and nominal purities exceeding 99% and 99.8%, respectively. Elemental powders with the proper Nb-Si ratio for the formation of Nb_5Si_3 (i.e. Nb-37.5 at.% Si) were milled in a Spex model 8000 high intensity mixer-mill for a variety of times ranging from 0.5 hour to 3.5 hours. It was found that milling times in excess of 3.25 hours were sufficient to produce Nb_5Si_3 compound formation as evidenced by X-ray diffraction patterns taken from interrupted millings. Figure 5 and **Paper 3** in the **Appendix** show X-ray diffraction patterns of the mechanically alloyed Nb-Si powders for times just prior to compound formation (e.g. 3 hours) as well as those just after compound formation (e.g. 3.25 hours).

Paper 4 included in the **Appendix** further details the results of TEM investigations of powders milled for various times and reveals that a small amount (i.e. not detectable by conventional X-ray techniques) of silicide formation occurs early in the milling procedure. Subsequent vacuum hot pressing was carried out to produce consolidated compacts of Nb_5Si_3 via the processing schedule shown in Figure 6 and reproduced in **Paper 3** in the **Appendix**. More recent work has succesfully utilized this technique to produce model laminates consisting of Nb and Nb_5Si_3 as shown in **Paper 3** in the **Appendix**. The following two papers included in the **Appendix** provide more details regarding the mechanism(s) of silicide formation, as well the details of laminate production:

Paper 3. J. Kajuch, J.D. Rigney, and J.J. Lewandowski, "Processing and Properties of Tough Nb_5Si_3/Nb Laminates", Materials Science and Engineering, A155, 1992, pp. 59-65.

Paper 4. J. Kajuch, J.W. Short, C. Liu, and J.J. Lewandowski, "On the Kinetics of Nb_5Si_3 Compound Formation", in Proc. Mater. Res. Symp., (R. Darolia, et al, eds.), 1993, in press.

2. Fracture Toughness Testing of Monolithic and Composite Intermetallics

a) Ni_3Al and NiAl Systems

Representative load-crack opening displacement (COD) traces for identically-sized monolithic aluminide specimens is shown in Figure 7, while Figure 8 summarizes the toughnesses obtained on the monolithic materials as well as the composites. Included in Figure 8 are the toughness values obtained for composites containing different TiB_2 particulate sizes. It is shown that 10 volume % of TiB_2 particulates increases the toughness of NiAl while decreasing the toughness of Ni_3Al and Ni_3Al + B. In-situ monitoring of fracture toughness tests revealed that the reinforcement additions to a brittle matrix such as NiAl produces toughening via crack tip bowing and deflection, while the addition of particulate reinforcement to a relatively "tough" intermetallic produces a decrease in toughness due to the preferential deformation and fracture of regions associated with the reinforcement in the "tough" matrix. The effects of particulate reinforcement on the fracture toughness were modeled with the aid of the in-situ fracture observations. **Papers 1 and 2** in the **Appendix** provide additional details of the experiments conducted on the Aluminide systems.

b) Nb_5Si_3 System

Similar experiments conducted on the monilithic Nb_5Si_3 revealed a toughness of approximately 2 MPa$\sqrt{m}$ for the monolithic silicide. In-situ testing of the ductile phase toughened material provided by collaborators at Wright Patterson Air Force Base revealed a significant increase in toughness and R-curve behavior in comparison to the monolithic silicide. Figure 9 shows the stress intensity vs. crack extension trace for one of the specimens tested inside the SEM. Included in Figure 9 is the behavior of the monolithic silicide. It is clear that significant increases in toughness were obtained, while the in-situ studies revealed extensive bridging of the crack by the "ductile" Nb ligaments. The details of such behavior are summarized in **Papers 5 and 6** in the **Appendix**. In particular, the papers enclosed in the **Appendix** illustrate the effects of deformation processing and interstitial contamination on the resulting R-curve behavior and damage tolerance in such systems. **Paper 3** in the **Appendix** summarizes the work conducted on laminated Nb_5Si_3/Nb specimens. In particular, the effects of systematic changes in the interface strength on the resulting toughness and the behavior of the Nb were investigated. It was demonstrated that the presence of a strong interface bond promoted cleavage fracture of the Nb, although the experiments also revealed that the mere appearance of cleavage fracture is not necessarily detrimental to the toughness of such materials because cleavage fracture in Nb and its alloys requires a large amount of energy. The following papers are included in the **Appendix** for this section:

Paper 5. J.D. Rigney, P.M. Singh, and J.J. Lewandowski, "Environmental Effects on Ductile Phase Toughening in In-situ Nb_5Si_3/Nb Composites" Jnl. of Metals, August 1992, pp. 36-41.

Paper 6. M.G. Mendiratta, J.J. Lewandowski, and D.M. Dimiduk, "Strength and Toughness in In-situ Silicide Composites", Metallurgical Transactions A, 22A, 1991, pp. 1573-1584.

3. Effects of Loading Rate on the Toughness of Nb_5Si_3/Nb In-situ Composites

The effects of loading rate on the fracture toughness of the ductile-phase toughened Nb_5Si_3 system was determined on notched bend specimens tested over the range of crosshead speeds shown in Figure 10. This work was conducted in collaboration with researchers at Wright Patterson Air Force Base. The resulting fracture toughness values were shown to be significantly affected by the crosshead speed utilized during the test. The fracture toughness (as calculated using the peak load in the load-displacement trace) decreased sharply with an increase in loading rate.

Fracture toughnesses in excess of 25 MPa$\sqrt{m}$ were obtained during typical tests conducted under nominally static testing conditions (i.e. 0.001 mm/sec), while toughness values of only 10 MPa$\sqrt{m}$ were obtained on nominally identical materials tested at 10 mm/sec.

The fracture surface details were quantified in the SEM for one of the toughest specimens (i.e. slowest loading rate) and one of the least tough specimens (i.e. fastest loading rate). It was found that the specimen tested at the faster loading rate exhibited a higher percentage of cleavage fracture of the Nb than did the specimen tested at the slower rate. Figure 11 shows a schematic of the regions analyzed by SEM as well as the percentage of cleaved Nb on the fracture surface for each position analyzed. It is clear that the specimen tested at the higher rate exhibited a higher percentage of cleavage for each location analyzed. These results strongly indicate that the deformation and fracture behavior of the "ductile" phase controls the development of high toughness in such systems.

Figure 12 presents a schematic of one interpretation of these results, although additional tests are being conducted on specimens tested at low temperatures in order to determine the generality of such an argument. In the tests conducted at slow loading rates, the Nb behaves in a ductile manner as shown in the schematic in Figure 12 and a high toughness is obtained. In such a case, the Nb ligaments deform to such an extent that ductile rupture occurs, while the stress-strain curve of such a ductile ligament could be as that shown in Figure 12. In contrast, the tests conducted at faster rates exhibited cleavage of the Nb. At this stage, such a result implies that the effective stress-strain curve of the Nb is truncated by cleavage fracture, thereby reducing the energy available to impart toughening. Additional experiments where identical specimens were tested at low temperatures to determine the generality of such features to the development of toughness in such systems has illustrated that the mere appearance of cleavage fracture is an insufficient indicator of low toughness in such systems. Tests conducted at low temperatures on both arc-cast composites and laminated Nb_5Si_3/Nb specimens revealed a predominance of cleavage fracture in the Nb, yet the specimens possessed high toughness. Examination of the stress-displacement curves in such cases revealed that the behavior of the Nb at high strain rate is different than that at low temperature, with the latter test conditions producing a larger area under the curve than the former conditions. The details of this work are currently being prepared for a journal publication.

C. RESEARCH PERSONNEL SUPPORTED 8/1/89 - 12/31/92

1.	John J. Lewandowski	-	Associate Professor
2.	Joseph D. Rigney	-	M.S./Ph.D. Student
3.	Jan Kajuch	-	Ph.D. Student
4.	Sunil Patankar	-	Research Associate (Half-time)
5.	Ben Goss	-	Undergraduate Student
6.	John Short	-	Undergraduate Student

D. PUBLICATIONS ACKNOWLEDGING AFOSR SUPPORT:

1. P. Khadkikar, J.D. Rigney, J.J. Lewandowski, and K.M. Vedula, in Proc. Mater. Res. Symp., (C.C. Koch, et al, eds.), vol. 133, 1988, pp. 523-528.

2. J. Rigney, P. Khadkikar, J.J. Lewandowski, and K.M. Vedula, in Proc. Mater. Res. Symp., (C.C. Koch, et al, eds.), vol. 133, 1988, pp. 603-608.

3. J.J. Lewandowski, D. Dimiduk, W.G. Kerr, and M. Mendiratta, in Proc. Mater. Res. Symp., (S. Fishman, et al, eds.), vol. 20, 1988, pp. 103-109.

4. P. Khadkikar, J.J. Lewandowski, and K.M. Vedula, Metall. Trans. A, 20A, 1989, pp. 1247-1255.

5. J.J. Lewandowski, G.M. Michal, I. Locci, and J.D. Rigney, in Proc. Mater. Res. Symp., (G.M. Stocks, et al, eds.), vol. 186, 1990, pp. 341-348.

6. J.D. Rigney and J.J. Lewandowski, in Proc. Second Int'l Ceramic Sci. and Tech. Congress - Advanced Composite Materials, (M.D. Sacks, ed.), 1990, pp. 519-525.

7. M.G. Mendiratta, D. Dimiduk, and J.J. Lewandowski, Metall. Trans. A, 22A, 1991, pp. 1573-1584.

8. J.D. Rigney, J.J. Lewandowski, L. Matson, M.G. Mendiratta, and D.M. Dimiduk, in Proc. Mater. Res. Soc. Symp., (D.P. Pope, et al, eds.), vol. 213, 1991, pp. 1001-1009.

9. J.D. Rigney and J.J. Lewandowski, Mater. Sci. and Eng., A149, 1992, pp. 143-151.

10. J.D. Rigney, P.M. Singh, and J.J. Lewandowski, Jnl. of Metals, August 1992, pp. 36-41.

11. J.D. Rigney and J.J. Lewandowski, Mater. Sci. and Eng., A158, 1992, pp. 31-45.

12. J. Kajuch, J.D. Rigney, and J.J. Lewandowski, Mater. Sci. and Eng., A155, 1992, pp. 59-65.

13. S. Patankar and J.J. Lewandowski, in Proc. Mater. Res. Symp., (R. Darolia, et al, eds.), 1993, in press.

14. J. Kajuch, J. Short, C. Liu, and J.J. Lewandowski, in Proc. Mater. Res. Symp., (R. Darolia, et al, eds.), 1993, in press.

15. J.D. Rigney and J.J. Lewandowski, Jnl. Mater. Sci., 1993, in press.

16. J.D. Rigney, R. Castro, and J.J. Lewandowski, Jnl. Mater. Sci., 1993, in press.

17. J. Kajuch, J. Short, and J.J. Lewandowski, Acta Metall. et Materialia, 1993, in preparation.

E. PRESENTATIONS ACKNOWLEDGING AFOSR SUPPORT:

1. J.J. Lewandowski, "Fracture of Nb-Nb Silicide Composites - Ductile Phase Toughening", WRDC, Dayton, Ohio, 9/11/87. **INVITED**

2. J.J. Lewandowski, "Fracture of Nb-Si Alloys", WRDC High Temperature Materials Workshop, Dayton, Ohio, 10/23/87. **INVITED**

3. J.J. Lewandowski, D. Dimiduk, W.G. Kerr, and M.G. Mendiratta, "Microstructual Effects on Nb-Nb Silicide Composite Properties", MRS Meeting, Reno, Nevada, 4/8/88.

4. D. Dimiduk, M.G. Mendiratta, and J.J. Lewandowski, "Microstructures and Phase Relationships in Nb-Nb_5Si_3 In-Situ Composites", MRS Meeting, Reno, Nevada, 4/9/88.

5. P. Khadkikar, J.J. Lewandowski, and K.M. Vedula, "Notch Effects on the Fracture of Ni_3Al and Ni_3Al + B", TMS Meeting, Chicago, Illinois, 9/26/88.

6. P. Khadkikar, J.D. Rigney, J.J. Lewandowski, and K.M. Vedula, "Notch Effects on the R.T. Tensile and Bend Properties of Ni_3Al", MRS Meeting, Boston, Massachusetts, 11/29/88.

7. J.D. Rigney and J.J. Lewandowski, "Composite Materials Based on Nickel Aluminide Matrices", MRS Meeting, Boston, Massachusetts, 12/1/88.

8. J.J. Lewandowski, "Use of Blunt Notched Specimens in Fracture Experiments", University of Michigan, Dept. Materials Science and Eng., Ann Arbor, Michigan, 5/2/89. **INVITED**

9. J.J. Lewandowski, "Fracture Toughness of Advanced Composites", WRDC, 12/14/89. **INVITED**

10. J.D. Rigney, J.J. Lewandowski, G.M. Michal, and I. Locci, "Effects of Stress State on the Fracture Behavior of Aluminides", MRS Meeting, San Francisco, California, 4/19/90.

11. J.D. Rigney, J.J. Lewandowski, and K.M. Vedula, "Fracture of Nickel Aluminide Composites", MRS Meeting, San Francisco, California, 4/20/90.

12. J.D. Rigney and J.J. Lewandowski, "Processing and Characterization of Nickel Aluminide Composites", TMS Meeting, Detroit, Michigan, 10/10/90.

13. J.D. Rigney and J.J. Lewandowski, "Processing and Characterization of Nickel Aluminide Composites", TMS Meeting, Detroit, Michigan, 10/10/90.

14. J.D. Rigney and J.J. Lewandowski, "Fracture Toughness of Monolithic and Composite Nickel Aluminides", TMS Meeting, Detroit, Michigan, 10/11/90.

15. J.D. Rigney and J.J. Lewandowski, "Ductile Phase Toughening of Silicides", Second Int'l Ceramic Sci. and Tech. Congress, Orlando, Florida, 11/14/90.

16. J.D. Rigney and J.J. Lewandowski, "Fracture Toughness and Effects of Stress State on Fracture of Aluminides", MRS Meeting, Boston, Massachusetts, 11/19/90.

17. J.D. Rigney, M.G. Mendiratta, D. Dimiduk, and J.J. Lewandowski, "Loading Rate Effects on Ductile Phase Toughening of Silicides", MRS Meeting, Boston, Massachusetts, 11/20/90.

18. J.J. Lewandowski, "Effects of Stress State on Deformation and Fracture of IMCs", WRDC High Temperature Materials Workshop, 2/12/91.

19. J.J. Lewandowski, "Issues in Ductile Phase Toughening in the Nb-Nb Silicide System", WRDC High Temperature Materials Workshop, 2/13/91. **INVITED**

20. J.D. Rigney, J. Kajuch, and J.J. Lewandowski,"Ductile Phase Toughening of SIlicides", ICCM/VII, Honolulu, Hawaii, 7/17/91.

22. J.J. Lewandowski, "Overview of Deformation and Fracture of Composites" Aeronautical Research Laboratory - Aircraft Materials Division, DSTO, Melbourne, Australia, 7/29/91. **INVITED**

21. J. Kajuch and J.J. Lewandowski, "Processing and Properties of Nb_5Si_3/Nb Composites", TMS Meeting, Cincinnati, Ohio, 10/23/91.

22. J.D. Rigney and J.J. Lewandowski, "Volume Fraction Effects on Ductile Phase Toughening in In-situ Nb/Nb_5Si_3 Composites", TMS Meeting, Cincinnati, Ohio, 10/23/91.

23. J.D. Rigney, J. Kajuch, and J.J. Lewandowski, "Processing and Properties of Silicide Composites", Workshop on Silicides, Gaithersburg, Maryland, 11/4/91. **INVITED**

24. J.D. Rigney, P.M. Singh, and J.J. Lewandowski, "Environmental Effects on Fracture of Nb/Nb_5Si_3 Composites", TMS Meeting, San Diego, California, 3/3/92.

25. J.J. Lewandowski, "Processing and Properties of Tough Silicides". WRDC High Temperature Materials Workshop, Dayton, Ohio, 4/19/92. **INVITED**

26. J.J. Lewandowski, "Processing of Advanced Materials", AFOSR/ONR Workshop on Processing, Aurora, New York, 5/18/92. **INVITED**

27. J.J. Lewandowski, "Microstructural Effects on Micromechanisms of Fracture in Advanced Metallic Materials", Gordon Conference on Physical Metallurgy, Plymouth, New Hampshire, 6/15/92. **INVITED**

28. J.D. Rigney, J. Kajuch, and J.J. Lewandowski, "Aspects of Ductile Phase Toughening in In-situ Composites", TMS Meeting, Chicago, Illinois, 11/2/92.

29. J. Zhang and J.J. Lewandowski, "Non-Destructive Evaluation of Interface Strength", TMS Meeting, Chicago, Illinois, 11/2/92.

30. J. Short, J. Kajuch, and J.J. Lewandowski, "A Kinetic Model for Formation of Nb_5Si_3", TMS Meeting, Chicago, Illinois, 11/3/92.

31. S. Parthasarathar and J.J. Lewandowski, "Processing and Properties of $MoSi_2$", MRS Meeting, Boston, Massachusetts, 11/30/92.

32. J.D. Rigney, J. Kajuch, andJ.J. Lewandowski, "Ductile Phase Toughened Silicides", MRS Meeting, Boston, Massachusetts, 11/30/92.

33. J. Kajuch and J.J. Lewandowski, "Kinetic Model for Nb_5Si_3 Formation", MRS Meeting, Boston, Massachusetts, 11/30/92.

F. AWARDS AND HONORS

1. John J. Lewandowski - Associate Professor

1. ASM Bradley Stoughton Award for Young Teachers (1989)
2. NSF Presidential Young Investigator Award (1989)
3. BAST/STAR Committee Member - National Academy of Sciences (1989-92)
4. Nominee - Tau Beta Pi Professor of the Year, CWRU (1990)
5. Invited Speaker - 15th International Nathiagali Summer College on Physics and Contemporary Needs (1990)
6. Nominee - Mortarboard Outstanding Professor of the Year, CWRU (1991)
7. Nominee - Carl F. Wittke Award for Undergraduate Teaching, CWRU (1991)
8. Invited Speaker - Gordon Conference on Physical Metallurgy (1992)
9. Invited Speaker - Los Alamos National Lab Conference on Interfaces (1992)
10. SAE Ralph R. Teetor Educational Award (1992)
11. Invited Member - NSF Young Investigator Panel - Institute for Mechanics and Materials (1992)

2. **Joseph D. Rigney - Graduate Student**

1. ASM Undergraduate Student Paper Contest Winner (1988)
2. MRS Graduate Student Paper Award Semi-finalist (1989, 1990)
3. MRS Graduate Student Poster Award Winner (1992)
4. ASM Graduate Student Paper Contest Winner (1992)

3. **Jan Kajuch - Graduate Student**

1. MRS Graduate Student Poster Award Winner (1992)

Table 1: The monolithic and composite materials hot-pressed, their designations and the fabrication parameters utilized during compaction.

Designation	Material Composition	Matrix Powder Size (Mesh)	Mean TiB_2 Size (μm)	HP Parameters T(K);P(MPa);t(h)
A	Ni_3Al	-325	-	1323; 48.3; 2
ACf1	$Ni_3Al+TiB_2(f)$	-80 +325	4.2	1398; 48.3; 4
ACf2	$Ni_3Al+TiB_2(f)$	-325	4.2	1423; 55.2; 2
ACc1	$Ni_3Al+TiB_2(c)$	-325	15	1423; 55.2; 2
B	Ni_3Al+B	-325	-	1423; 55.2; 2
BCf1	$Ni_3Al+B+TiB_2(f)$	-80 +325	4.2	1398; 48.3; 4
BCf2	$Ni_3Al+B+TiB_2(f)$	-325	4.2	1423; 55.2; 2
BCc1	$Ni_3Al+B+TiB_2(c)$	-325	15	1373; 55.2; 2
C	NiAl	-200	-	1498; 55.2; 0.5
CCf1	$NiAl+TiB_2(f)$	-100 +325	4.2	1673; 48.3; 2
CCf2	$NiAl+TiB_2(f)$	-200	4.2	1623; 48.3; 1
CCc1	$NiAl+TiB_2(c)$	-200	15	1623; 51.7; 1

*f and c on the composite compositions refer to fine (4.2μm) and coarse (15μm) reinforcement mean particle size, respectively.

Table 2: Microstructural characteristics of the as-hot-pressed monolithic and composite materials.

Designation	Material Composition*	Contiguity Ratio (C_t)	Matrix Grain Size (μm)
A	Ni_3Al	-	9.0 ± 0.8
ACf1	$Ni_3Al+TiB_2(f)$	0.508 ± 0.042	49.4 ± 2.7
ACf2	$Ni_3Al+TiB_2(f)$	0.322 ± 0.015	14.4 ± 1.2
ACc1	$Ni_3Al+TiB_2(c)$	0.299 ± 0.055	16.1 ± 0.6
B	Ni_3Al+B	-	8.6 ± 1.2
BCf1	$Ni_3Al+B+TiB_2(f)$	0.495 ± 0.042	38.8 ± 6.0
BCf2	$Ni_3Al+B+TiB_2(f)$	0.290 ± 0.021	14.1 ± 1.5
BCc1	$Ni_3Al+B+TiB_2(c)$	0.274 ± 0.026	15.0 ± 1.3
C	NiAl	-	19.7 ± 2.4
CCf1	$NiAl+TiB_2(f)$	0.477 ± 0.026	42.7 ± 2.6
CCf2	$NiAl+TiB_2(f)$	0.449 ± 0.050	30.5 ± 1.7
CCc1	$NiAl+TiB_2(c)$	0.331 ± 0.045	32.9 ± 2.6

*f and c on the composite compositions refer to fine (4.2μm) and coarse (15μm) reinforcement mean particle size, respectively.

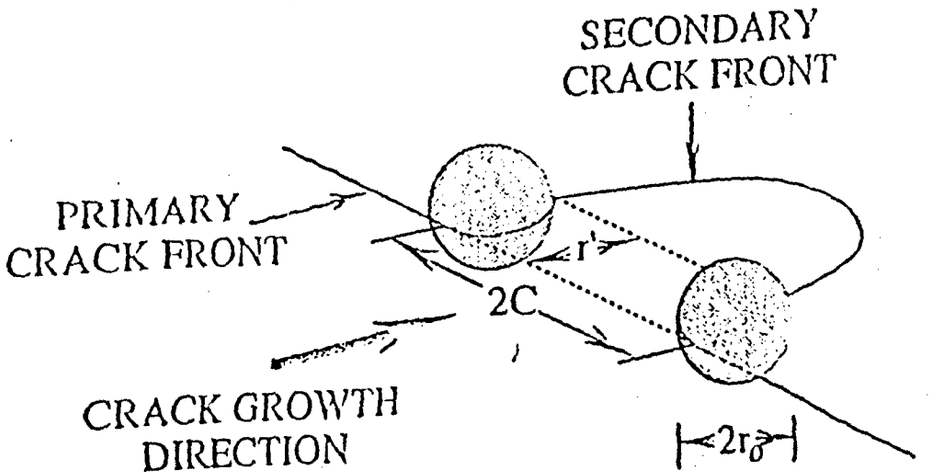

FIGURE 1. TOUGHENING DUE TO CRACK BOWING AROUND REINFORCEMENT.

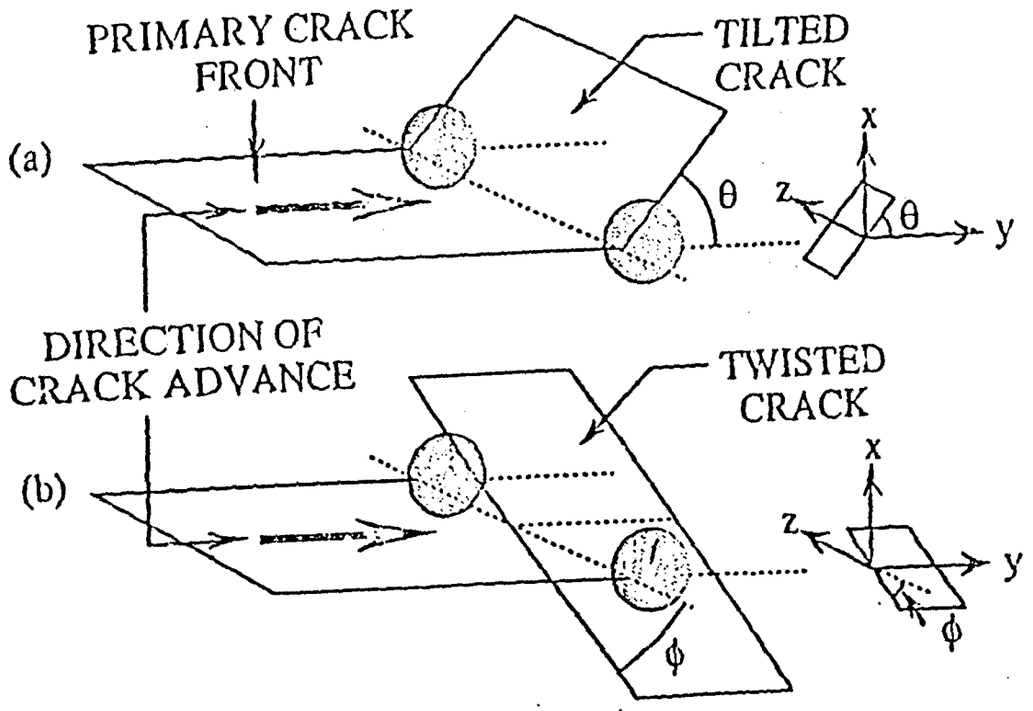

FIGURE 2. TOUGHENING DUE TO CRACK DEFLECTION.
a) CRACK TILTING
b) CRACK TWISTING

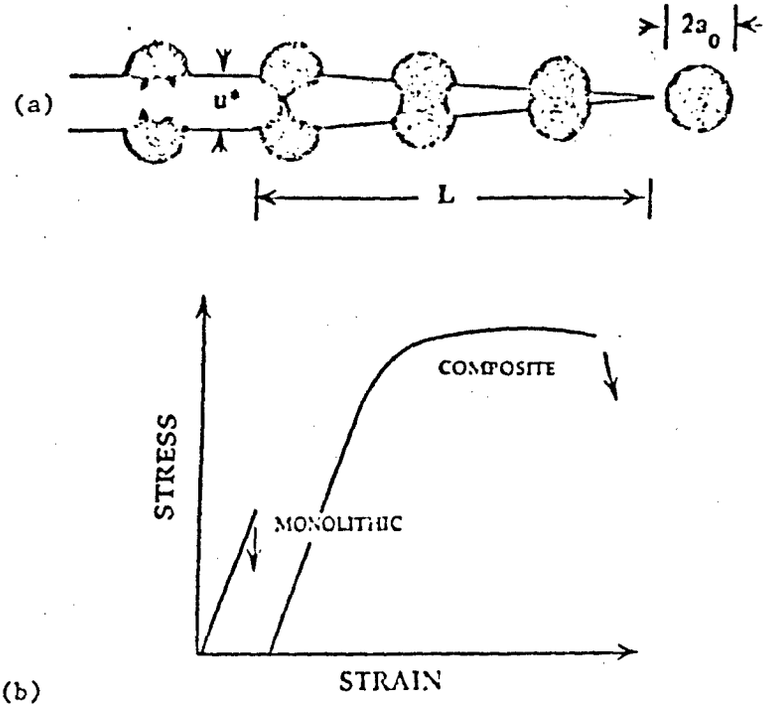

FIGURE 3. DUCTILE PHASE TOUGHENING. INTRODUCTION OF DUCTILE PARTICLES INTO BRITTLE MATRIX (a) PRODUCES DAMAGE TOLERANT COMPOSITE (b).

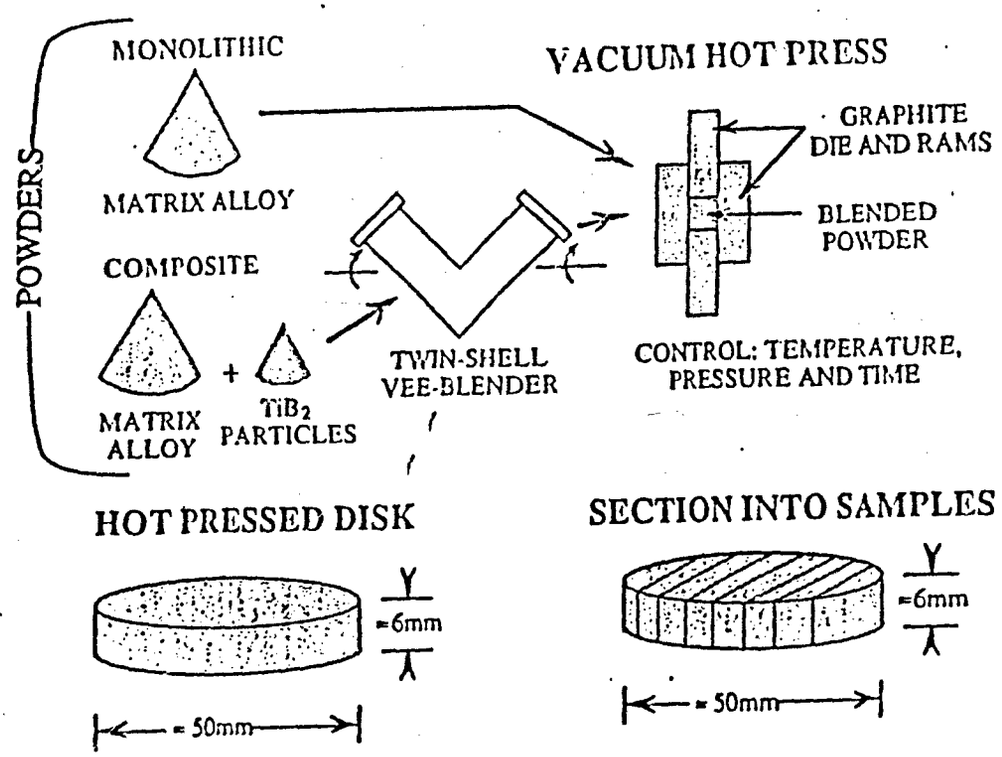

FIGURE 4. PROCESSING ROUTE FOR ALUMINIDES.

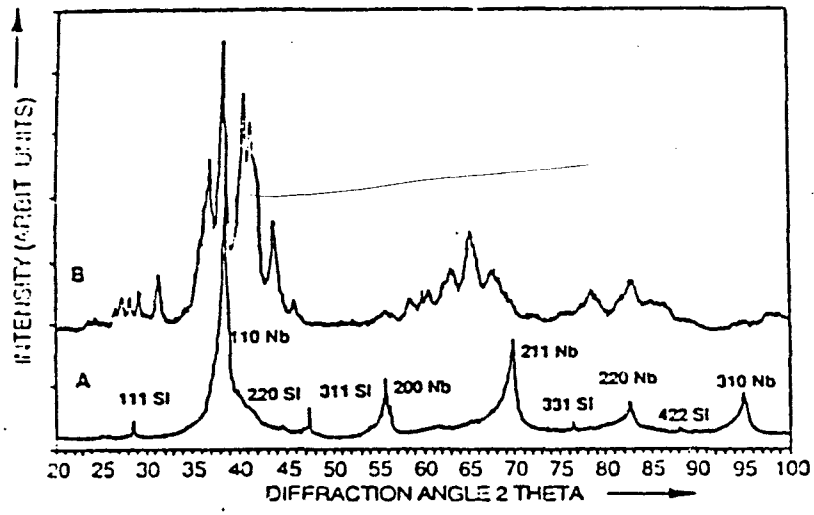

FIGURE 5. X-ray DIFFRACTION PATTERNS TAKEN OF MECHANICALLY ALLOYED Nb-Si POWDERS AFTER 3 HOURS (A) AND AFTER 3.25 HOURS (B).

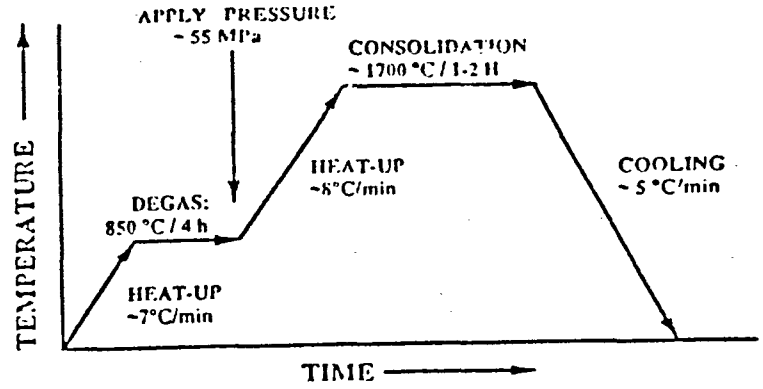

FIGURE 6. HOT PRESSING SCHEME UTILIZED TO CONSOLIDATE Nb_5Si_3.

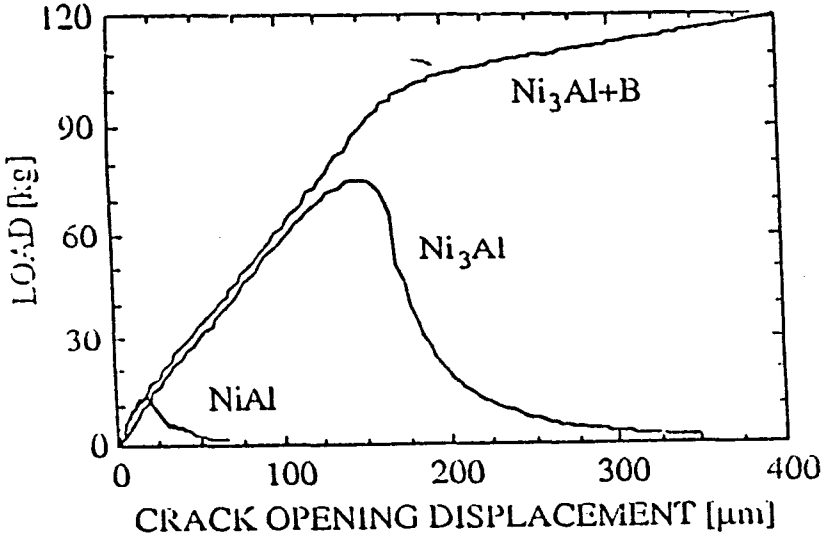

FIGURE 7. LOAD-COD TRACES FOR ALUMINIDES.

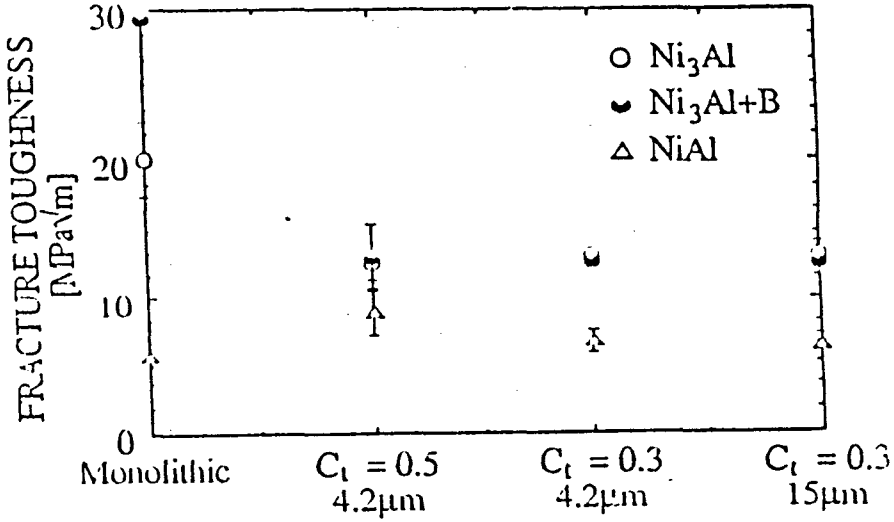

FIGURE 8. EFFECT OF TiB_2 ON ALUMINIDE TOUGHNESS.

IN-SITU TESTING

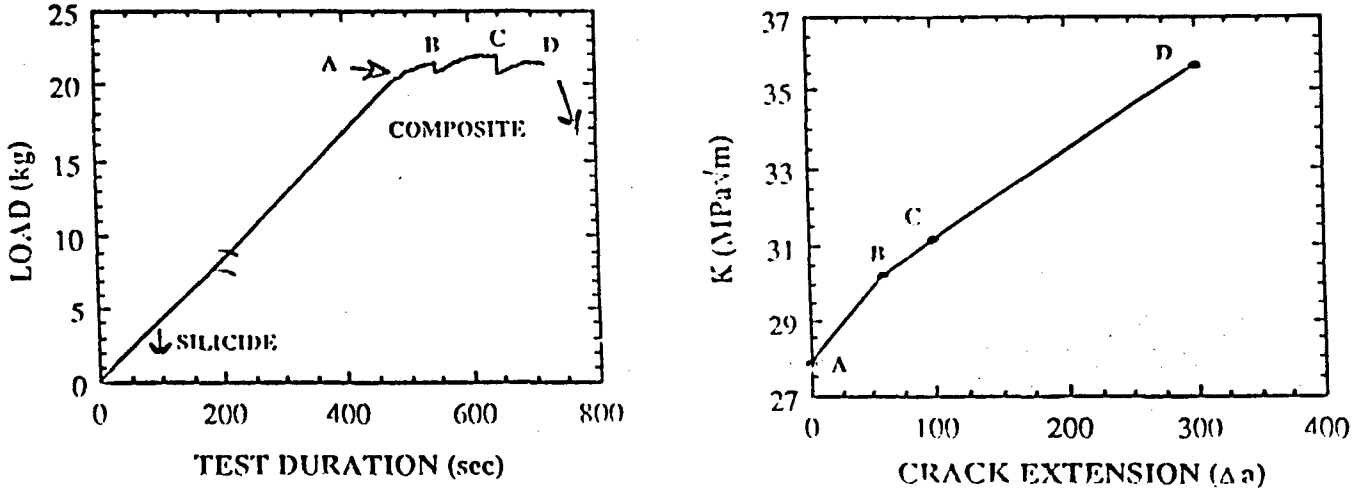

FIGURE 9. RESULTS ON IN-SITU FRACTURE TESTS ON SILICIDE COMPOSITES. R-CURVE BEHAVIOR AND SIGNIFICANT TOUGHNESS IS OBTAINED IN THE DUCTILE PHASE TOUGHENED SILICIDE.

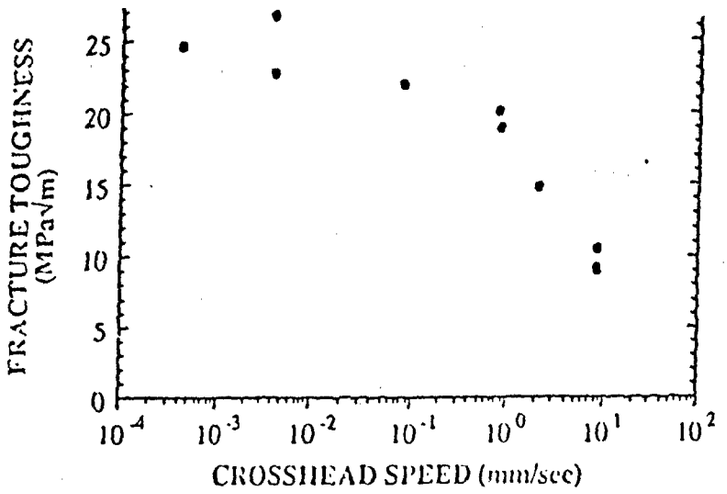

FIGURE 10. EFFECT OF LOADING RATE ON TOUGHNESS OF DUCTILE PHASE TOUGHENED SILICIDE.

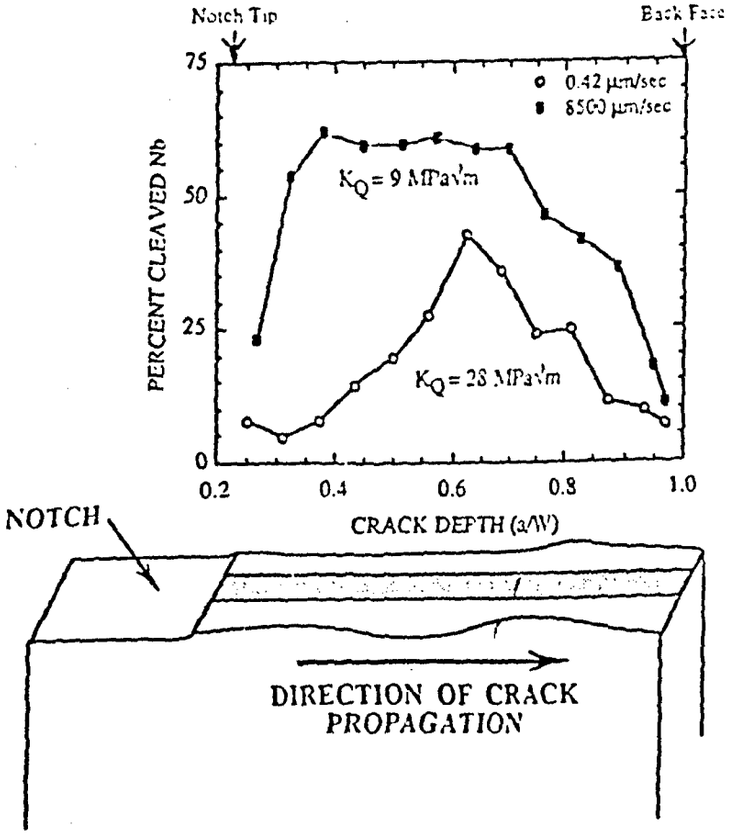

FIGURE 11. QUANTIFICATION OF FRACTURE SURFACE DETAILS VIA SEM. TESTS CONDUCTED AT FAST RATE EXHIBITED MORE CLEAVAGE AND LOWER TOUGHNESS.

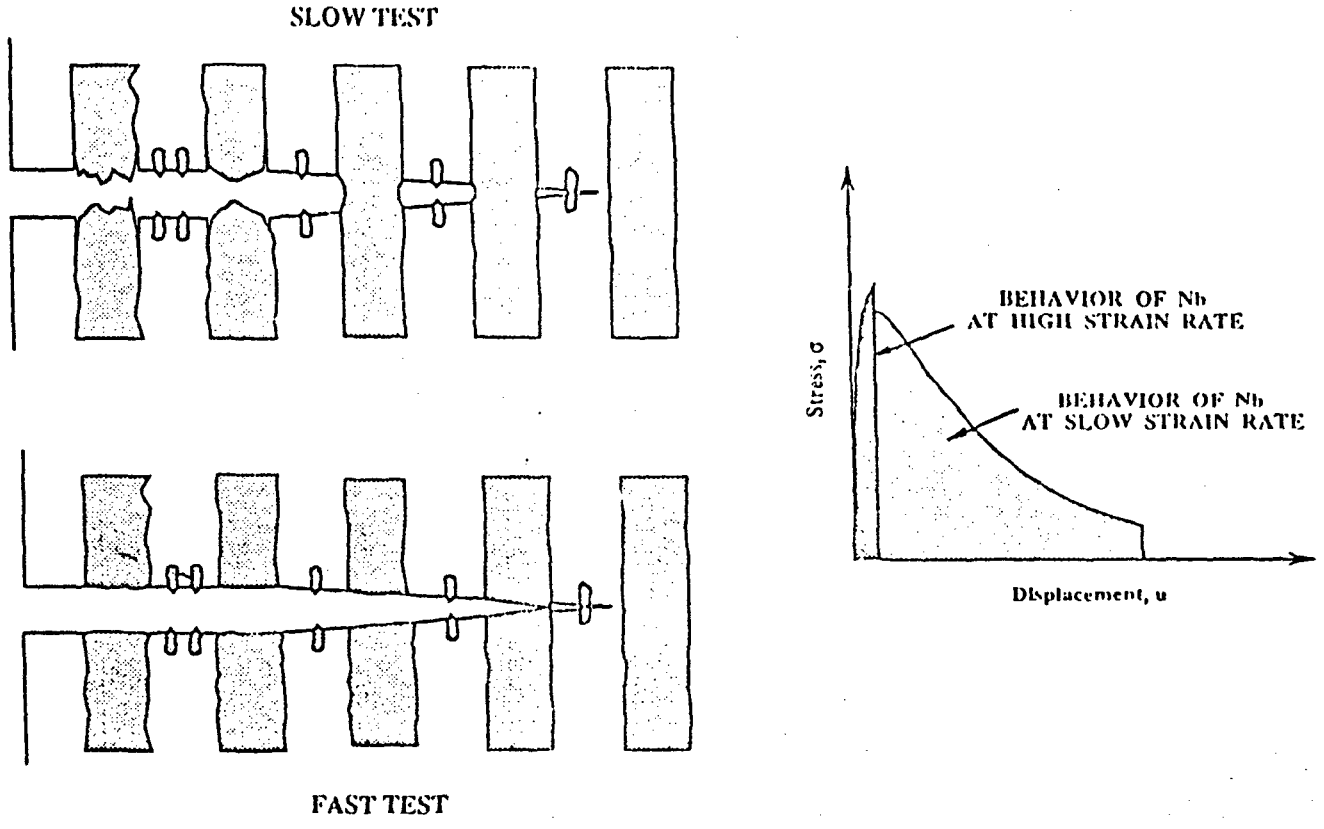

FIGURE 12. SCHEMATIC SHOWING THE EFFECT OF LOADING RATE ON FRACTURE OF Nb LIGAMEN DUCTILE RUPTURE OF Nb IS OBTAINED IN TESTS AT SLOW RATES, PRODUCING A LARGE WORK OF FRACTURE. BRITTLE FAILURE OF Nb IS OBTAINED IN TESTS FAST RATES, REDUCING THE WORK OF RUPTURE.

APPENDIX

Materials Science and Engineering, A149 (1992) 143–151

Fracture toughness of monolithic nickel aluminide intermetallics

Joseph D. Rigney and John J. Lewandowski

Department of Materials Science and Engineering, Case Western Reserve University, Cleveland, OH 44106 (USA)

(Received July 24, 1991; in revised form August 21, 1991)

Abstract

The fracture toughness of several nickel aluminide intermetallics have been determined in accordance with standard testing techniques. The intermetallics tested, Ni_3Al (24 at.% Al), Ni_3Al + 0.2 at.% B and NiAl (45 at.% Al), were produced by conventional vacuum hot-pressing techniques while processing conditions were varied to produce systematic changes in grain size. The toughnesses obtained and details of the fracture behavior were distinctly different for the materials studied. Ni_3Al exhibited an initiation toughness of 20 MPa $m^{1/2}$, while the boron-doped material had a toughness exceeding 30 MPa $m^{1/2}$. NiAl, on the contrary, demonstrated toughness values of about 5 MPa $m^{1/2}$. These differences are discussed in the light of deformation and fracture mechanisms operating at the crack tip in the cases described. *In situ* fracture monitoring and post-failure analyses are utilized in support of the discussion.

1. Introduction

Current emphasis on extebnding gas turbine engine operating temperatures for applications above which superalloys are now viable has focused renewed interest on ordered intermetallics, as revealed in a recent review article [1]. Nickel aluminide intermetallic alloys are of potential interest because of their high melting temperatures, low density and favorable oxidation resistance. Despite these advantages, such ordered alloys as Ni_3Al and NiAl suffer owing to their brittleness, especially at ambient temperatures. This brittleness is manifested as low tensile ductility, with fracture generally propagating intergranularly and/or transgranularly [2]. Studies dating a decade or more ago have shown that microalloying additions of boron to substoichiometric Ni_3Al significantly increases the room temperature ductility to values exceeding 50%, with an accompanying fracture mode change from intergranular to transgranular tearing [3, 4]. In contrast, such tensile ductility improvements in NiAl have yet to be realized, despite similar attempts at alloying [5]. Ductility has been achieved with modest success via careful control of purity level and processing conditions [6, 7] and grain size [8, 9] in binary NiAl, while recent work [10] has demonstrated significant ductility improvements during high pressure testing.

Many intermetallics are considered to be "brittle" and possess low fracture toughness based on observations of low tensile ductility and/or fractographic indications of intergranular or transgranular fracture. Fracture-related properties of monolithic Ni_3Al and Ni_3Al + B obtained under more severe stress states (*e.g.* notched K_{Ic} conditions) are virtually unreported in the literature. While low tensile ductility often accompanies low fracture toughness in non-deforming (*e.g.* ceramic-based) monolithic materials, such correlations may be misleading in many semibrittle metallic- and intermetallic-based systems. Furthermore, evaluation of such properties are necessary for the successful service application of these materials, as severe stress states may exist or become important in fatigue applications. The present authors are unaware of any such experimental studies, other than related high cycle fatigue studies on Ni_3Al-based intermetallics (reviewed by Stoloff *et al.* [11]) or notched tensile studies [12] on monolithic Ni_3Al and Ni_3Al + B. A more extensive study on powder-processed binary NiAl [13] and composites of NiAl with grain boundary Ni_3Al has been conducted to determine the effects of composition and heat treatment on the chevron-notched fracture toughness. Additional work on cast- and heat-treated stoichiometric NiAl revealed changes in fracture toughness as a function of testing temperature, processing technique and heat treatment [14].

This study was undertaken to explore the mechanisms controlling the fracture toughness of monolithic Ni_3Al (24 at.% Al), Ni_3Al + B and NiAl (45 at.% Al) and represents a continuation of work presented elsewhere [12, 15–17]. The interest in the former two materials was to investigate the fracture toughness of Ni_3Al and the effects of boron additions to these values, as boron has been shown to increase both smooth tensile [3, 4] and notched tensile ductility [12]

0921-5093/92/$5.00

Effects of reinforcement size and distribution on fracture toughness of composite nickel aluminide intermetallics

Joseph D. Rigney and John J. Lewandowski

Department of Materials Science and Engineering, Case Western Reserve University, Cleveland, OH 44106 (USA)

(Received December 11, 1991; in revised form March 23, 1992)

Abstract

The effects of particulate size and distribution on the fracture toughness of nickel aluminide composites based on Ni_3Al, Ni_3Al+B and NiAl with additions of 10 vol.% TiB_2 reinforcement were determined. Composites were fabricated by conventional vacuum hot-pressing consolidation of blends of pre-alloyed matrix powder and TiB_2 platelet reinforcement. It is shown that reinforcement additions produced a decrease in the toughness of Ni_3Al and Ni_3Al+B and an increase in the toughness of NiAl while the range of reinforcement distributions and sizes tested at present did not produce a significant change in the measured composite toughness values. The mechanisms responsible for such behavior are discussed with the aid of *in-situ* fracture studies.

1. Introduction

Nickel aluminide intermetallics are of potential interest for high temperature service where nickel- and cobalt-based superalloys have reached their highest temperature capabilities. The intermetallics based on Ni_3Al and NiAl have been investigated extensively in the past decade as evidenced by recent review articles [1] and conference proceedings [2]. These materials possess good oxidation resistance with higher melting temperatures and lower densities than superalloys. Although ambient temperature tensile ductility is low for Ni_3Al and fracture occurs in a brittle intergranular manner, recent work [3] has shown that Ni_3Al possesses a high toughness (*e.g.* above 20 MPa $m^{1/2}$) and exhibits resistance curve behavior. The improvement in tensile ductility of substoichiometric Ni_3Al via boron additions [4, 5] accompanies an improvement in fracture toughness [3]. The ductility of single-phase NiAl is generally low (*e.g.* less than 2% reduction in area) despite attempts at alloying [6] and grain size refinement [7, 8], although injection of mobile dislocations via superimposed hydrostatic pressure and testing under high pressures has produced reduction of areas in excess of 10% at room temperature [9, 10]. The fracture toughness of NiAl is generally low in as-processed material (*e.g.* 5 MPa $m^{1/2}$) [3, 11].

It should be noted that, while Ni_3Al was considered to be brittle (*i.e.* not tough) based on observations of low tensile ductility, recent fracture toughness experiments show that tensile ductility is not necessarily a good indicator of toughness in these materials [3]. It is also generally accepted that the creep resistance and high temperature strength of these alloys [12] is less than that attained by the superalloys. While the high temperature properties of these systems [13–15] has been improved somewhat by a composite approach, little work has been reported on their toughness. The schematic diagram in Fig. 1 shows the typical effects of reinforcement on the toughness of various matrices. It is shown that discontinuous metal matrix composites typically exhibit a loss in toughness with an increase in volume fraction [16], while ceramic matrix systems may gain some toughness provided that interfacial characteristics are considered [17]. The case for nickel aluminide intermetallics is not as clear, partly because

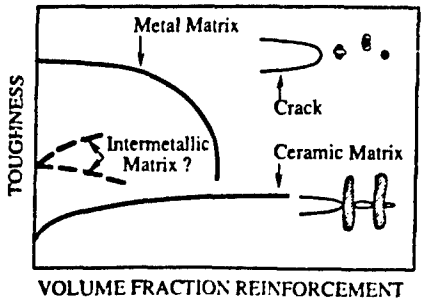

Fig. 1. General fracture toughness behavior of metal and ceramic matrix materials with additions of hard particle reinforcement. The values of intermetallic toughness or trends followed with addition of reinforcement is virtually unknown.

Processing and properties of Nb_5Si_3 and tough Nb_5Si_3/Nb laminates

Jan Kajuch, Joseph D. Rigney and John J. Lewandowski
Department of Materials Science and Engineering, Case Western Reserve University, Cleveland, OH 44106 (USA)

Abstract

Both mechanical alloying (MA) and reactive sintering (RS) techniques were successfully used to produce Nb_5Si_3. The homogeneity of the mechanically prealloyed powders and that of the Nb–Si powder blend before RS significantly affected the microstructures produced after hot-press consolidation. Model laminates of mechanically alloyed Nb_5Si_3 and nominally pure niobium were prepared via vacuum hot pressing. Room temperature toughness tests were conducted inside a scanning electron microscope equipped with a deformation stage to evaluate the effect of the niobium reinforcement on the composite fracture behavior. Significant toughness increases were obtained in the laminates, while the niobium exhibited both cleavage and ductile fracture. These results are discussed in light of recent work on ductile phase toughening of brittle materials. It is also shown that the RS process may offer an alternative approach, other than *in situ* and arc melting and casting processes, for producing both monolithic and ductile-phase reinforced Nb_5Si_3.

1. Introduction

Refractory metal silicides are receiving interest as potential candidate materials for replacing nickel and cobalt superalloys in high temperature (1473–1873 K) applications. While much of the recent work has focussed on monolithic $MoSi_2$ [1–5] and composites based on this matrix, the present work investigates the production of Nb_5Si_3 and Nb_5Si_3/Nb to evaluate the variables affecting ductile phase toughening [6–9]. *In situ* composites of niobium-based silicides investigated most recently were processed via conventional arc melting and casting processes [6–8]. However, powder processing approaches may be more versatile by providing homogeneous and/or tailorable microstructures with minimal contamination. Mechanical alloying (MA) and reactive sintering (RS) processes were used in this research for the production of Nb_5Si_3 powders and compacts, while other recent work in our laboratory [10] has utilized identical technology to produce $MoSi_2$ and other high temperature materials systems.

The MA process involves repeated fragmentation and coalescence of a mixture of powder particles until the interatomic distance between elements decreases to the point that true alloying occurs [11]. In our previous work [12] it was shown that Nb_5Si_3 is formed by a self-propagating exothermic reaction near room temperature (*i.e.* 323 K). Differential thermal analysis (DTA) of a 50/50 (at.%) Nb–Si elemental powder mixture demonstrated that Nb_5Si_3 begins to form spontaneously at approximately 1523 K [13] and that this temperature is lowered when the powders are milled and more intimately mixed prior to DTA [14]. These recent results are consistent with the proposal [15] that the activation energy for the reaction in the MA process is supplied by cold work accumulated during milling.

RS [16] provides another means of producing a compound from elemental powders and is generally possible in systems with large negative heats of formation. In this process, blended powders are isostatically cold pressed and are often ignited by torch in air or by electrical spark in vacuum to start a self-propagating exothermic reaction. RS may also occur without such external input provided that one element is molten in the reaction zone. Thus, in contrast to the MA process where alloying is a result of solid state processes, RS begins to occur at temperatures near the lowest eutectic where one element or component is in the molten state in the reaction zone [16].

This paper summarizes the results of production and consolidation of Nb_5Si_3 by both the MA and RS methods, and fabrication of laminated Nb_5Si_3/Nb composites by the use of vacuum hot pressing. The mechanism of toughening in the model Nb_5Si_3 laminates is presented, while continuing work on the production and evaluation of $MoSi_2$ and toughened $MoSi_2$ is presented elsewhere [3, 4, 9].

2. Materials and procedures

Elemental silicon (Aldrich Chemical Company) and niobium powders (Cabot Corporation) were obtained with a particle size of −325 mesh (less than 44 μm)

Elsevier Sequoia

and nominal purities exceeding 99% and 99.8% respectively. For MA, elemental powders with the proper Nb–Si ratio for the formation of Nb_5Si_3 (Nb–37.5at.%Si) were weighed and placed into a tungsten carbide vial while in an argon-gas-filled glove box. MA was carried out in a Spex model 8000 high intensity mixer–mill using 100 gf of hardened 52100 steel balls (12 mm diameter) and 10 gf of elemental powders for a 10:1 balls/powder weight ratio. The vial temperature was monitored with a portable digital thermometer with contact thermocouple type J probe. Fifty MA runs were employed to produce enough silicide powder (*e.g.* 350 g) to enable subsequent consolidation in a vacuum hot press. Prior to reactive sintering, 250 g of the elemental powder mixture was blended using a horizontal roller mixer.

Three types of powder batches were prepared for the vacuum hot pressing operation, as follows.

Mechanically alloyed Nb_5Si_3. The continuous milling process established in previous work [12] indicated that a minimum milling time of 3.25 h is required for Nb_5Si_3 compound formation. All batches of Nb–Si powders were mechanically alloyed for this length of time. In all cases, the vial was air fan cooled to assure a near-constant milling temperature.

Prealloyed Nb–Si mixture. In addition to using MA to produce Nb_5Si_3, Nb–Si mixtures were alloyed for times less than that required for compound formation (less than 3.25 h). The 45 batches were mechanically alloyed for 2 h, blended in a horizontal roller mixer for 2 h, then consolidated in the vacuum hot press. The resulting powder mixture, prior to hot pressing, contained an intimate blend of elemental niobium and silicon powders.

Blended mixture of Nb–Si powders. Elemental powders of niobium and silicon in the proper ratio for Nb_5Si_3 formation were also blended for 24 h using a horizontal roller mixer. As the powder homogeneity and/or segregation in a blending operation depends on various factors related to the blending equipment, and the size, density and volume per cent fill of elemental powders [17], a standard blending time of 24 h was selected for this work to produce a sufficient mixture. It is assumed that a more homogeneous blend will be obtained with longer blending times.

Powder consolidation was accomplished with a vacuum hot press capable of operating at up to 69 MPa pressure and 2573 K using graphite dies and plungers and a graphite resistance heating element. The general hot pressing scheme is shown schematically in Fig. 1. The degassing stage at 1123 K for 4 h may be particularly important for powders prepared by the MA process, as significant microcracking was observed in compacts not degassed for sufficient time at this temperature. RS was conducted under 55 MPa pressure in

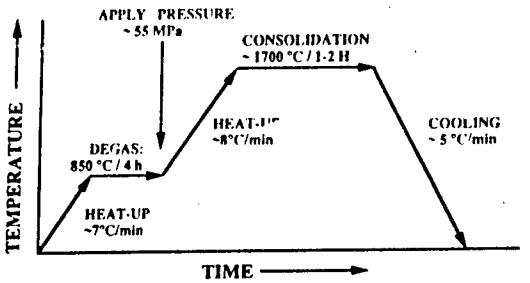

Fig. 1. Schematic of the powder consolidation process.

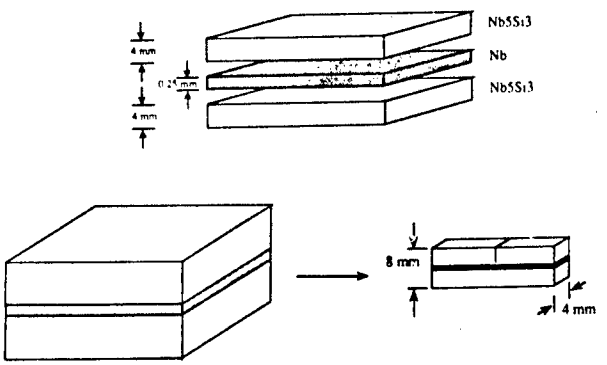

Fig. 2. Schematic of laminate bonding and sample orientation for three-point bending.

order to enhance densification. The final compacts were disc shaped 50 mm in diameter and 21 mm in height. Electrodischarge machining (EDM) was employed to prepare the samples for X-ray diffraction, metallographic analysis, and density measurements (using the Archimedes principle).

X-ray diffraction was performed on elemental powders, the mechanically alloyed silicide, prealloyed powders, the reaction-sintered material, and the material consolidated via vacuum hot pressing. A Philips X-ray Autodiffractometer operated in the continuous step scanning mode using a Cu Kα radiation source was used for the X-ray analysis. A JEOL 840A scanning electron microscope and Nikon optical microscope were used for the microstructural examinations.

The hot-pressed mechanically alloyed Nb_5Si_3 powders were electrodischarged machined and laminated with pure niobium foils 250 μm thick (grain size 10 μm) obtained from Aldrich Chemical Company. The schematic in Fig. 2 shows the laminate production scheme while the bonding was accomplished in a vacuum hot press at 10 MPa and 1473 K for 5 h. The laminates were subsequently electrodischarge machined into 4 mm × 8 mm × 45 mm single-edge-

notched bend bars for subsequent metallographic analysis and testing in three-point bending. The EDM notch of 125 μm root radius was placed in the silicide, roughly 250 μm from the silicide–Nb interface. Subsequent notching with a wire saw was utilized to extend the notch to 125 μm from the interface with a 50 μm root radius.

Metallographic analysis and mechanical testing were accomplished in a JEOL 840A scanning electron microscope equipped with an Oxford Instruments deformation stage. The bend bars were tested in three-point bending at a loading rate of 1 μm s^{-1} and continuous video monitoring enabled accurate calculation of fracture initiation loads and monitoring of the behavior of the niobium ligament. Postfailure analysis included scanning electron microscope examination of the fracture surfaces and quantification of fracture modes present.

3. Results and discussion

3.1. Powder production

Figure 3 shows the X-ray diffraction spectrum of Nb–Si elemental powders (*i.e.* curve A) as well as that of the Nb_5Si_3 compound (*i.e.* curve B) formed after 3.25 h of MA. The peaks shown in curve B correspond to a mixture of both low temperature α-Nb_5Si_3 phase (JCPDS card 30-874) and high temperature (above 2273 K) β-Nb_5Si_3 phase (JCPDS card 30-875). Diffraction spectrum A represents patterns obtained on the Nb–Si mixture and the prealloyed powders with niobium peaks as given in JCPDS card 35-789 and silicon peaks as given in JCPDS card 35-1158.

3.2. X-ray, metallographic analysis and density measurements

Figure 4 shows the X-ray diffraction patterns of the consolidated compacts obtained from the various powder processing techniques. Comparison of the diffraction spectra with the JCPDS card file shows that Nb_5Si_3 exists as both the α phase (unmarked peaks) and carbon-stabilized γ phase (filled squares) in the RS material. In contrast, MA-processed material contains the β phase as well as the α and γ phases. The β phase is a high temperature phase stabilized by the accumulated cold work experienced during the MA process [18], while the carbon in the graphite die is responsible for the formation of the carbon-stabilized γ phase. Since the hot press consolidation temperature was below that of the α-to-β phase transformation (2273 K), the β phase was retained in the compacts.

Figure 5 shows microstructures of compacts obtained from the powder processing techniques. Compacts produced from mechanically alloyed Nb_5Si_3

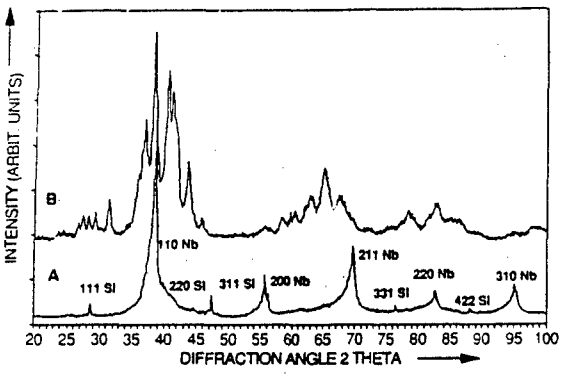

Fig. 3. X-ray diffraction patterns of mechanically alloyed Nb–Si powders: curve A, just before (3 h) compound formation; curve B, just after (3 h 15 min) compound formation.

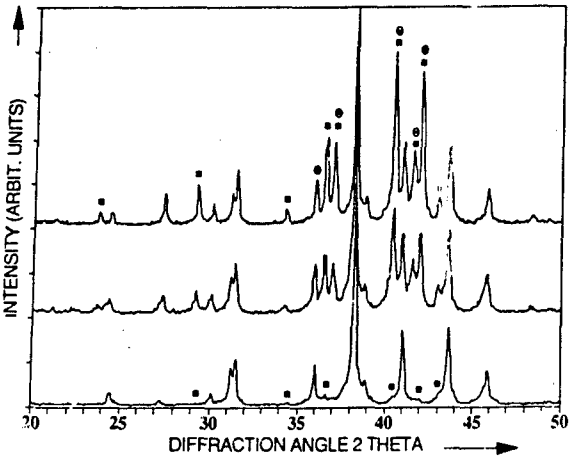

Fig. 4. X-ray diffraction patterns of consolidated powders: top, mechanically alloyed Nb–Si mixture; middle, mechanically alloyed Nb_5Si_3; bottom, reaction-sintered and hot-pressed Nb–Si mixture; ■, γ phase; θ, β phase.

exhibit a single-phase microstructure (Nb_5Si_3) with an average grain size of 5 μm. Compacts obtained from prealloyed niobium and silicon powders contain a small amount (less than 3 vol.%) of unreacted niobium confirmed by energy-dispersive X-ray analysis on the scanning electron microscope with the remaining microstructure consisting of Nb_5Si_3 with an average grain size of 5 μm. The RS compact, in addition to exhibiting a larger volume per cent of unreacted niobium (*i.e.* 5 vol.%), displayed a bimodal grain size distribution with grains of average size 2–3 μm and 15 μm. Results of the immersion density measurements are reported in Table 1. All micrographs (*i.e.* Fig. 5) show porosity levels apparently exceeding 98% of theoretical density; however, subsequent work has

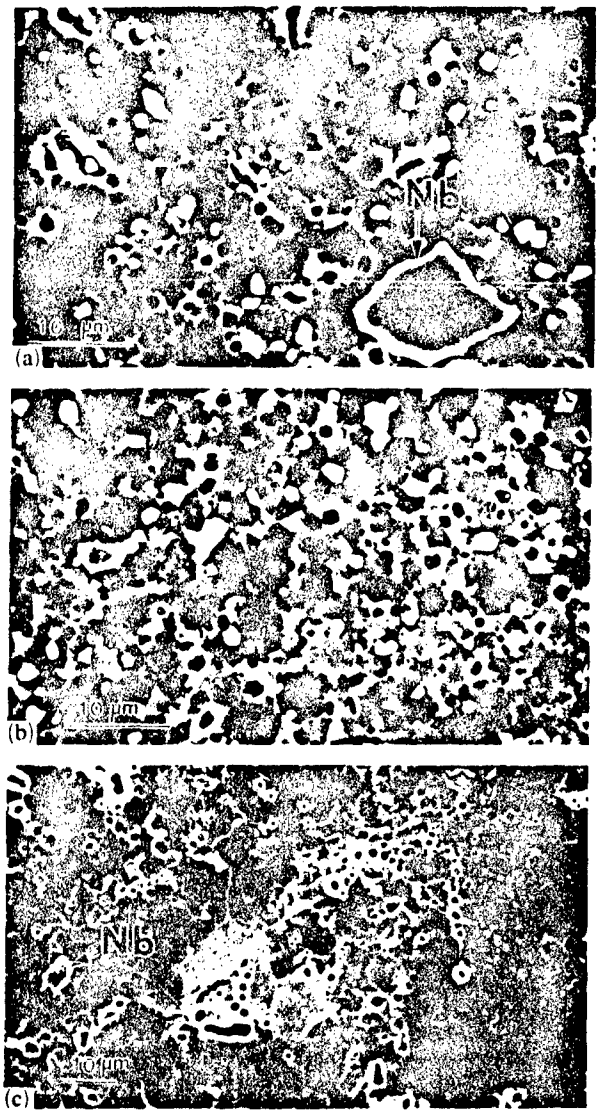

Fig. 5. Microstructures obtained: (a) mechanically prealloyed Nb–Si mixture, hot pressed; (b) mechanically alloyed Nb_5Si_3, hot pressed; (c) reaction-sintered Nb_5Si_3, hot pressed.

TABLE 1. Results of powder compaction

Initial powders	Hot-pressed density (% theoretical)	Nb_5Si_3 phases present[a]	Microstructure[b]
Nb_5Si_3	97.6	α, β, γ	Nb_5Si_3
Alloyed Nb–Si	97.7	α, β, γ	Nb_5Si_3 + Nb[c]
Nb–Si blend	98.5	α, γ	Nb_5Si_3 + Nb[d]

[a]From X-ray analysis.
[b]From scanning electron microscopy.
[c]Less than 3 vol.%.
[d]About 5 vol.%.

shown that the additional "holes" result from silicide grain pull-out during metallographic preparation.

Although RS of elemental powders typically involves the formation of a transient liquid phase (*e.g.* silicon in Nb–Si mixture), the formation of the desired phase is controlled by the mass transport of atoms with higher diffusivity [19]. In the Nb–Si system, silicon (melting point 1687 K) diffusion into niobium grains controls the formation of Nb_5Si_3. In both the reaction-sintered and mechanically alloyed Nb–Si mixtures, the inhomogeneity of the initial powder apparently results in the microstructure of unreacted niobium and Nb_5Si_3. In mechanically prealloyed Nb–Si mixtures, the niobium and silicon interparticle spacing is somewhat smaller than that of the simply blended material used for RS. Thus, the amount of unreacted niobium is somewhat less than that of the reaction-sintered powder. Additional work where the milling times and/or powder particle sizes are varied is necessary to establish a more quantitative relationship between the resulting two-phase microstructures and the starting particle sizes and interparticle spacing.

Figure 6 shows the notched specimen and the laminate interfacial region. No interfacial reactions between Nb_5Si_3 and niobium were observed. Also, no cracks were observed in the as-electrodischarge-machined specimens. Figure 7 shows the load–displacement trace obtained on the three-point bending laminate tested inside the scanning electron microscope, while Fig. 8 presents a sequence of photographs taken at the locations marked in Fig. 7. The shaded area in Fig. 7 represents the notch-bend behavior of monolithic Nb_5Si_3. The significant toughness increase (*i.e.* area under the load–displacement trace) results from the niobium ligament and its ability to blunt propagating cracks in the Nb_5Si_3 as shown in Fig. 8. This was also observed in much of our previous work on arc-cast and

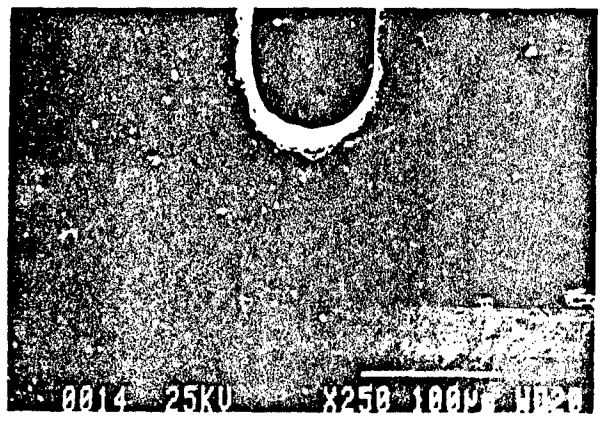

Fig. 6. Micrograph of a notched Nb_5Si_3/Nb/Nb_5Si_3 sample (three-point bending).

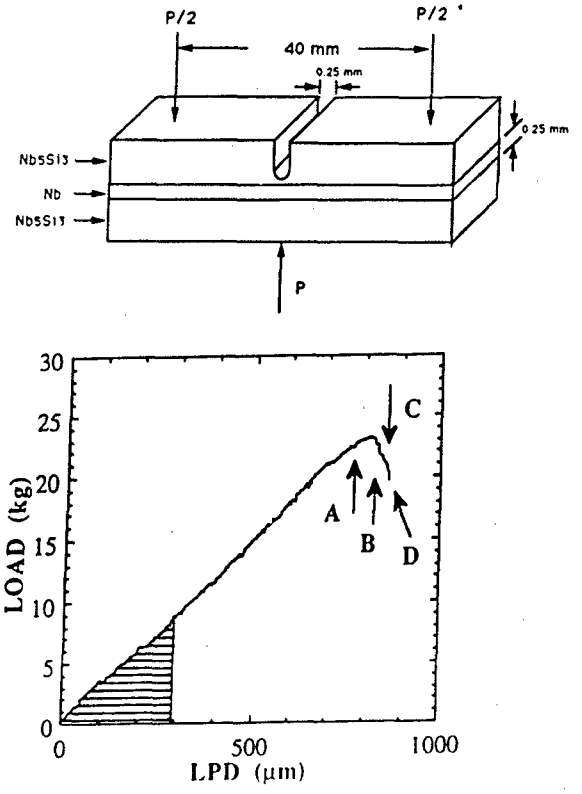

Fig. 7. Load-displacement trace of a three-point bending notched sample.

extruded *in situ* composites of Nb_5Si_3/Nb [6–8, 20, 21]. The Nb_5Si_3–Nb interface is well bonded, while Fig. 8 shows arrested microcracks in the niobium. Examination of the fracture surfaces obtained from the laminate tested at room temperature (Fig. 9) indicates that the niobium exhibits both cleavage and ductile fracture in the proportion of 40% and 60% respectively. The arrested microcracks in the niobium ligament shown in Fig. 8 are cleavage microcracks which are blunted by the ductile niobium.

The appearance of room temperature cleavage fracture of niobium in the present tests is apparently due to a combination of several factors, as pure niobium does not typically cleave at room temperature [22]. The high-temperature vacuum hot-press bonding procedure used to produce laminates enables diffusion of silicon into niobium and grain growth in the niobium ligament. The large grains are obvious from the large cleavage facets shown in Fig. 9. The effects of grain size on the propensity for cleavage fracture are well documented in ferrous materials [23]. Materials containing larger grains typically exhibit a greater tendency for cleavage fracture since the cleavage fracture stress decreases with an increase in grain size [23]. Secondly, silicon is a potent solid solution hardener and embrittler of niobium as shown in previous work [6–8, 24]. However, recent work [24, 25] has shown that smooth tension specimens of niobium containing silicon in solid solution are ductile while notched specimens of the same material [24, 25] exhibit cleavage fracture and much lower ductility.

Table 2 summarizes the effects of grain size and silicon diffusion on the properties of niobium foils 250 μm thick [24]. Tension specimens were prepared from the as-received foil as well as those exposed to vacuum at 1473 K for 5 h and those exposed to Nb_5Si_3 at 1473 K for 5 h. The second treatment provided large niobium grains, while the third provided both large grains and silicon diffusion into niobium. The tensile results in Table 2 show that silicon increases the yield stress of the smooth specimens without significantly decreasing the ductility. In light of the present results, it appears that the constraint provided by the Ni_5Si_3 is sufficient to elevate the local stresses to levels high enough to induce cleavage in the niobium ligament. This is consistent with recent finite element analyses [26] and experiments [27] which have shown significant stress elevation in ductile particles bridging brittle cracks. Thus, the combination of silicon diffusion into niobium, large niobium grain size, and constraint is responsible for cleavage fracture in the niobium. Areas of ductile niobium fracture in the laminates result in part from multiple cracks in the silicide which effectively reduce the constraint locally in the niobium, as shown in Fig. 8 and similar to other recent work on a Pb–glass model system [27]. Nonetheless, while significant toughness increases are observed in the present tests, additional toughness increments may be realized by optimizing the microstructure and properties of the niobium ligament as well as those of the interfacial region. Recent work [27, 28] has shown beneficial effects of a weak interface in increasing the toughness of such systems, due to the relaxation of constraint on the ductile ligaments.

4. Conslusions

(1) MA and RS techniques were used to produce Nb_5Si_3 from elemental Nb–Si mixtures. Consolidation of the powders in a vacuum hot press resulted in crack-free dense compacts.

(2) Homogeneity of the prealloyed and blended powders played a major role in the microstructural homogeneity of consolidated compacts. It was shown that unreacted niobium existed in both the mechanically prealloyed Nb–Si and powder-blended reaction-sintered materials. This technique may be utilized to produce composite microstructures of Nb_5Si_3 and

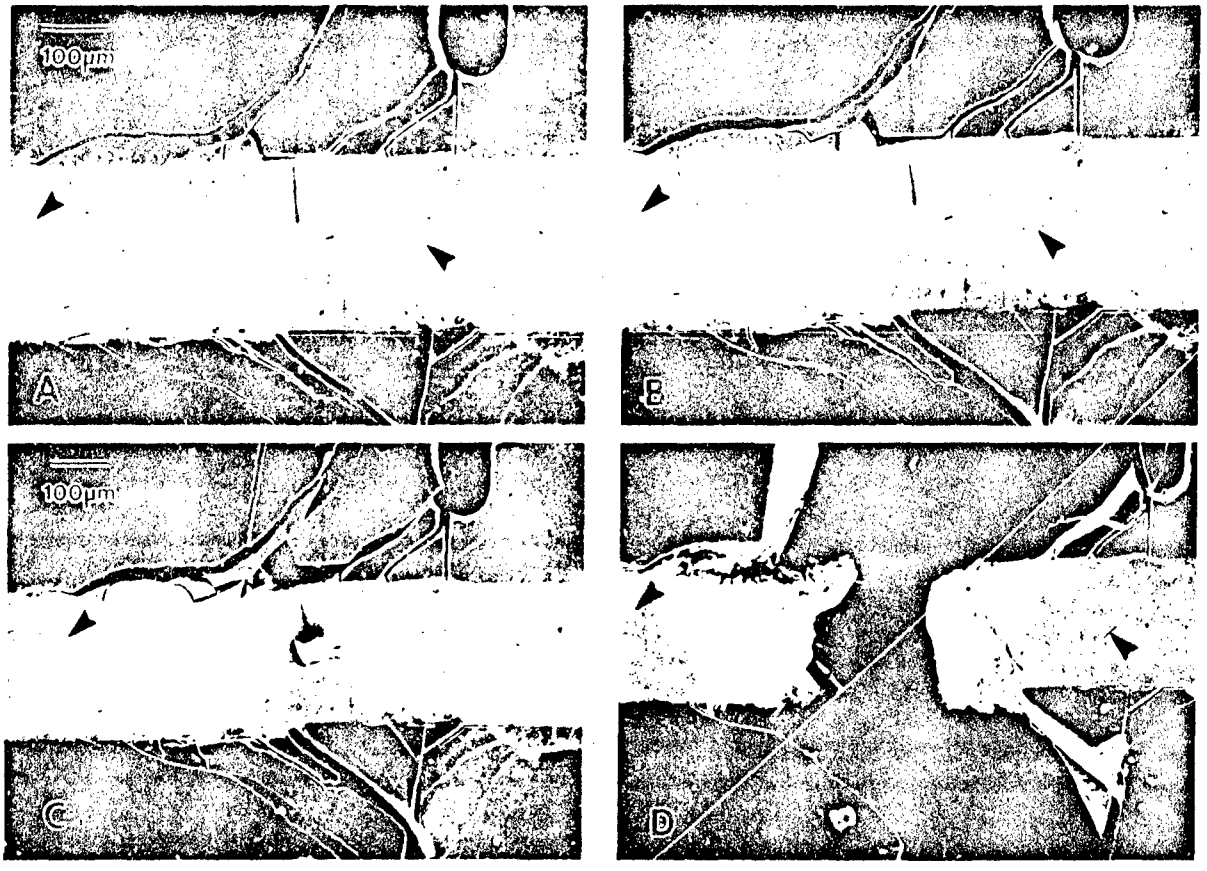

Fig. 8. Scanning electron micrographs of niobium ligament deformation at the loads marked A, B, C and D respectively in Fig. 7. Arrows indicate arrested cleavage microcracks in niobium.

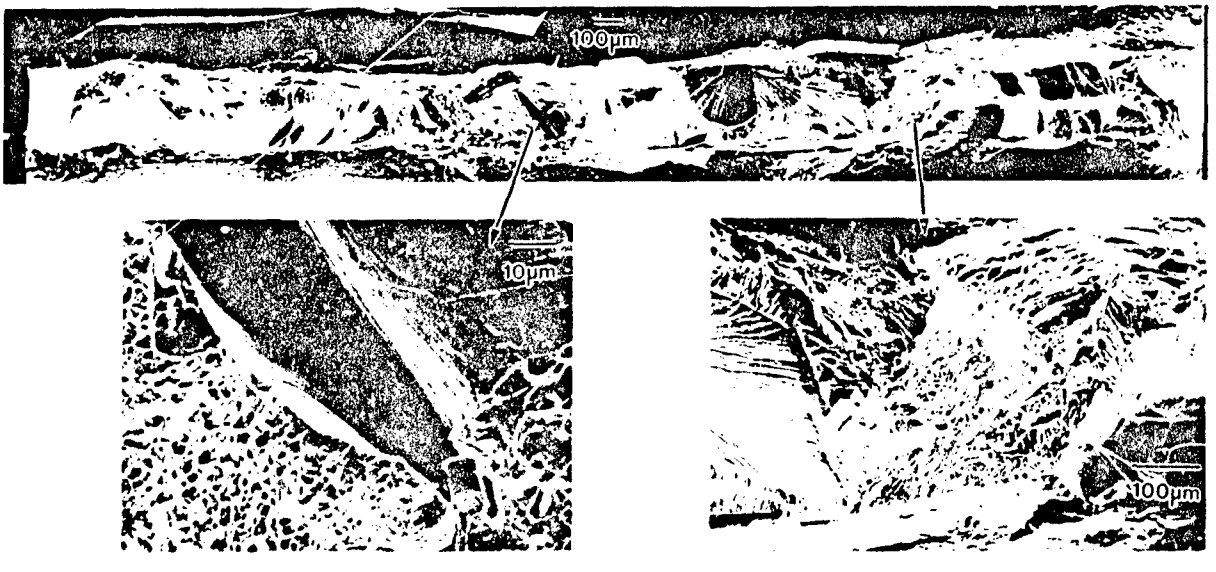

Fig. 9. Fracture surface of a niobium ligament showing 40% cleavage and 60% ductile fracture.

TABLE 2. Tensile properties of Nb foil

Material[a] condition	Grain size (μm)	σ_y (MPa)	UTS[b] (MPa)	Elongation (%)	Reduction of area (%)
As received	10	251.8	344.8	9.0	78.2
1473 K for 5 h in vacuum	210	185.6	222.2	23.4	82.0
1473 K for 5 h exposed to Nb_5Si_3	210	363.2	390.0	11.3	75.5

[a]Niobium foil.
[b]Ultimate tensile strength.

niobium, or other combinations of phases in different systems.

(3) Nb_5Si_3/Nb laminates were successfully produced and exhibited significant toughness increases over that of the monolithic Nb_5Si_3. *In situ* fracture monitoring revealed crack blunting by the niobium and stable cleavage microcracks in the niobium. Dual fracture characteristics of niobium were observed and possible reasons for this behavior were provided.

Acknowledgments

The authors would like to acknowledge the support of the US Air Force Office of Scientific Research through contract 89-0508 and the program manager Dr. Alan Rosenstein, with partial support (J. D. Rigney) by MTS Systems Corporation.

References

1 F. D. Gac and J. J. Petrovic, *J. Am. Ceram. Soc., 68* (1985) C 200.
2 J. M. Yang and S. M. Jeng, *Mater. Res. Soc. Symp. Proc., 194* (1990) 139.
3 S. A. Maloy, A. H. Heuer, J. J. Lewandowski and J. J. Petrovic, *J. Am. Ceram. Soc., 74* (1991) 2704–2706.
4 S. A. Maloy, J. J. Lewandowski, A. H. Heuer and J. J. Petrovic, *Mater. Sci. Eng., A155* (1992) 159.
5 J. D. Cotton, Y. S. Kim and M. J. Kaufman, *Mater. Sci. Eng., A144* (1991) 287–291.
6 J. J. Lewandowski, D. Dimiduk, W. Kerr and M. G. Mendiratta, *Mater. Res. Soc. Symp. Proc., 120* (1988) 103–108.
7 M. G. Mendiratta and D. M. Dimiduk, *Mater. Res. Soc. Symp. Proc., 133* (1989) 441–446.
8 M. G. Mendiratta, J. J. Lewandowski and D. M. Dimiduk, *Metall. Trans. A, 22* (1991) 1573–1583.
9 J. D. Rigney, R. Castro and J. J. Lewandowski, *J. Mater. Sci. Lett.*, submitted for publication.
10 S. Patankar, J. Kajuch and J. J. Lewandowski, unpublished results, Case Western Reserve University, 1991.
11 D. R. Maurice and T. H. Courtney, *Metall. Trans. A, 21* (1990) 289.
12 J. Kajuch and K. Vedula, *Adv. Powder Metall.*, (2) (1990) 187.
13 N. N. Thadhani, M. J. Costello, I. Song, S. Works and R. A. Graham, in A. C. Claver and J. J. de Barbadillo (eds.), *Solid State Powder Processing*, TMS-AIME, Warrendale, PA, 1990, p. 97.
14 J. Kajuch, I. Locci and J. J. Lewandowski, unpublished results, Case Western Reserve University, 1992.
15 C. C. Koch, *Annu. Rev. Mater. Sci., 19* (1989) 121.
16 Z. A. Munir and U. Anselmi-Tamburini, *Mater. Sci. Rep., 3* (1989) 277.
17 J. O. G. Parent, J. Iyengar, M. Kuhni and H. Henein, *AFOSR Annu. Rep., Contract F49620-87-C-0017*, Carnegie Mellon University, Pittsburgh, PA, 1988, p. 9.
18 K. S. Kumar and S. K. Mannan, *Mater. Res. Soc. Symp. Proc., 133* (1989) 415.
19 J. D. Whittenberger, in A. C. Claver and J. J. Barbadillo (eds.), *Solid State Powder Processing*, Metallurgical Society of AIME, Warrendale, PA, 1990, p. 137.
20 J. D. Rigney and J. J. Lewandowski, in M. D. Sacks (ed.), *Proc. 2nd Int. Ceramic Science and Technology Congr.—Advanced Composite Materials*, America Ceramic Society, Westerville, OH, 1990, p. 519.
21 J. D. Rigney, J. J. Lewandowski, M. G. Mendiratta and D. M. Dimiduk, *Mater. Res. Soc. Symp. Proc., 213* (1991) 1001.
22 *Proc. Int. Symp. on Niobium, San Francisco, CA*, 1981, p. 253.
23 J. F. Knott, *Fundamentals of Fracture Mechanics*, 1st edn., Butterworths, London, 1973.
24 J. Kajuch, J. D. Rigney and J. J. Lewandowski, unpublished results, Case Western Reserve University, 1991.
25 M. Mendiratta and D. Dimiduk, unpublished results, 1991.
26 A. G. Evans and R. McMeeking, *Acta Metall., 34* (1986) 241.
27 M. F. Ashby, F. J. Blunt and M. Bannister, *Acta Metall., 37* (1989) 1847.
28 L. Xiao and R. Abbaschian, in M. N. Gungor, E. J. Lavenia and S. G. Fishman (eds.), *Proc. Int. Symp. on Advanced Metal Matrix Composites for Elevated Temperatures, ASM International Materials Park, OH*, 1991, pp. 33–40.

PAPER 4

MRS Proceedings.
1993, in press

ON THE KINETICS OF Nb_5Si_3 COMPOUND FORMATION

Jan Kajuch, John W. Short, Changqi Liu and John J. Lewandowski
Dept. of Materials Science and Engineering
Case Western Reserve University, Cleveland, OH

ABSTRACT

The kinetics of intermetallic Nb_5Si_3 compound formation via the mechanical alloying process was investigated. Interrupted milling process, X-ray diffraction, SEM examination and TEM imaging and diffraction were utilized to characterize changes in the milled powders, while DTA analyses were used to determine the critical and onset temperatures of reaction as a function of milling time. On the basis of experimental results, a kinetic model was proposed for formation of Nb_5Si_3 via the interrupted MA process. It is suggested that precipitation of Nb_5Si_3 particles during cooling in the interrupted milling process is responsible for the exothermic reaction after resumption of milling.

INTRODUCTION

Mechanical alloying (MA) is a simple but effective process for the production of intermetallic compounds of high temperature refractory metals. Its main advantage as compared to the standard melting and casting process is in the capability to maintain exact composition (stoichiometry), low degree of contamination, and flexibility in producing monolithic and composite powders. MA is a non-equilibrium processing technique analogous to Rapid Solidification (RS). In contrast to the RS process, the MA process is entirely a solid state operation at or near room temperature. The MA process has been defined as a dry, high energy ball milling process that produces composite metal powders with extremely fine microstructures. Interdispersion of the powders occurs by the repeated cold welding and fracturing process of free powder particles, trapped between two colliding steel balls[1]. The force of the impact deforms the particles and creates atomically clean surfaces which weld together on contact. To prevent oxidation of these surfaces, the milling operation is carried out in an inert gas atmosphere. Refinement of the structure is approximately a logarithmic function of time and depends on the mechanical energy input into the milling process and the work hardening of the powders being processed[2]. The microstructural refinement continues into the steady-state period despite the fact that the hardness saturates and a constant agglomerate particle size distribution is achieved.

Several authors studied the formation of intermetallic compounds by the MA process. Atzmon determined the parameters affecting phase formation in the Al-Ni system[3]. While NiAl formed by an explosive, self-propagating reaction, Al_3Ni formed in a reaction with layer diffusion as a predominant factor. Kumar and his co-workers were the first to study the mechanism of MA in group V transition metal/silicon systems[4]. In order to study the progress of mechanical alloying, the ball mill was stopped periodically and cooled to room temperature in order to enable removal of small amounts of the powder for analysis. This "interrupted process" resulted in the formation of Nb_5Si_3 in 75 minutes, while milling for 73 minutes and cooling to room temperature produced elemental Nb and Si. Whittenberger in his analysis of the solid state processing of high temperature alloys and composites[5] believes that "enhanced diffusivity" plays a major role in the alloying process.

Schaffer and McCormick studied the mechanism of compound formation in the "interrupted process" in several systems with the conclusion that room temperature "enhanced diffusivity" facilitates the exothermic reaction which occurs almost instantaneously after milling is resumed[6].

This investigation concentrates on proposing a kinetic model of the formation of Nb_5Si_3 via interrupted milling utilizing Differential Thermal Analyses, X-ray diffraction and Scanning Electron and Transmission Electron Microscopy. The work represents a continuation of work reported elsewhere[7].

EXPERIMENTAL PROCEDURES

Elemental silicon (Aldrich Chemical Company) and niobium powders (Cabot Corporation) were obtained with a particle size of -325 mesh (less than 44 μm) and nominal purities exceeding 99% and 99.8% respectively. For MA, elemental powders with the proper Nb-Si ratio for the formation of Nb_5Si_3 (Nb-37.5 at% Si) were weighed and placed into a tungsten carbide vial while in an argon-gas-filled glove box. MA was carried out in a Spex model 8000 high intensity mixer-mill using 100 g of hardened 52100 steel balls (12 mm diameter) and 10 g of elemental powders for a 10:1 bal's/powder weight ratio. The vial temperature was monitored with a portable digital thermometer with a contact thermocouple type J probe.

X-ray diffraction was performed on elemental powders and the mechanically alloyed powders for time intervals of 1 to 3.5 hrs. A Phillips X-ray Autodiffractometer operated in the continuous step scanning mode using a Cu Kα radiation source was used for the X-ray analyses. A JEOL 840A scanning electron microscope (SEM) and JEOL 200CX transmission electron microscope (TEM) were used for the microstructural examinations. SEM characterization of agglomerate size and microstructural refinement was performed on powders milled for various times as well as on reacted powders. Back scattered electron imaging was used for the studies of microstructural refinement.

A Netzsch STA 429/409 Differential Thermal Analyzer at NASA Lewis Research Laboratories and a modified DTA unit built at Case Western Reserve University were used to determined the critical and onset reaction temperatures on prealloyed powders as well as on reacted powders (Nb_5Si_3). Prealloyed powders (1 hr) aged at room temperature for times of 1 to 1000 hrs were held at -196°C when the DTA equipment was not immediately available. For the DTA tests at CWRU, powder samples (2 to 5 grams) were cold pressed into small discs and a center hole was drilled for the insertion of a K type thermocouple, while another K type thermocouple was placed in the alumina crucible as a reference. Argon gas was used to prevent powder oxidation during the analysis and post-analysis cooling. Some of these sintered samples were crushed and x-rayed to determine the phase evolution during DTA analysis.

For the TEM observations, Nb-Si milled powders were dispersed on a piece of carbon film which was supported on a copper grid (3mm in diameter). An additional layer of carbon film was deposited on top of the dispersed powders in order to avoid contamination of the microscope. Both bright field and dark field imaging techniques were employed to observe and identify the particles.

RESULTS AND DISCUSSION

In our previous work on the synthesis of Nb_5Si_3 by the "interrupted process" it was found that compound formation proceeded by self-propagating exothermic reaction upon

resumption of the milling process[7]. Two major variables controlling compound formation were identified. A minimum milling time of 1 hour and a minimum cooling time of 2 hours was required before milling was resumed (Figure 1). The following observations were analyzed to determine the reasons for the critical milling time and hold time at room temperature.

Figure 2 shows the microstructural refinement in a Nb-Si agglomerate after MA for 1 hour. Particles within the agglomerate are not uniformly refined, with an average inter-particle spacing on the order of 1 μm although there are areas where refinement is on a much smaller scale. According to the theory of mechanical alloying, true alloying occurs when the microstructural refinement is no longer visible in an optical microscope, roughly a particle spacing of 0.5 μm. This leads us to conclude that there are small areas where intensive MA energy input promotes Si dissolution in Nb, creating a supersaturated solid solution with respect to its equilibrium solubility at low processing temperatures (≈600-900 K). Upon cooling, Nb_5Si_3 particles precipitate from solid solution as expected from the equilibrium diagram. Upon resumption of milling, a self-propagating exothermic reaction takes place, due to a large heat of formation release upon growth of Nb_5Si_3 particles.

Differential Thermal Analyses (DTA) were conducted on powders milled for a total time of 1 hour immediately after the milling process was stopped as well as after room temperature "aging" for up to 1000 hours (Figure 3). Figure 4 shows the onset reaction temperature of Nb_5Si_3 vs. "aging" time at room temperature, with a total temperature differential of less than 9°C. This small reaction temperature drop suggests that although "enhanced diffusivity" occurred, it does not play a significant role in the compound formation in the interrupted process. In order for the reaction to take place as shown in Figure 5, enhanced diffusivity would have to decrease critical reaction temperature on the order of 50°C. Here, the critical reaction temperature is the temperature at which the heat of reaction is large enough to cause a positive increase in the temperature differential between the sample and the reference thermocouple, while the onset temperature is designated as the temperature at which the reaction is self-propagating.

TEM electron diffraction of Nb-Si powders milled for 1 hour (Figure 6) show particles of Nb+Si mixture as well as Nb_5Si_3 compound. No other metastable, amorphous, or equilibrium phases were observed.

CONCLUSIONS

The initiation of Nb_5Si_3 compound reaction in the interrupted milling process occurred via the precipitation of Nb_5Si_3 particles upon cooling from the milling temperature. Two major parameters controlling the precipitation process are the minimum milling time of 1 hour and the minimum cooling time of 2 hours. The most plausible explanation for the precipitation process is the creation of a non-equilibrium supersaturated solid solution of Si in Nb. TEM observations of powders milled for 3 hours failed to show precipitates other than Nb_5Si_3, supporting the mechanism of Nb_5Si_3 precipitation.

ACKNOWLEDGEMENTS

The authors would like to acknowledge the support of the US Air Force Office of Scientific Research through contract 89-0508 and the program manager Dr. Alan Rosenstein. The use of DTA equipment at NASA Lewis Research Center and the assistance of Dr. Ivan Locci is also appreciated.

REFERENCES

[1]P.S. Gilman and J.S. Benjamin, *Annual Rev. Mater. Sci.*, 13, 279 (1983).
[2]J.S. Benjamin and T.E. Volin, *Metall. Trans.*, 5, 1929 (1974).
[3]M. Atzmon in A.H. Clauer and J.J. deBarbadillo (eds.), *Solid State Processing*, The Minerals, Metals & Materials Society, Warrendale, 173 (1990).
[4]K.S. Kumar and S.K. Mannan, *Mater. Res. Soc. Symp. Proc.*, 133, 415 (1989).
[5]J.D. Whittenberger in A.H. Clauer and J.J. deBarbadillo (eds.), *Solid State Powder Processing*, The Minerals, Metals & Materials Society, Warrendale, 137 (1990)
[6]G.B. Schaffer and P.G. McCormick, *Metall. Trans A*, 22A, 3019 (1991).
[7]J. Kajuch, J.D. Rigney, and J.J. Lewandowski, *Materials Sci. and Eng.*, A155, 59 (1992).

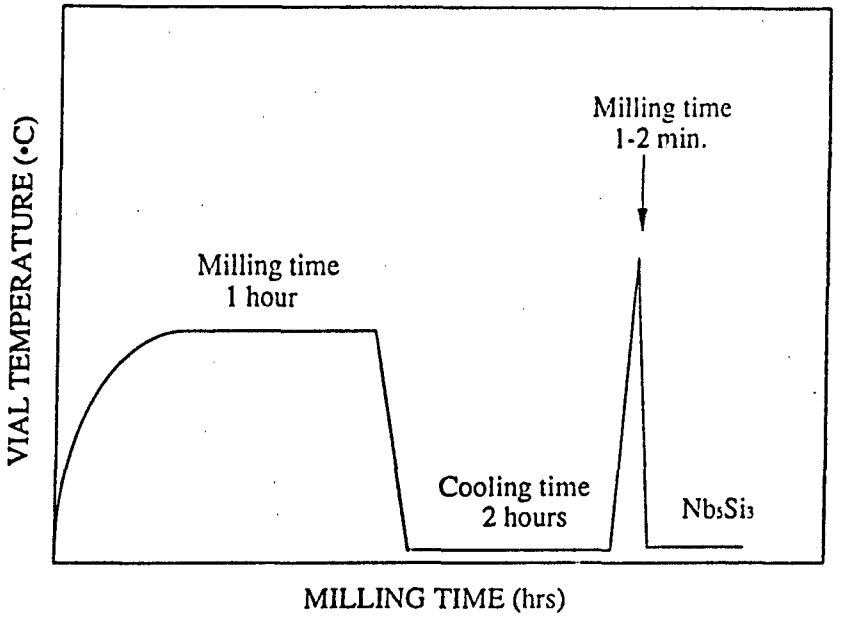

Figure 1. Schematic of interrupted milling process

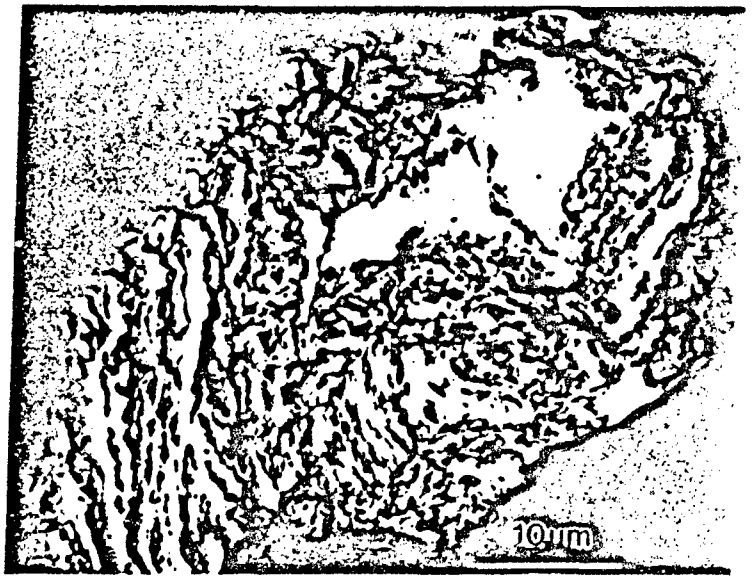

Figure 2. SEM micrograph of Nb-Si mixture milled for 1 hr

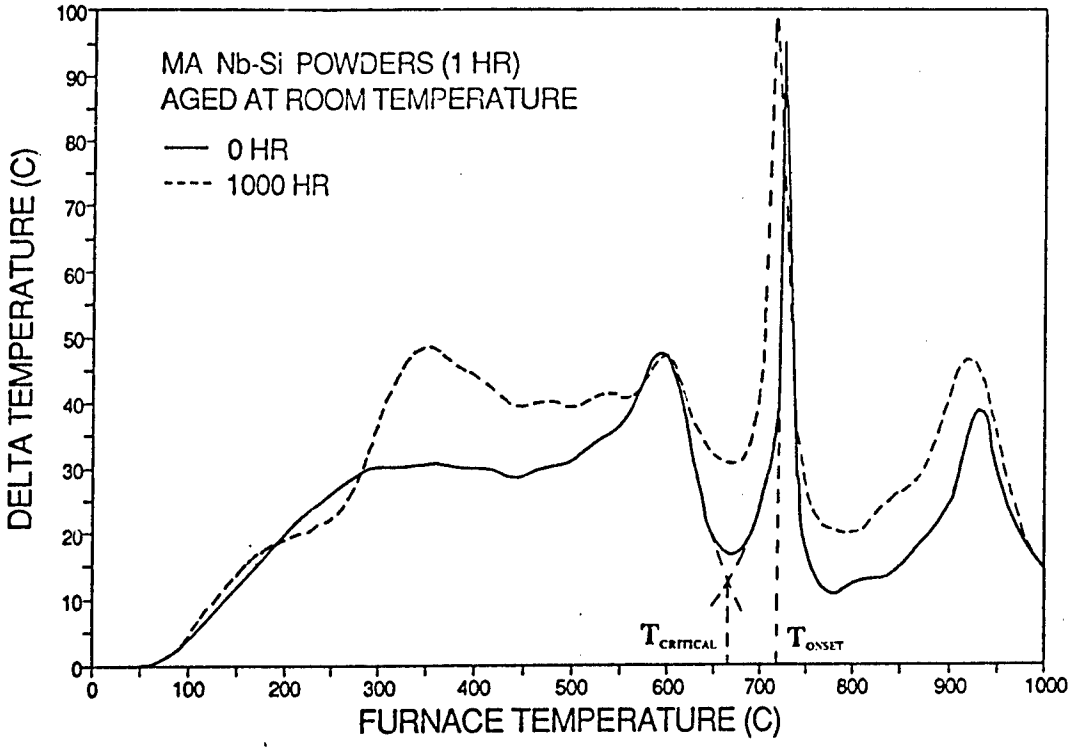

Figure 3. DTA trace of MA Nb-Si powders (1 hr) aged at RT

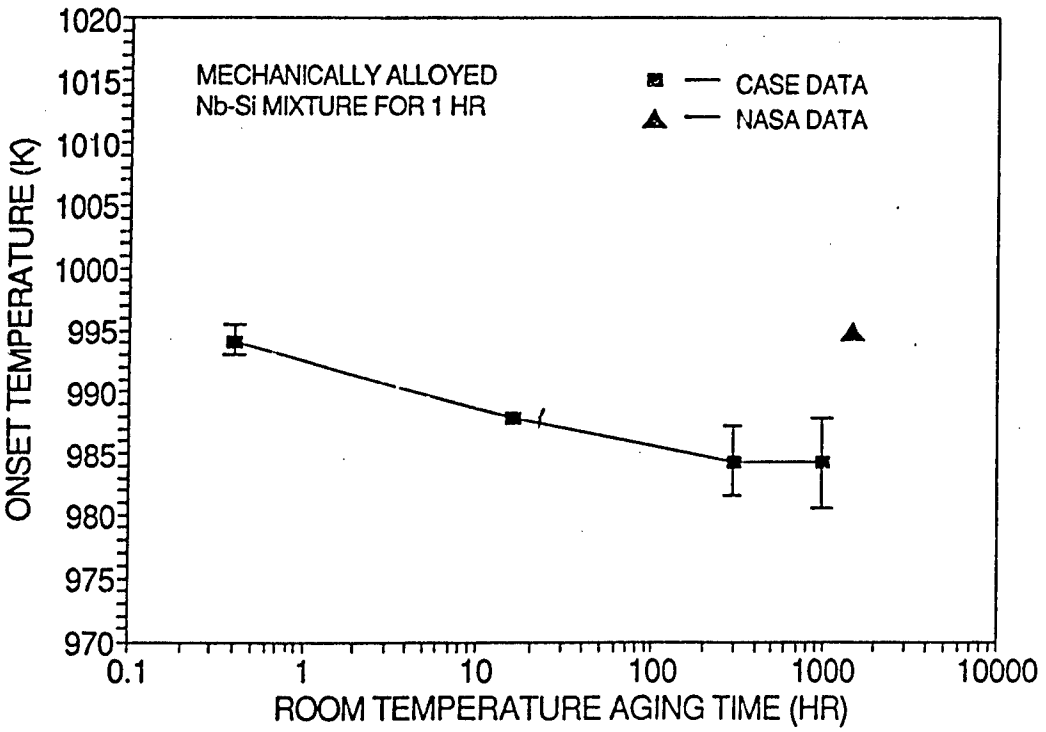

Figure 4. Reaction onset temperature vs. aging time at RT

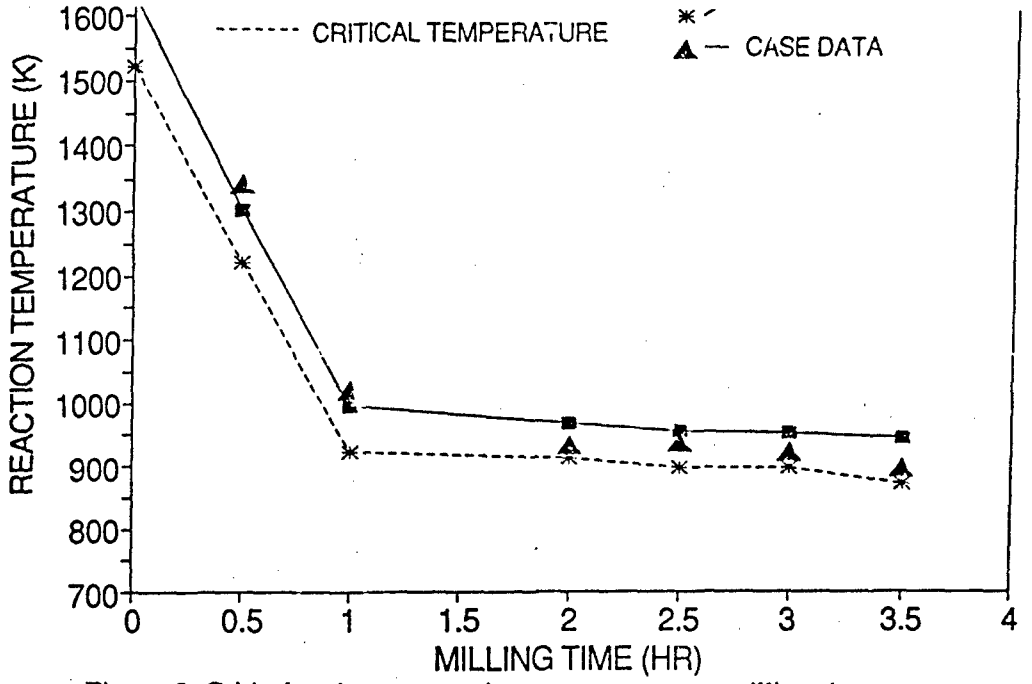

Figure 5. Critical and onset reaction temperature vs. milling time

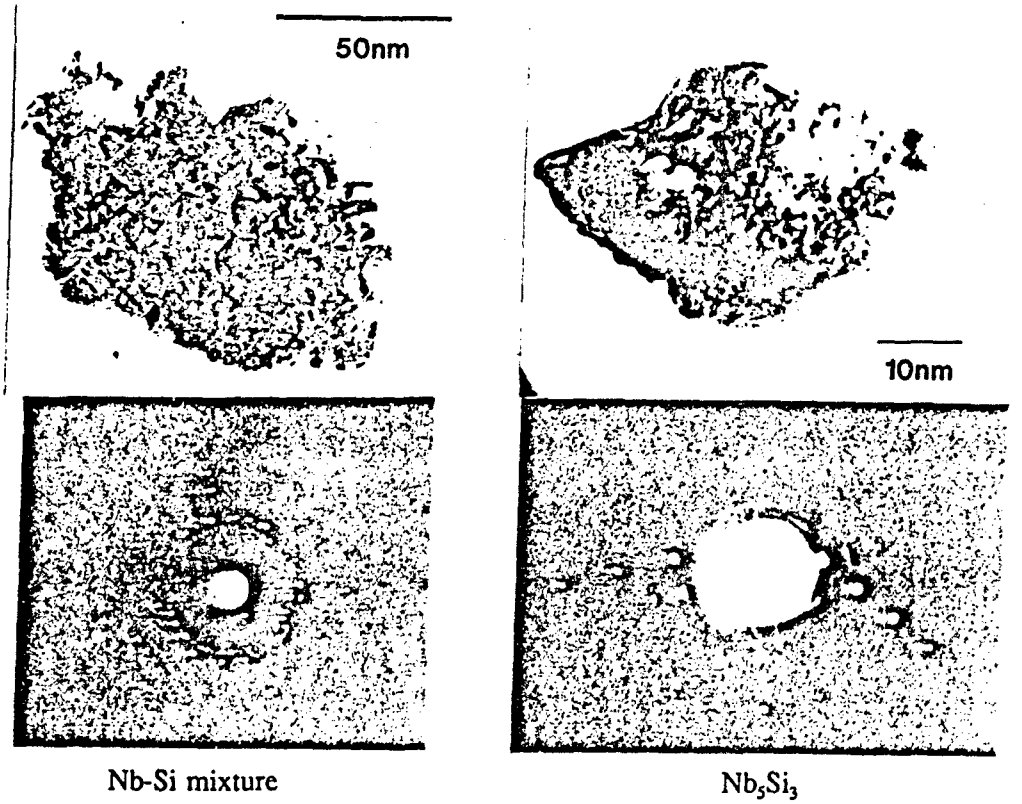

Figure 6. TEM micrograph and diffraction of MA Nb-Si mixture (1 hr)

Environmental Effects on Ductile-Phase Toughening in Nb_5Si_3-Nb Composites

Joseph D. Rigney, Preet M. Singh, and John J. Lewandowski

A variety of materials have been toughened via the addition of a ductile phase. Brittle silicide intermetallics such as Nb_5Si_3 have been significantly toughened by niobium particles incorporated during in-situ processing techniques. In the work described here, toughness tests conducted on Nb_5Si_3-Nb were monitored in a scanning electron microscope to view the process of toughening provided by the niobium particles. In particular, the behavior of the ductile phase was monitored and related to the toughness obtained. In an attempt to vary the behavior of the ductile phase, the composite materials were exposed to a variety of gaseous environments and subsequently tested in air. The resulting toughness, resistance-curve behavior, and in-situ results highlight the importance of the behavior of the ductile phase on subsequent properties.

INTRODUCTION

Silicides and silicide-based composites provide a number of attractive features for potential high-temperature service.[1-5] The 5:3 transition-metal silicides in particular are attractive since they have higher melting temperatures and lower densities than many of the other intermetallic compounds with different crystal structures.[6] Some of these materials (those based on Zr, Nb, Mo, Hf, Ta, W, and Re) have melting temperatures in the range of 2,200 K to 2,800 K. These transition-metal silicides are extremely stable, existing as line compounds or over only a limited range of stoichiometry.[7,8] Of the transition-metal 5:3 silicides, Nb_5Si_3 has the highest melting temperature (2,757 K) of those with densities below that of the nickel-based superalloys (Figure 1). The Nb-Si system has been of recent interest[1-5] as a model experimental system to study the mechanical behavior of in-situ composites and the concept of ductile-phase toughening, because Nb_5Si_3 exhibits a low value of fracture toughness (1–3 MPa$\sqrt{m}$) and inadequate ambient ductility at room temperature.[4,9,10]

Improving the fracture toughness of the silicide can be accomplished through reaction synthesis,[10] where niobium is incorporated into a niobium-silicide matrix, or via lamination,[10] while in-situ composites may be studied by selecting alloys from the niobium-rich end of the Nb-Si binary phase diagram[2,7] (i.e., Nb-10 at.% Si or Nb-15 at.% Si), as pictured in Figure 2. Processing materials in this region will precipitate niobium particles in the Nb_5Si_3 matrix. Vacuum arc casting followed by extrusion and heat treatment has incorporated elongated primary and secondary ductile, refractory niobium solid solution (~0.8 at.% Si) particles within a Nb_5Si_3 matrix.[3] The silicide and refractory metal are virtually immiscible[2] up to 1,943 K and differ in coefficient of thermal expansion by 1×10^{-6}/K, providing a degree of thermal (chemical) and mechanical compatibility in these composites to high temperatures. The only other 5:3 transition-metal silicides that exist in equilibrium with their terminal refractory metal phase are Re_5Si_3/Re and W_5Si_3/W; however, these silicides have higher densities and lower melting temperatures than Nb_5Si_3. The in-situ-formed Nb_5Si_3/Nb composite system produced during solidification is thus an ideal model system for studying factors influencing toughness in these materials systems and is a reasonable base alloy system for further development.

The incorporation of niobium particles into the silicide matrix has increased the room-temperature fracture toughness of Nb_5Si_3[1-4] to values exceeding 25 MPa$\sqrt{m}$, and resistance-curve behavior has also been reported in these systems.[11] Other brittle-matrix systems have been toughened by a dispersed ductile phase, such as Al_2O_3/Al,[12,13] TiAl/(Nb or NbTi),[14] $MoSi_2$/Ta,[15] and $MoSi_2$/Nb,[16,17] in addition to model systems such as glass/Pb[18,19] and glass/(Al or Ni).[20]

Several analyses have proposed that ductile-phase toughening is accomplished via ductile bridging of intact ligaments behind the crack tip along the fracture plane (see Figure 3).[18-22] The degree of toughening depicted by these analyses depends primarily on the stress-strain behavior or χ-function of the ductile ligament with the constraint imposed by the surrounding elastic matrix. The degree of matrix-ductile phase debonding will affect the stress-strain behavior of the ligament. Toughening is also proposed to be related to the size (a_0) and area fraction (V_f) of the ligaments in the fracture plane as well as the uniaxial yield strength (σ_0) of the ligaments. These dependencies are depicted in the following relation:[18-22]

$$\Delta G = V_f \cdot \chi \cdot \sigma_0 \cdot a_0$$

Recent work[10,11] has begun to measure the extent of bridging and its effects on resultant resistance (R)-curve behavior in the Nb_5Si_3/Nb systems.

Although it has been previously demonstrated that incorporation of "ductile" particles is effective in enhancing toughness, a variety of factors may affect the ductility of a body-centered cubic phase used for such toughening. In particular, little work has investigated the effects of interstitial elements on such processes. One way to examine such effects is to study the room-temperature fracture behavior after exposure to high-temperature gaseous environments.

It is possible that exposure to air, or the major components of air (i.e., oxygen and nitrogen) and hydrogen, may affect the yield and fracture strengths and ductility of the "ductile" phase, thereby affecting the magnitude of toughening. Although some

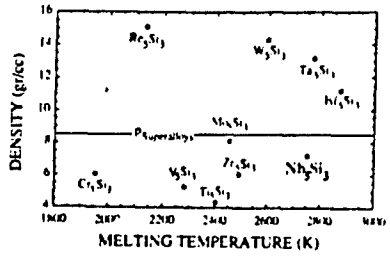

Figure 1. Density vs. melting temperature for 5:3 transition-metal silicides.

The work reported here is part of a larger effort undertaken to investigate the behavior of the ductile phase in such systems in order to provide insight into the factors affecting toughness in other brittle/ductile systems. In particular, the development of bridged zones and the resistance curve in Nb_5Si_3/Nb composites has been quantified by monitoring in-situ fracture studies. These results have then been compared to the room-temperature fracture behavior of samples simply exposed to air, oxygen, nitrogen, or hydrogen at temperatures up to 873 K to document the effect of these exposures on the mechanical behavior of the niobium in in-situ composite systems.

EXPERIMENTAL PROCEDURES

The materials investigated were initially vacuum arc-cast with a composition of Nb-10 at.% Si or Nb-15 at.% Si (Westinghouse, Pittsburgh, Pennsylvania). Secondary processing—such as hot extrusion (in molybdenum cans at 5.5:1 and 1,923 K by Wright-Patterson Air Force Base, Dayton, Ohio) and vacuum heat treatment (1,773 K for 100 h)—was utilized to change the morphology and fracture behavior of the primary and secondary niobium contained within the Nb_5Si_3 matrix. Notched three-point bend bars were then machined from the extrusions such that the notch was perpendicular to the extrusion direction while testing was conducted in accordance with standard testing procedures.[24] The sides of the samples were polished to a 1 μm finish to facilitate fracture monitoring via optical or scanning electron microscopy (SEM) techniques.

Mechanical tests on the three-point bend specimens were conducted at a load point displacement rate of 1 μm/s on a JEOL 840A scanning electron microscope equipped with an Oxford Instruments deformation stage. The deformation stage may be operated in tension, compression, or bending and provides a range of loading rates in addition to real-time monitoring of load, displacement, and crack length. The polished sample surfaces were oriented perpendicular to the electron beam so that surface cracking events could be monitored. Computer-aided data acquisition was used to record load versus time traces for the various tests that were conducted, and the data were later converted to load-load point displacement (LPD) traces. The loads (P_Q) at which initial and subsequent cracking events were observed were used in the following equation[24] to determine the initiation toughness of the sample as well as R-curve behavior. (Variables are defined above.)

$$K_Q = \left(\frac{P_Q S}{BW^{3/2}}\right) \cdot f\left(\frac{a}{W}\right)$$

Post-failure analysis consisted of SEM examination of the fracture surfaces in locations neighboring the notch tip in order to observe the fracture behavior of the niobium.

Environmental exposure to air, N_2, O_2, and H_2 was conducted in either a tube furnace or a Cahn 3000 microbalance under 1 atm pressure of the gases. Heat-treatment schedules were kept the same at 873 K for 4 h except for additional exposures to H_2 at 473 K and 673 K. Samples were exposed at 873 K, as this temperature is close to the temperature that gives maximum weight gain for niobium in an oxygen environment.[25] Vickers microhardness indentations with 10 g loads for 15 s were additionally made on the unexposed and exposed samples to try to detect differences in mechanical response.

MECHANICAL BEHAVIOR

Figure 4 shows the typical appearance of the extruded and heat-treated Nb_5Si_3/Nb composites taken in three orientations; the orientation of the notched three-point bend specimen with respect to the microstructure is also shown. In the Nb-10 at.% Si material, the large primary niobium particles occupy ~51 vol.%, while the continuous phase is the Nb_5Si_3 + Nb eutectoid microconstituent. In the case of Nb-15 at.% Si, the silicide Nb_5Si_3 occupies ~20 vol.%.

In-Situ Testing

Figure 5a shows a typical load-LPD trace obtained during in-situ fracture toughness testing of Nb-10 at.% Si composite samples and the corresponding K versus Δa plots in Figure 5b. Figure 6 shows a sequence of photomicrographs of a well-developed crack at several points in the load-displacement trace with increasing load from 6a to 6d. In Figure 6a, bridging events are clearly visible in the microcrack "damage zone" in the Nb_5Si_3 extending over 300 μm ahead of the contiguous crack. With increasing load (Figure 6b), the microcrack damage zone intercepts a large niobium particle (light contrast), and then extends on the other side with an increase in load (Figure 6c). Significant deformation in this niobium particle is clearly visible; in Figure 6d, the deformation is so extensive that the particle has almost necked to a point. The bridged zone remains roughly constant with increasing load. After fracture, SEM micrographs

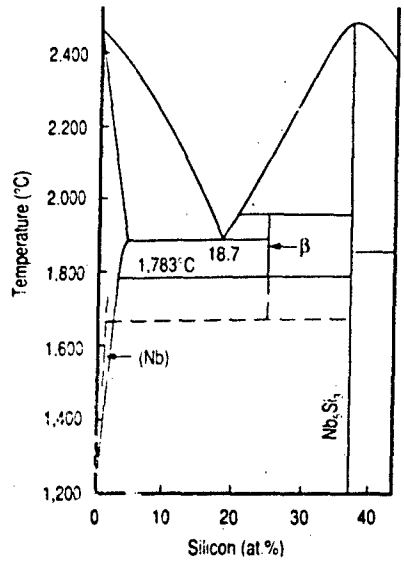

Figure 2. The relevant portion of the recently modified niobium-rich end of the Nb-Si phase diagram.[2]

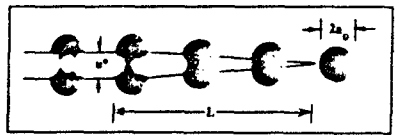

a

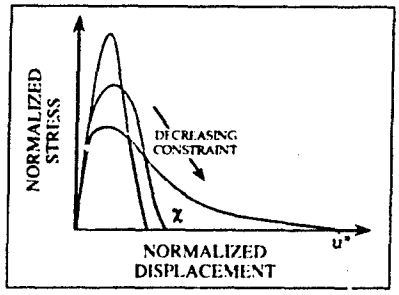

b

Figure 3. (a) A schematic view of the ductile-phase toughening phenomenon. (b) Normalized stress-strain curves depicting differences that result from constraint changes in the particles.[16,22]

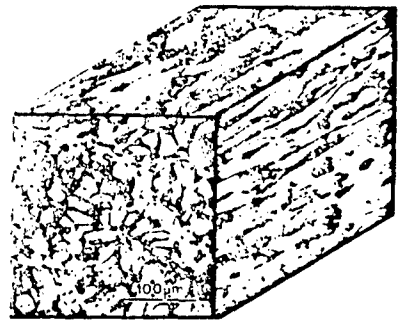

a

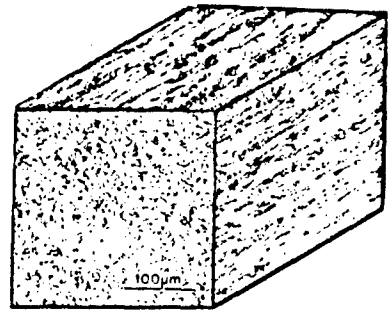

b

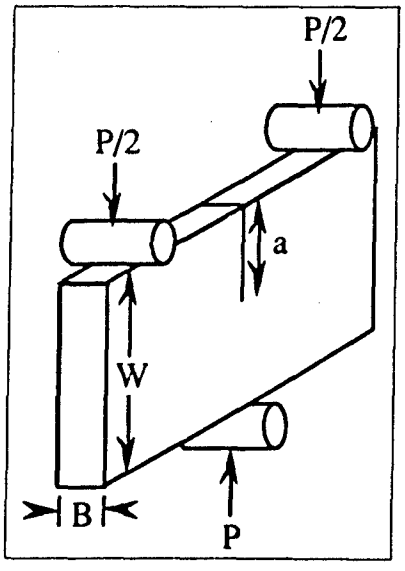

c

Figure 4. Microstructures of the arc-cast, extruded, and heat treated (a) Nb-10 at.% Si and (b) Nb-15 at.% Si composites. The light phase is the niobium and the darker phase is the Nb_5Si_3. (c) The orientation of the mechanical testing with respect to the microstructures shown.

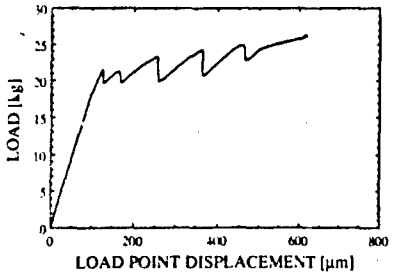

a

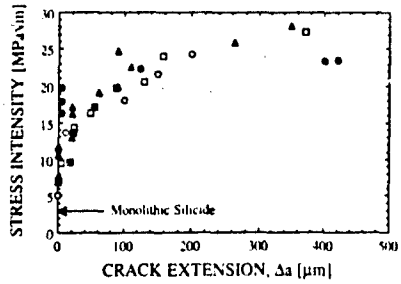

b

Figure 5. (a) Typical load-load point displacement traces from the three-point bend mechanical tests. (b) The corresponding stress intensity (K) vs. crack extension (Δa) plots for Nb-10 at.% Si.

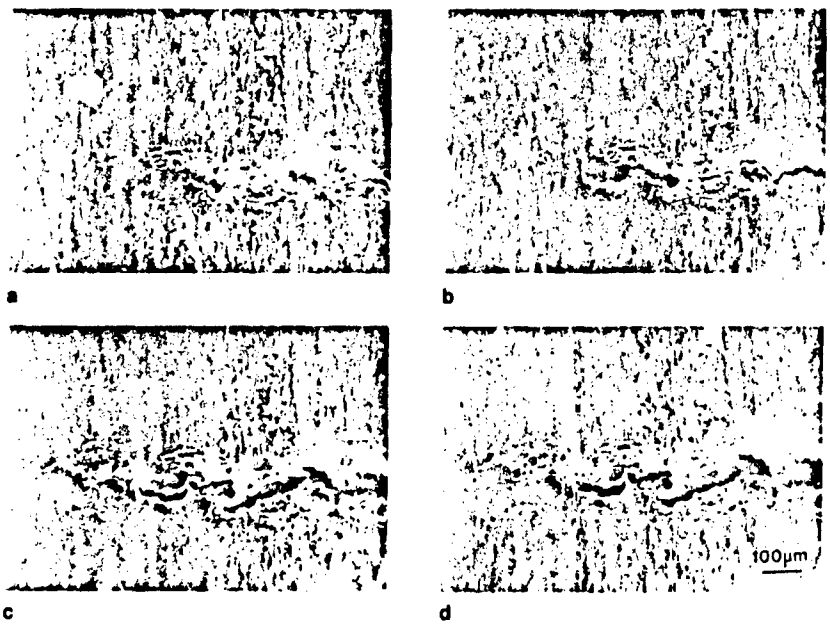

a b c d

Figure 6. (a–d) A sequence of micrographs showing the effects of increasing load and load displacement obtained from in-situ testing a Nb-10 at.% Si composite in the SEM.

were taken of the fracture surface in areas ahead of the notch within the rising portion of the resistance curve. The niobium was observed to behave in a ductile manner (Figure 7), stretching to a point at several locations. This ductility contributes to the resistance-curve behavior and the high peak toughness detected in the Nb_5Si_3/Nb composites.

Exposure to Air

Figures 8 and 9 show the results of in-situ SEM bend testing after exposure to air at 873 K for 4 h and removal of the white oxide scale from the surface and polishing to a 1 μm finish. These results are clearly different from that found in the unexposed material shown in Figures 5 and 6. Although cracks are observed to initiate at approximately the same values and grow stably, the rise in the resistance curve is significantly shallower than the unexposed material, and the sample catastrophically fractured at 19 MPa$\sqrt{m}$, at about one-half the stress intensity measured prior to air exposure. In Figure 9, a sequence of photographs of a crack propagating from the notch is shown with increasing load from Figure 9a to 9d. In contrast to Figure 6, the crack is planar (i.e., minimal damage zone) and the niobium is clearly behaving in a macroscopically brittle fashion, although some deformation is evident at the tip of the crack.

It is clear that exposure to air at 873 K has significantly reduced the toughness of the Nb-15 at.% Si composite, although the resulting toughness is still significantly in excess of the monolithic silicide. The niobium has been embrittled, at least at the surface of the sample, causing fracture before significant macroscopic deformation can take place. It was summarized above that changes in the stress-strain response of the niobium can affect the resulting toughnesses dictated by the ductile-phase toughening phenomenon. In the unexposed case, the niobium can deform extensively without fracture. However, lower toughness is obtained after air exposure as fracture precedes significant deformation.

Nitrogen Exposure

Both composite types were exposed in their as-notched condition to N_2 at 873 K for 4 h and subsequently tested at room temperature on the SEM bend stage. Samples did not exhibit visible scaling or measurable weight gain during exposure. When tested, peak toughnesses were slightly higher than those found in the unexposed cases. Unlike the results after air exposure, fracture propagated with visible plasticity of the niobium and a microcrack process zone. Fracture surfaces were similar to those observed in the as-processed unexposed material (Figure 7).

Vickers indentations were made in niobium particles on the sample surfaces and in the bulk. Hardness values of the niobium on the surface were 265 ± 22.8 VHN, while those in the bulk were 167 ± 17.4 VHN; unexposed hardnesses were about 164 VHN. The surface was significantly hardened by nitrogen, while the bulk was unaffected.

From these results and observations of plasticity in the notch-tip regions, it is reasonable to suggest that the nitrogen has increased the yield strength without causing brittle fracture of the niobium, providing for a greater degree of toughening. The effect of solid solution strengthening of niobium with nitrogen has been previously observed.[26] These results indicate that nitrogen at these levels does not contribute to embrittlement of composites or a drop in toughness observed in the specimens given an air exposure at 873 K.

Oxygen Exposure

Samples were exposed to pure O_2 at 873 K for 0.5 h in either the notched or unnotched conditions, producing a surface oxide that was removed by polishing. Toughness tests indicated a lack of macroscopic ductility in the niobium accompanied by a drop in toughness to 20 MPa$\sqrt{m}$ for the Nb-10 at.% Si sample. Fracture surfaces (Figure 10) showed that the niobium in the center of the sample deformed in a ductile manner, as observed in the nonexposed cases. However, in areas near the surface (within ~30 μm) the niobium fractured in a brittle transgranular fashion, as shown in the schematic in Figure 11. A ring of transgranular fracture along the exposed surfaces of the specimen was exhibited, while microhardness indentations in these regions indicated that the niobium was hardened to 255 ± 37 VHN by oxygen dissolution to a depth roughly corresponding to the depth of the brittle fracture. The hardnesses in the bulk of the specimen remained unchanged and these areas fractured in a ductile manner.

To determine whether the decrease in toughness and stable crack growth resulted from this affected surface layer, an unnotched sample was exposed to 1 atm O_2 at a temperature of 873 K for 0.5 h. Fifty micrometers were then removed from each face and the specimen was then notched to the standard depth. The toughness of this sample was nearly identical to that exhibited by the unexposed specimen, and the fracture was ductile. Thus, the effect of the oxidation was found to be only on the exposed surface, and removal of the embrittled layer restored the original properties.

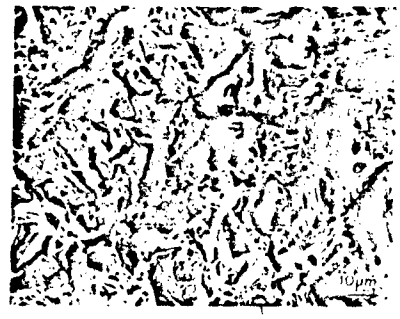

Figure 7. The fracture surface of Nb-10 at.% Si in the region of the rising resistance curve. Ductile stretching of the niobium is observed.

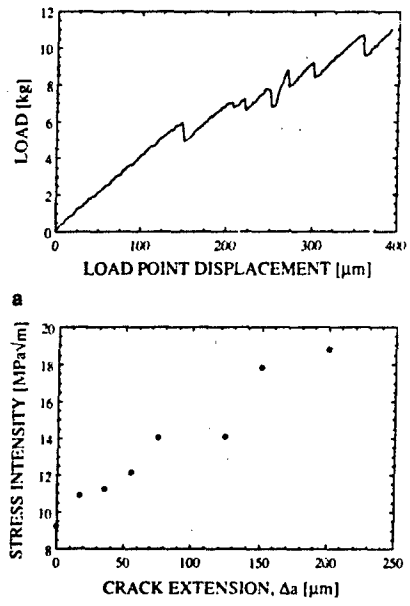

Figure 8. (a) The load-load point displacement trace obtained when testing an air-exposed (873 K, 4h) sample in the SEM bend stage. (b) The corresponding K-Δa curve obtained with the observation of stable crack growth on the outer surface (cf. Figure 9).

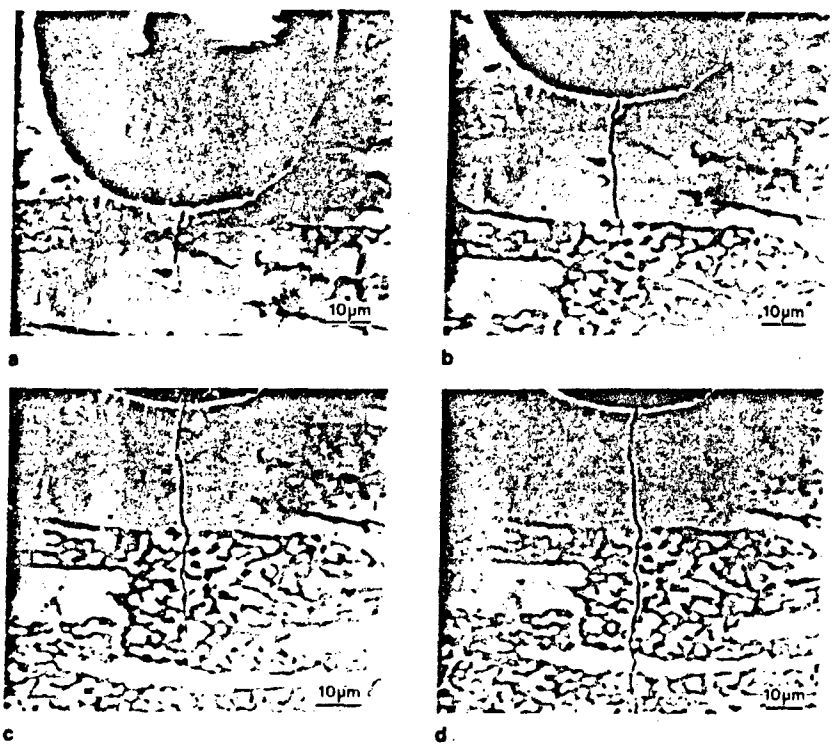

Figure 9. (a–d) A sequence of micrographs depicting the effects of increasing load and LPD on a crack extending from the notch in a sample exposed to air at 873 K for 4 h.

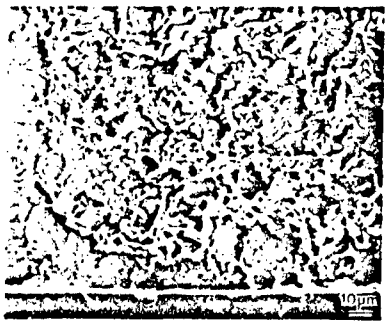

Figure 10. The fracture surface of the Nb-10 at.% Si samples exposed to oxygen for 0.5 h at 873 K. A surface layer has been embrittled by the oxidation.

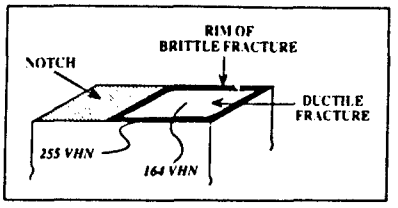

Figure 11. A schematic summarizing the fracture surface details and the hardnesses of the niobium in various positions on the oxidized samples.

Figure 13. A view of a crack initiated from a notch in a hydrogen-embrittled sample.

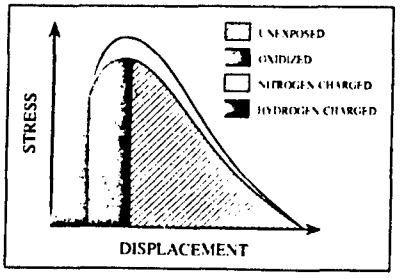

Figure 14. A schematic comparing the envisioned stress-strain diagrams for the unexposed and embrittled samples.

Table I. Room-Temperature Toughness of Nb-15 at.% Si Composites After Hydrogen Exposure

Temp. (K)	Nb-15 at.% Si	Nb-15 at.% Si After Bakeout*	Comments
473	24.7 MPa$\sqrt{m}$ (R-curve behavior)	—	No embrittlement
673	7.69 MPa$\sqrt{m}$ (Unstable crack growth)	Weight loss	Reversible embrittlement
873	5.65 MPa$\sqrt{m}$ (Unstable crack growth)	Weight loss (28.5 MPa$\sqrt{m}$)	Reversible embrittlement
Unexposed	24.5 MPa$\sqrt{m}$ (R-curve behavior)		

* 873 K, 4 h exposure.

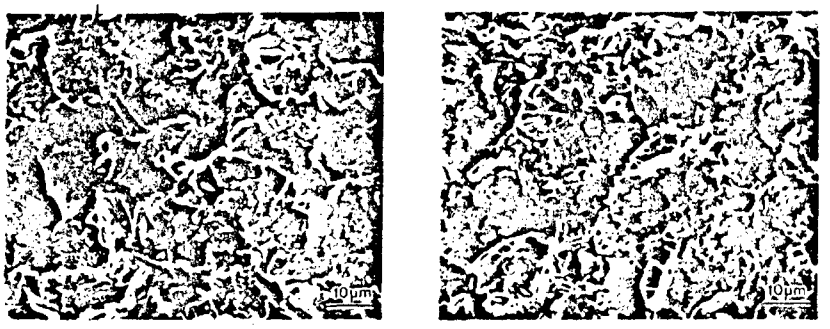

a b

Figure 12. The fracture surfaces of hydrogen-embrittled (a) Nb-10 at.% Si and (b) Nb-15 at.% Si showing transgranular fracture of the niobium.

Hydrogen Exposure

Samples of Nb-15 at.% Si were exposed to 1 atm of H_2 at different temperatures between 473 K and 873 K for 4 h and tested in the SEM bend stage. The results of the toughness tests and observations are presented in Table I. After charging at 673 K and above, fracture was often catastrophic, and the toughnesses were substantially decreased. The decrease in fracture resistance was accompanied by a change in fracture mode from ductile tearing to cleavage over the entire fracture surface (Figure 12). A crack that had initiated from a notch during in-situ testing is pictured in Figure 13. The crack is contained in one plane rather than in a "damage zone" as exhibited in the untreated case (cf. Figure 6). After exposure at 473 K, no embrittlement was observed, because the sample behaved as in the untreated case. Samples given a vacuum heat treatment after hydrogen charging similarly showed no embrittlement, indicative of the reversibility of the hydrogen embrittlement.

The drop in the toughness resulted from the brittle fracture of the niobium over the entire fracture surface. Unstable crack growth and low toughness were observed because the niobium was unable to deform significantly before fracture intervened.

CONCLUSIONS

It is clear that the niobium particles in Nb_5Si_3/Nb composites produce resistance-curve behavior and significantly increased toughness over that of Nb_5Si_3. As illustrated schematically in Figure 14, the niobium is able to stretch and deform prior to fracture, absorbing a large amount of energy (the large area beneath the stress-strain curve). Simple exposure to different gases at high temperatures and returning to room temperature clearly alters the mechanical behavior of the niobium, thereby altering the peak toughness. In the air- and oxygen-exposed cases, the toughnesses were decreased because brittle fracture of the niobium preceded extensive macroscopic deformation on the specimen surfaces, although resistance-curve behavior was exhibited due to the ductile behavior of the niobium in the remaining portions of the specimen. Figure 14 schematically presents the behavior of the niobium in the oxidized cases. Nitrogen exposure increased the hardness of the niobium without causing brittle fracture, while Figure 14 suggests that the net effect was a slight increase in energy absorbed via an increase in area underneath the stress-strain curve, leading to higher fracture toughnesses than in the unexposed cases. After hydrogen charging, all niobium in the structure fractured in a brittle manner with low toughness, suggesting a severe truncation of the stress-strain curve (Figure 14), thereby producing a low toughness.

This work highlights the importance of understanding the role of interstitial contaminants as well as the behavior of the "ductile" phase on the resulting properties. The limited work presented here clearly shows that the "ductile" phase is affected in different ways by high-temperature gaseous exposure. Additional work is necessary

to investigate the mechanism(s) responsible for embrittlement by oxygen and hydrogen, as well as the relatively benign effects of exposure to nitrogen. Such work highlights the continuing need to develop material systems more resistant to the interstitial contaminants and environments that may be present in processing and service.

References

1. D.L. Anton and D.M. Shaw, "High Temperature Ordered Compounds for Advanced Aero-Propulsion Applications," *High Temperature Ordered Intermetallic Alloys III* (Pittsburgh, PA: MRS, 1989), p. 361.
2. M.G. Mendiratta and D.M. Dimiduk, "Phase Relations and Transformation Kinetics in the High Nb Region of the Nb-Si System," *Scripta Met.*, 25 (1991), p. 237.
3. M.G. Mendiratta, J.J. Lewandowski, and D.M. Dimiduk, "Strength and Ductile-Phase Toughening in the Two-Phase Nb/Nb_5Si_3 Alloys," *Met. Trans. A*, 22A (1991), p. 1573.
4. J.J. Lewandoski, D. Dimiduk, W. Kerr, and M.G. Mendiratta, *High Temperature/High Performance Composites* (Pittsburgh, PA: MRS, 1988), p. 103.
5. R.L. Fleischer, "High-Strength, High Temperature Intermetallic Compounds," *J. Mater. Sci.*, 22 (1987), p. 2281.
6. R.L. Fleischer, "Selection of Intermetallic Compounds for High Temperature Mechanical Use," *Plasma Synthesis and Etching of Electronic Materials* (Pittsburgh, PA: MRS, 1985), p. 405.
7. T.B. Massalski, *Binary Alloy Phase Diagrams*, vols. 1 and 2 (Metals Park, OH: ASM, 1986).
8. G. Stauthoff, "Intermetallic Phases as High Temperature Materials," *Z. Metallkunde*, 77 (1986), p. 654.
9. J. Kajuch, unpublished research (1992).
10. J. Kajuch, J.D. Rigney, and J.J. Lewandowski, "Processing and Properties of Niobium Silicide (Nb_5Si_3) and Tough Nb_5Si_3/Nb Laminates," *Mater. Sci. Eng.*, in press (1992).
11. J.D. Rigney and J.J. Lewandowski, "In-Situ Monitoring of Fracture in Tough Silicide Composites," *Advanced Composite Materials* (Westerville, OH: American Ceramic Society, 1990), p. 519.
12. B.D. Flinn, M. Ruhle, and A.G. Evans, "Toughening of Composites of Al_2O_3 Reinforced with Al," *Acta Met.*, 37 (1989), p. 3001.
13. L.S. Sigl et al., "On the Toughness of Brittle Materials Reinforced with a Ductile Phase," *Acta Met.*, 36 (1988), p. 945.
14. H.C. Cao et al., "A Test Procedure for Characterizing the Toughening of Brittle Intermetallics by Ductile Reinforcement," *Acta Met.*, 37 (1989), p. 2969.
15. J.D. Rigney, R. Castro, and J.J. Lewandowski, "In-Situ Fracture Monitoring of Ductile-Phase Toughened Arc-Sprayed Molybdenum Disilicide-Tantalum Composites," *J. Mater. Sci.*, submitted (1992).
16. T.C. Liu et al., "Toughening of $MoSi_2$ with a Ductile (Niobium) Reinforcement," *Acta Met.*, 39 (1991), p. 1853.
17. L. Xiao et al., "Processing and Mechanical Properties of Niobium-Reinforced $MoSi_2$ Composites," *Mater. Sci. Eng.*, A144 (1991), p. 277.
18. M.F. Ashby, F.J. Blunt, and M. Bannister, "Flow Characteristics of Highly Constrained Metals Wires," *Acta Met.*, 37 (1989), p. 1847.
19. M. Bannister and M.F. Ashby, "The Deformation and Fracture of Constrained Metal Sheets," *Acta Met.*, 39 (1991), p. 2575.
20. V. Krstic and P.S. Nicholson, "Toughening of Glasses by Metal Particles," *J. Amer. Ceram. Soc.*, 64 (1981), p. 499.
21. B. Budianski, J.C. Amazigo, and A.G. Evans, "Small-Scale Bridging and the Fracture Toughness of Particulate-Reinforced Ceramics," *J. Mech. Phys. Solids*, 36 (1988), p. 167.
22. P.A. Mataga, "Deformation of Crack-Bridging Ductile Reinforcements in Toughened Brittle Materials," *Acta Met.*, 37 (1989), p. 3349.
23. D. Hardie and P. McIntyre, "The Low Temperature Embrittlement of Niobium and Vanadium by Both Dissolved and Precipitated Hydrogen," *Met. Trans. A*, 4A (1973), p. 1247.
24. "Standard Test Method for Plane Strain Fracture Toughness of Metallic Materials," E 399-83, *Annual Book of ASTM Standards*, vol. 03.01 (Philadelphia, PA: ASTM, 1988).
25. D.W. Bridges and W.M. Fassel, Jr., "High Pressure Oxidation of Niobium," *J. Electrochem. Soc.*, 103 (1956), p. 326.
26. H.W. Paxton and J.M. Seehan, "The Influence of Hydrogen and Nitrogen on Some Mechanical Properties of Niobium," (Pittsburgh, PA: Metals Research Laboratory, Carnegie Institute of Technology, 1957).

ACKNOWLEDGEMENTS

This work was supported in part by a graduate research assignment (JDR) at Wright R&D Center through the Air Force Office of Scientific Research (AFOSR)/ Graduate Student Research Program (AFOSR F49620-88-C-0053) with additional support (JDR, JJL) at Case Western Reserve (AFOSR 89-0508). We also acknowledge the help of Drs. M. Mendiratta (Universal Energy Systems) and D. Dimiduk (Wright-Patterson Air Force Base).

ABOUT THE AUTHORS

Joseph D. Rigney earned his M.S. in materials science and engineering at Case Western Reserve University in 1990. He is currently a graduate student at the same institution. Mr. Rigney is also a student member of TMS.

Preet M. Singh earned his Ph.D. in materials science and engineering at the University of Newcastle-upon-Tyne, United Kingdom, in 1989. He is currently a research associate at Case Western Reserve University. Dr. Singh is also a member of TMS.

John J. Lewandowski earned his Ph.D. in metallurgical engineering and materials science at Carnegie Mellon University in 1983. He is currently an associate professor at Case Western Reserve University. Dr. Lewandowski is also a member of TMS.

If you want more information on this subject, please circle reader service card number 54.

Strength and Ductile-Phase Toughening in the Two-Phase Nb/Nb_5Si_3 Alloys

MADAN G. MENDIRATTA, JOHN J. LEWANDOWSKI, and DENNIS M. DIMIDUK

The effect of heat treatment on the mechanical properties of Nb-Nb_5-Si_3 two-phase alloys having compositions Nb-10 and 16 pct Si (compositions quoted in atomic percent) has been investigated. This includes an evaluation of the strength, ductility, and toughness of as-cast and hot-extruded product forms. The two phases are thermochemically stable up to ~1670 °C, exhibit little coarsening up to 1500 °C, and are amenable to microstructural variations, which include changes in morphology and size. The measured mechanical properties and fractographic analysis indicate that in the extruded condition, the terminal Nb phase can provide significant toughening of the intermetallic Nb_5Si_3 matrix by plastic-stretching, interface-debonding, and crack-bridging mechanisms. It has been further shown that in these alloys, a high level of strength is retained up to 1400 °C.

I. INTRODUCTION

ADVANCES in aerospace technology are paced by the continuing search for light weight durable materials which retain their strength and stiffness at very high temperatures. There are a large number of intermetallic compounds, some of which have the potential for being developed into structural materials for service in turbine engines and hypersonic vehicles at temperatures from 1000 °C to 1600 °C.[1-4] Most of the intermetallics with high melting temperatures have complex, low-symmetry crystal structures which possess strong directional atomic bonds. It is generally believed that the strong bonding is responsible for retention of mechanical properties, such as high strength, stiffness, and creep resistance (due to low diffusivity) at high temperatures, and the compiled data on these materials have shown that these properties directly scale with melting temperature.[1] However, this same attribute often contributes to a lack of ductility and low fracture resistance at low temperatures. These compounds may be exploited for high-temperature structural use provided their low-temperature fracture resistance can be enhanced without compromising the attractive high-temperature properties.

The microstructural aspects of toughening and fracture have been treated in numerous studies of conventional multiphase metallic alloys, and the results have been summarized in a recent review article.[5] However, only limited research has been carried out on toughening mechanisms in brittle intermetallic compounds. Conventional approaches to intermetallics have employed appropriate alloying and thermomechanical processing to enhance toughness; an example of this is the toughening of titanium aluminide alloys.[6,7,8] The addition of brittle reinforcements which provide crack-deflection, crack-bridging, and pull-out toughening is an approach which is being explored in ceramic-matrix composites and may be exploited in the intermetallic systems. An example[9] of the latter material is the α_2-based titanium aluminide (Ti-24 at. pct Al-11 at. pct Nb) reinforced by continuous silicon carbide fibers (SCS-6). An additional possibility is to provide damage tolerance by the addition of a well-dispersed ductile phase in a brittle matrix. In general, this latter case may be achieved by "phase blending,"[10] provided that thermochemical stability is unimportant in the final product. However, for high-temperature structural use, thermochemical stability is an important consideration, and, therefore, composite systems whose components exhibit a high degree of inherent thermochemical stability (*e.g.*, stable *in situ* two-phase systems) are more suitable for long-term high-temperature applications. Among these systems, those with the highest phase stability temperatures and lowest lattice permeability will provide the greatest thermal resistance to chemical and morphological changes.

A number of systems consisting of brittle matrices have been investigated in which considerable toughening is achieved by incorporating ductile inclusions or binders. Some examples of these systems are Glass-Al,[11] WC-Co,[12] Al_2O_3-Al,[13] and TiAl-Nb.[10] In these systems, the plastic-stretching of the ductile particles which bridge advancing cracks in the brittle matrix reduces the crack tip stresses, thereby yielding an increment in toughness over that of the matrix. The challenge for designing these systems is the ability to predict the toughening increment for a set of ductile-phase properties. For this, the stress supported by the ductile phase must be known as a function of crack-opening displacement under the conditions of constraint provided by the composite matrix. Recent theoretical investigations have utilized three approaches to analyze the variation of nominal stress, $\sigma(u)$, carried by stretching particles with the crack-opening displacement, u. The three approaches[13]—the finite element method, the slip-line field analysis, and the Bridgeman analysis for necking—are complementary and have the following major assumptions: the particles are strongly bonded (*i.e.*, fully constrained by the surrounding elastic matrix) and fail by pure plastic rupture without interface decohesion. Within these approximations,

MADAN G. MENDIRATTA, Group Manager, Metals and Ceramics, is with the Materials Research Division, Universal Energy Systems, Inc., Dayton, OH 45432-1894. JOHN J. LEWANDOWSKI, Associate Professor, is with the Department of Materials Science and Engineering, Case Western Reserve University, Cleveland, OH 44106. DENNIS M. DIMIDUK, Group Leader, is with WRDC/MLLM, Materials Laboratory, Wright-Patterson AFB, OH 45433-6533.

Manuscript submitted March 28, 1990.

the toughening increment can then be calculated as the area under the $\sigma(u)$-u curve, with the maximum value of u being that for which the ductile particles rupture. However, recent experimental work by Ashby *et al.*[14] involving ductile lead wires constrained by thick-walled pyrex capillary tubing has shown that the assumptions involved in the above-mentioned analyses are not true and that a number of mechanisms contributed to the failure of the lead wires. These mechanisms strongly correlate with varying degree of constraint and, therefore, varying degree of toughening. They include internal void growth in the ductile lead wires, interface decohesion, and a combination of cracking the brittle matrix and interface decohesion. The toughness increased with increased propensity of interface debonding prior to the final failure of the lead wires.

The phase relationships within the Nb-Si system[15] indicate that this system offers the possibility of providing composite-like materials consisting of a refractory metal (*i.e.*, terminal Nb phase with Si in solid solution) and an intermetallic having a high melting temperature (*i.e.*, Nb_5Si_3 phase). Recent work on the microstructural evolution in the equilibrium (Nb + Nb_5Si_3) two-phase field has shown that the microstructures are thermochemically and morphologically stable (low coarsening rates) for times at least up to 100 hours at 1500 °C.[16,17] The present research is concerned with an investigation of the mechanical behavior of the two-phase Nb/Nb_5Si_3 alloys which may be best understood as discontinuously reinforced brittle matrix composites. Special emphasis has been put on the low-temperature toughness and high-temperature strength. It is shown that in this system, a range of microstructures can be produced through composition variation and various thermomechanical treatments. This system is much more complex than the model system comprised of glass encapsulated lead wires. This complexity is associated with solidification microstructures and slow kinetics of phase transformation, geometry/morphology of various microconstituents, and subtle metallurgical changes (recrystallization and silicide precipitation) which might occur in the terminal Nb phase.[16,17] Nevertheless, it is shown that under certain conditions, the Nb phase behaves in a ductile manner and provides considerable toughening of the silicide matrix. The fracture mechanisms are documented through extensive scanning electron microscopy (SEM) fractography and are discussed in light of recent theoretical and experimental research on the concept of ductile-phase toughening of brittle matrices.

II. EXPERIMENTAL PROCEDURE

Two hypoeutectic compositions, Nb-10Si and Nb-16Si (all compositions are in atomic percent), were selected for the present investigation. For the Nb-10Si alloy, mechanical properties were measured in three conditions: (a) as-cast + heat-treated, (b) as-cast + hot-extruded, and (c) as-cast + hot-extruded + heat-treated condition; however, the Nb-16Si alloy was tested only in the as-cast + hot isostatically pressed (HIP) + heat-treated condition. Except for the hot extrusion, the alloys were prepared in the form of 250-g buttons which were cast employing triple nonconsumable arc-melting of elemental Nb machine turnings and elemental Si pellets. For the hot extrusion, a casting 6.35 cm in diameter × 13-cm long was prepared by consumable double AC arc-melting.*

*Procured from the Westinghouse Corporation, Pittsburgh, PA.

Vacuum fusion analysis was carried out on the castings to obtain the interstitial impurity content. The oxygen content varied from 0.02 to 0.03 wt pct, the nitrogen from 0.007 to 0.01 wt pct, and the carbon from 0.015 to 0.03 wt pct. The wet chemical analysis revealed Si content to be within 0.1 wt pct of the nominal, and spectrographic analysis revealed the presence only of trace amounts of metallic impurities, *i.e.*, total content less than 500 ppm by weight. The large casting of the Nb-10Si alloy was sealed in a 0.634-cm-thick Mo can; the can was heated to 1426 °C and extruded through dies maintained at 260 °C at a 4.5 : 1 extrusion ratio. The hot isostatic pressing of the 250-g buttons of the Nb-16Si alloy was carried out at 1700 °C/210 MPa/4 h without canning using commercial purity argon gas.

Samples machined from the buttons and the extrusion were wrapped in Ta foils (to minimize oxygen pick-up) and heat-treated in 10^{-6} torr vacuum at a temperature of 1500 °C for 100 hours. The temperature and time were chosen to ensure that the microstructure consisted of equilibrium Nb + Nb_5Si_3 phases.[17] The mechanical properties, *i.e.*, strength, ductility, and fracture toughness, were measured as a function of test temperature by performing bending tests in vacuum at a crosshead speed of 0.0254 cm/min. Bend strength was measured by performing four-point bending tests on bars having dimensions 3.175-cm long × 0.635-cm wide × 0.317-cm thick. The bars were machined using electrical discharge machining (EDM) and were polished to 600 grit finish on SiC paper prior to testing. The bending test also provided a qualitative indication of ductility. The fracture toughness, K_Q, was determined by three-point bend testing utilizing single-edge notch specimens at a crosshead speed of 0.0254 cm/min; this speed is in compliance with ASTM specification E-399. The bend bar dimensions for K_Q tests were 5.08-cm long × 1.25-cm wide × 0.953-cm thick, and the EDM notch dimensions were 0.254-cm deep × 0.02-cm root radius.

The microstructures were characterized mainly by SEM using the backscattered electron mode which provides contrast primarily dependent upon the atomic number and the proportion of elements present in a given phase. X-ray diffraction and quantitative electron probe microanalysis (EPMA) using ZAF iterative corrections were carried out to identify various phases. Finally, SEM fractography was carried out to characterize the fracture modes.

III. RESULTS

A. *Microstructures*

The phase relations, general microstructural evolution, and kinetics of phase transformation in a number of Nb-Si alloys (composition range: Nb-0.25 to 29Si) have been presented in recent publications[16,18] and are to be published in the near future.[17] In this paper, we

present results only on Nb-10Si and Nb-16Si; specifically, a description of the microstructural features pertinent to the mechanical properties. Figure 1 consists of SEM micrographs for the Nb-10Si alloy in the as-cast condition and after heat treatments at 1500 °C for 3 and 100 hours. As revealed by EPMA and X-ray diffraction, in the as-cast condition, the microstructure consists of large primary-Nb particles (bright phase) and a fine two-phase eutectic mixture of Nb_3Si (dark matrix) and Nb rods (bright phase). Thin-foil transmission electron microscopy (TEM) observations revealed that the large primary-Nb particles contained incoherent small particles (~0.5 μm) which were presumed to be silicide precipitates. This precipitation most likely occurred due to decreasing Si solubility in the terminal Nb phase with decreasing temperature. The backscattered SEM image of primary-Nb (Figure 1) shows a mottled dark contrast associated with the silicide precipitates. The presence of the Nb_3Si phase (instead of the equilibrium Nb_5Si_3 phase) indicates that the alloy is in metastable equilibrium in the as-solidified condition. After a 100-hour heat treatment at 1500 °C, the eutectic microstructure exhibited some coarsening (Figure 1(c)), with the Nb_3Si phase completely transforming to the equilibrium Nb_5Si_3 and Nb phases *via* a eutectoid transformation. The high magnification examination of the eutectoid microconstituent (Figure 2), revealed that the Nb_5Si_3 phase is the continuous matrix. Therefore, the overall composite equilibrium microstructure can be viewed as large dendritically formed Nb particles and small eutectically formed Nb particles uniformly distributed in the silicide matrix. For the 1500 °C/3 h heat treatment, the Nb particles in the eutectic mixture grew slightly; X-ray diffraction revealed the presence of intense Nb and Nb_3Si peaks (JCPDS Card #220763) and weak Nb_5Si_3 (JCPDS Card #30-874) peaks.

The microstructure of the Nb-16Si alloy in the as-cast + HIP + 1500 °C/100 h heat-treated condition was similar to that for the Nb-10Si alloy described above except for a difference in the relative volume fractions of the primary-Nb phase and the eutectoid microconstituent.

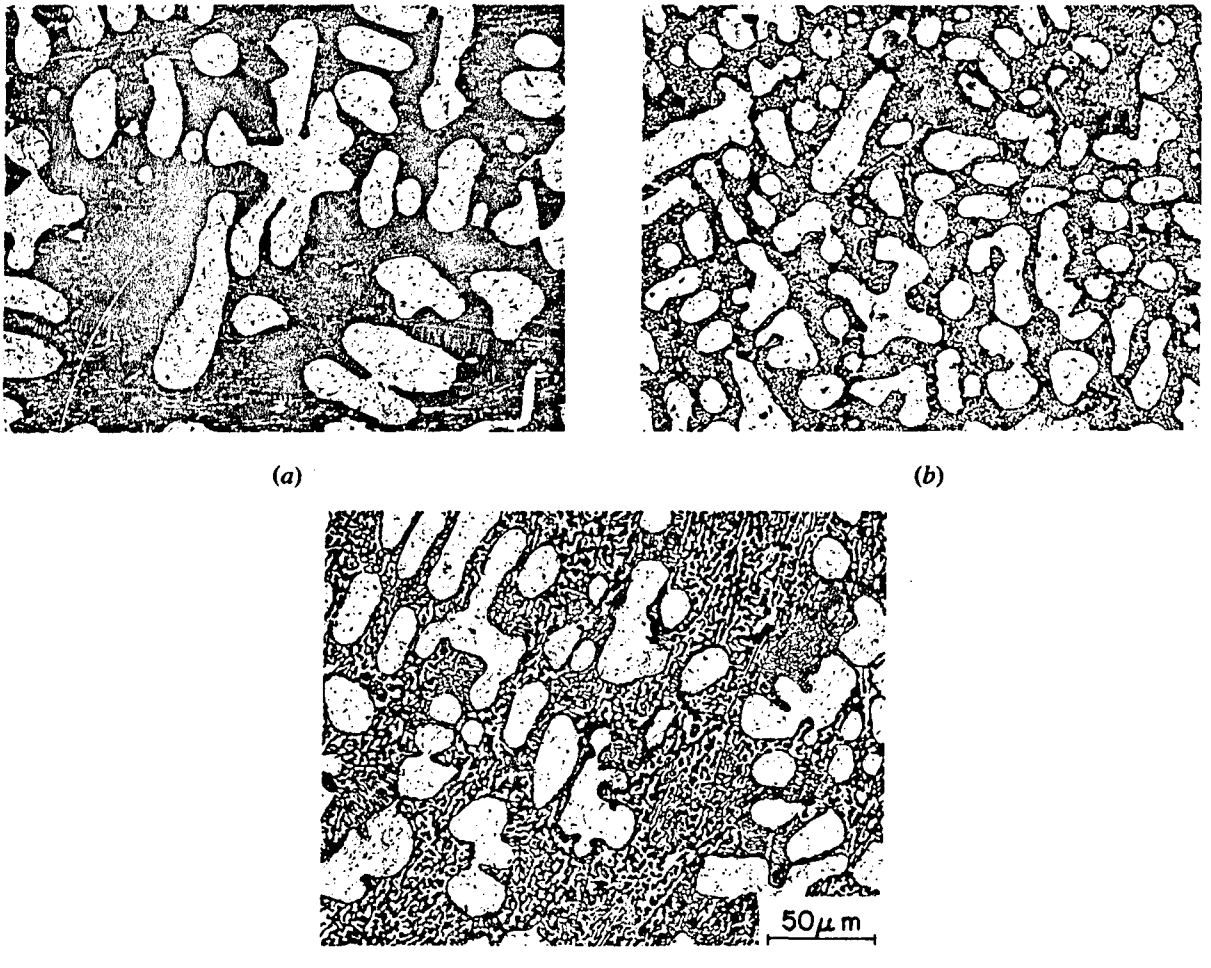

(a) (b) (c)

Fig. 1 — Microstructure in the cast Nb-10Si alloy: (*a*) as-cast; (*b*) 1500 °C/3 h; and (*c*) 1500 °C/100 h.

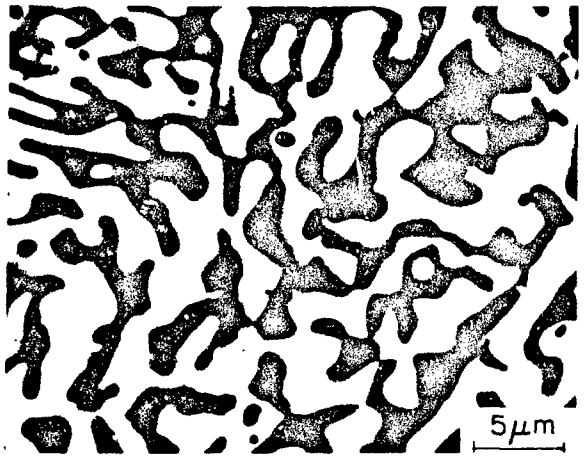

Fig. 2—Microstructure of the equilibrium eutectoid microconstituent (Nb_5Si_3 matrix containing secondary Nb-phase particles) in the as-cast + heat-treated (1500 °C/100 h) Nb-10Si.

Quantitative descriptions of the microstructural parameters (*i.e.*, volume fraction, size, *etc.*) for the two alloys are presented below.

In order to investigate the microstructures and properties of the wrought alloy, the Nb-10Si alloy was hot-extruded. Figures 3(a) and (b) are the SEM micrographs at respectively higher magnifications of the longitudinal section of the Nb-10Si alloy extruded at 1426 °C at an extrusion ratio of 4.5 : 1 and heat-treated at 1500 °C/100 h. It can be clearly seen that the primary-Nb particles are aligned in the extrusion direction. This microstructure should be compared to that of the as-cast + heat-treated Nb-10Si alloy (Figure 1(c)) which shows a distribution of the nonaligned large primary-Nb phase. The morphology of the smaller Nb particles in the eutectoid microconstituent with the Nb_5Si_3 matrix appears to be irregular in both the as-cast + heat-treated and as-cast + extruded + heat-treated conditions (Figures 2 and 4, respectively).

Statistical quantitative metallographic analysis[19] was carried out on a large number of SEM micrographs to quantify the microstructures in the Nb-10Si alloy in the as-cast + heat-treated, as-cast + extruded, and as-cast + extruded + heat-treated conditions. The determined microstructural parameters were (a) volume fractions of primary- and secondary-Nb phases, (b) size distribution of primary- and secondary-Nb phases, and (c) surface-to-surface interparticle spacing for primary-Nb particles along a planar front. The volume fractions were measured using a standard point-counting technique, and the size and interparticle spacing distributions were measured using a standard linear intercept analysis.[19] The volume fractions (within one standard deviation) and sizes are given in Table I, while the distribution of the surface to surface distance, λ, is plotted in Figure 5 for the Nb-10Si alloy in the three thermomechanical conditions. The measured volume fractions were found to be in close agreement (within the experimental error) with values calculated using the presently accepted Nb-Si phase diagram[15] by lever rule. For instance, the equilibrium volume fractions of the Nb and Nb_5Si_3 phases, as calculated

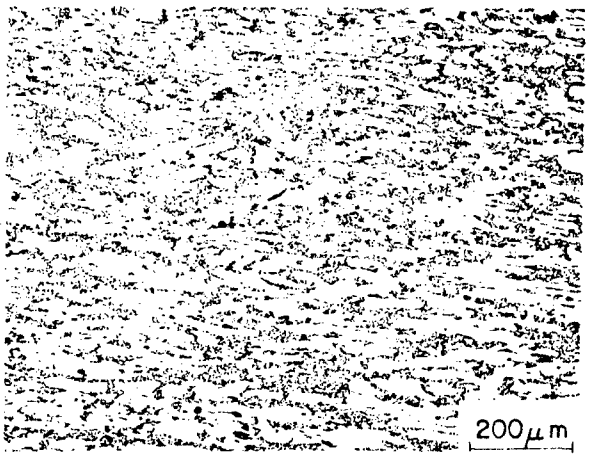

(*a*)

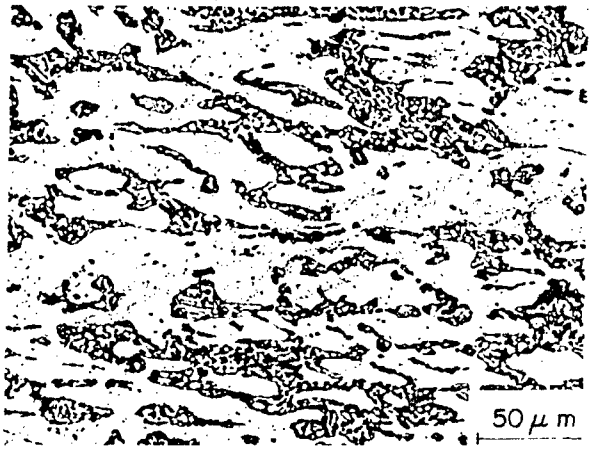

(*b*)

Fig. 3—(*a*) and (*b*) Microstructure of the longitudinal section of the extruded + heat-treated (1500 °C/100 h) Nb-10Si alloy. The primary Nb-phase particles are aligned parallel to the extrusion direction (horizontal in these micrographs).

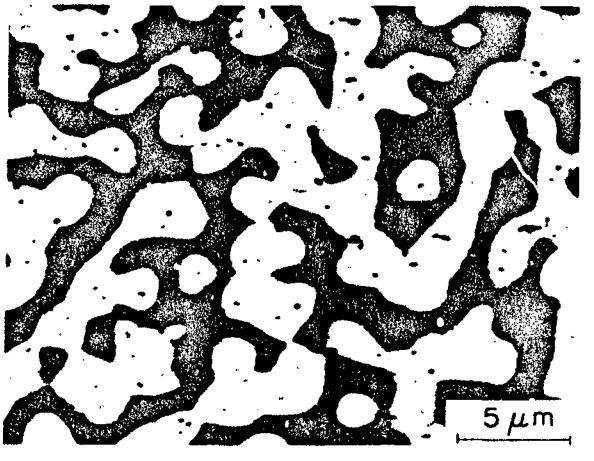

Fig. 4—Irregular morphology of the secondary-Nb particles within the Nb_5Si_3 matrix in the as-extruded + heat-treated (1500 °C/100 h) Nb-10Si alloy.

Table I. Volume Fraction and Size of Various Phases in Nb-Si Alloys

Alloy	Thermomechanical Condition	Volume Fraction ± σ			Size	
		Primary-Nb	Secondary-Nb	Silicide	Primary-Nb	Secondary-Nb
Nb-10Si	As-cast + 1500 °C/100 h	0.443 ± 0.08	0.279 ± 0.04	0.277 ± 0.04 (Nb_5Si_3)	dendrite arm length 20 to 150 μm, average cross-sectional diameter = 12.5 μm	length = 2 to 6 μm, average cross-sectional diameter = 1.33 μm
	As-cast + extruded	0.505 ± 0.08	0.173 ± 0.02	0.321 ± 0.02 (Nb_3Si)	aspect ratio = 5 to 10, average cross-sectional diameter = 12 μm	length = 2 to 8 μm, average cross-sectional diameter = 1 μm
	As-cast + extruded + 1500 °C/100 h	0.485 ± 0.05	0.274 ± 0.01	0.241 ± 0.01 (Nb_5Si_3)	aspect ratio = 5 to 10, average cross-sectional diameter = 15 μm	length = 15 to 20 μm, average cross-sectional diameter = 3.5 μm
Nb-16Si	As-cast + HIP + 1500 °C/100 h	0.246 ± 0.04	0.371 ± 0.03	0.383 ± 0.03	dendrite arm length 20 to 120 μm, average cross-sectional diameter = 10 μm	length = 1.5 to 5 μm, average cross-sectional diameter = 2 μm

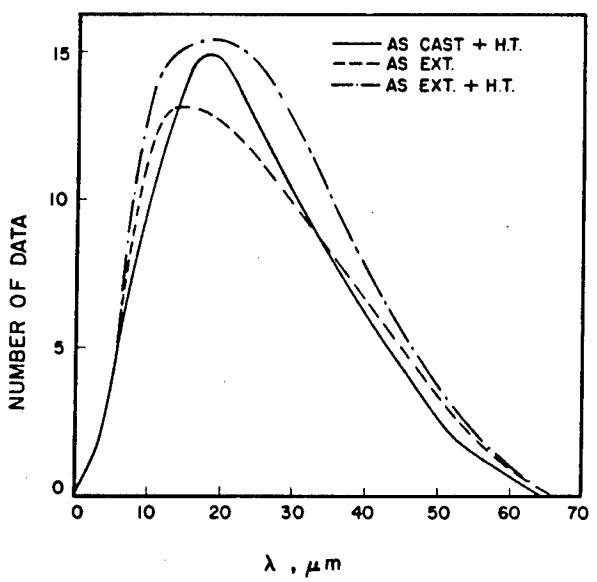

Fig. 5—Distribution of surface-to-surface interparticle spacing for primary-Nb particles in the Nb-10Si alloy for the three thermomechanical conditions.

using lever rule, are 0.758 and 0.242, respectively; these values compare well with the observed values for the cast + heat-treated (0.722 and 0.277) and extruded + heat treated (0.759 and 0.241) alloys. From Figure 5, it can be seen that there is little difference in the distribution curves for λ in the three thermomechanical conditions for the Nb-10Si alloy; the significance of this observation in the context of fracture behavior will be discussed later in this paper.

The microstructure of the HIP + heat-treated Nb-16Si alloy consisted of a low-volume fraction (~0.25) of large dendritically formed primary-Nb particles in a eutectoid matrix consisting of equilibrium Nb_5Si_3 matrix and small secondary-Nb particles. The size distributions of the two types of Nb particles was nearly similar to those for the as-cast + heat-treated Nb-10Si alloy, indicating that hot isostatic pressing at 1700 °C did not affect the microstructure significantly. This is in accord with the kinetic data[17] which exhibit extremely slow coarsening rates in alloys in the Nb-Si system.

B. *Mechanical Properties*

1. *Microhardness of the primary-Nb*

The present investigation indicated that in the Nb-10Si alloy, the primary-Nb plays an important role in the fracture process. Therefore, the microhardness as an approximate representation of the flow stress of the primary-Nb was determined in the as-cast + heat-treated, as-cast + extruded, and as-cast + extruded + heat-treated conditions. A Knoop diamond indentor was employed using a 10-g load on metallographically polished and etched samples. This indentation load was sufficiently small such that the Knoop impression was completely contained within the large Nb particles. Eight indentations were made for each condition. The microhardness values were 338 ± 41 (one standard deviation), 181 ± 14, and 161 ± 19 DPH, for the as-cast + heat-treated, as-cast + extruded, and as-cast + extruded + heat-treated conditions, respectively. These values clearly indicate that the extrusion process renders the primary-Nb much softer than its initial condition in the cast + heat-treated alloy. A reasonable estimate of the uniaxial yield strength of the Nb phase can be made from the hardness values using the following simple relationship: $\sigma_y = 0.8 \times 3$ DPH.[20] The estimated yield-strength values are 811,

434, and 386 MPa, respectively, for the three conditions. It should be mentioned here that as reported in a previous publication,[16] the room-temperature elastic-limit strength for the cast + heat-treated solid solution Nb-0.25Si alloy was measured in four-point bending to be ~560 MPa, while the room-temperature fracture strength of the as-cast + heat-treated Nb-1.25Si alloy (solid-solution Nb-Si matrix with silicide precipitates) was ~840 MPa; these values bracket the estimated strength of the primary-Nb phase in the present alloy for the cast + heat-treated condition.

2. *Bend Properties*

The smooth-bar four-point bending properties of the cast Nb-10Si alloy heat-treated to produce equilibrium Nb + Nb_5Si_3 phases (1500 °C/100 h; Figure 1) are presented in Figure 6, along with the properties in the as-cast + 1500 °C/3 h heat-treated condition. In this figure, the elastic limit strength is given by σ_E and implies the occurrence of some nonlinearity in the load-deflection curve (possibly due to plasticity or stable microcracking) during bending, while σ_F is the elastic fracture stress implying no nonlinearity (*i.e.*, no plasticity or stable microcracking). Data could not be obtained below 1000 °C for the cast alloy without the prolonged equilibrium heat treatment due to its extreme brittleness. After the long heat treatment, however, the elastic-fracture strength data were obtained down to room temperature and the brittle-to-ductile transition (as indicated by the nonlinearity in the load-deflection curve and the permanent curvature of the bend bars without surface microcracking) occurred at 1200 °C as compared to 1400 °C for the as-cast + 1500 °C/3 h condition. These minor improvements in bending properties are thought to be due to decreased Si content in the primary-Nb and due to some coarsening and an increased volume fraction of the Nb phase as a result of $Nb_3Si \rightarrow Nb_5Si_3$ + eutectoid transformation. It should be mentioned here that even though the alloy exhibited some ductility at 1200 °C after the prolonged heat treatment, this ductility was very small (<1 pct) and that with further temperature increase (*i.e.*, at 1400 °C), the ductility increase was not significant.

Alloys with a Si content higher than 10 at. pct contained numerous microcracks which occurred during cooling from the melt and, thus, precluded the possibility of obtaining meaningful bending test data. Therefore, the Nb-16Si alloy was HIP to weld shut internal cracks. Bend bars were machined from the HIP alloy, heat-treated at 1500 °C for 100 hours, and polished using a 5 μm Al_2O_3 polish. No microcracks were visible on the surfaces. The microstructure of the HIP + heat-treated Nb-16Si alloy consisted of a low-volume fraction of large primary-Nb particles (Table I) and a high-volume fraction of a fine eutectoid (Nb + Nb_5Si_3) microconstituent similar to that shown in Figure 1. Figure 7 shows the bend properties of the HIP + heat-treated Nb-16Si alloy. The alloy exhibited fracture strengths of ~483 MPa (70 ksi) at room temperature and ~400 MPa (58 ksi) at 1400 °C and a brittle-to-ductile transition at 1500 °C. The strength dropped rapidly above 1500 °C, having a value of ~124 MPa (18 ksi) at 1600 °C.

The bending properties of the extruded + 1500 °C/100 h heat-treated Nb-10Si alloy are presented in Figure 8. Data on the cast + 1500 °C/100 h heat-treated Nb-10Si alloy are also included in this figure for comparison. The extruded alloy exhibited a significant change in the bending properties as compared to the cast alloy. At room temperature, the extruded alloy fractured at a stress value of ~828 MPa (120 ksi) and also exhibited a slightly nonlinear load-deflection trace, indicating the occurrence of plasticity or stable microcracking. Above 1000 °C, the ductility of the extruded alloy increased significantly with temperature, as indicated by highly curved bend bars (at 1000 °C, the bend bar bottomed out without fracture; this corresponds to an outer fiber strain of ~6 pct).

The measured notch-toughness values, as a function of composition and processing/heat treatment, are given

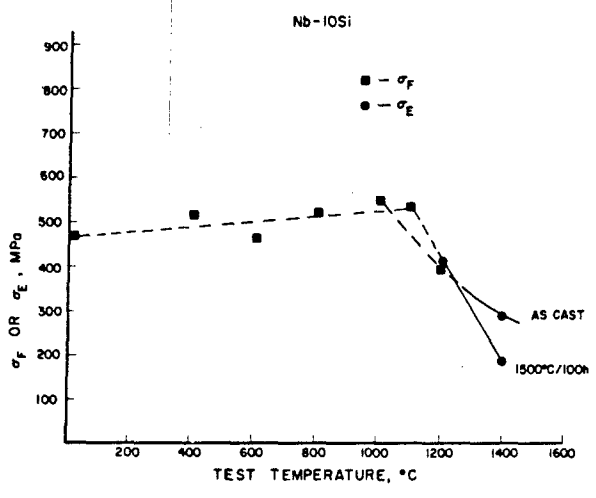

Fig. 6—Variations of bending strength with temperature for the Nb-10Si alloy in the as-cast + 1500 °C/100 h and as-cast + 1500 °C/3 h conditions. The term σ_F represents (premature) fracture strength with no nonlinearity in load-deflection curves, while σ_E represents proportional limit strength implying nonlinearity in load-deflection curves.

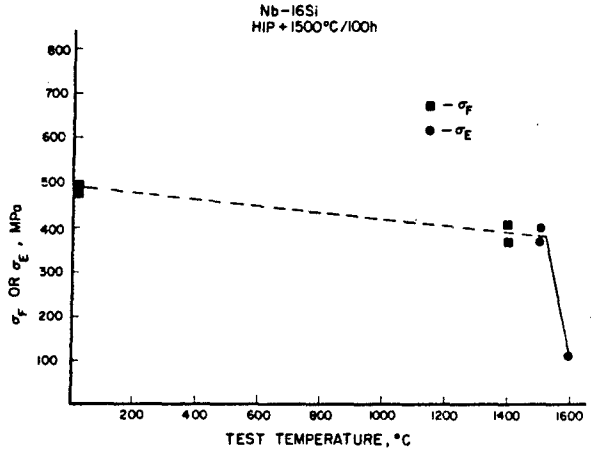

Fig. 7—Variation of bending strength with temperature for the Nb-16Si alloy in the HIP + heat-treated condition.

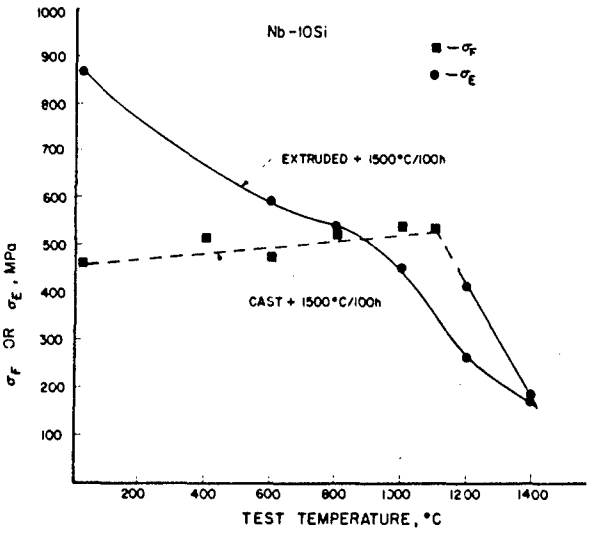

Fig. 8—Variation of bending strength with temperature for the extruded + heat-treated Nb-10Si alloy. Data on the cast + heat-treated Nb-10Si alloy are also shown for comparison.

in Table II. Since the ASTM specifications for fracture toughness testing (E-399) were not rigorously followed in the present investigation, the measured toughness values are denoted as K_Q. Most of the data are for tests conducted at room temperature; however, for the cast + heat-treated Nb-10Si alloy, tests were also carried out at 600 °C and 800 °C. It can be seen that for the cast Nb-10Si, the K_Q values appear to be independent of heat treatment and test temperature. As shown in Table II, the extruded Nb-10Si alloy exhibited a significant increase in toughness over that in the cast + heat-treated condition. Heat treatment of the extrusion further increased the toughness. For the toughness tests on the extruded alloy, the long direction of the bend bars was oriented parallel to the extrusion direction, with the notch plane and crack propagation direction perpendicular to the extrusion direction. This orientation ensures, at least macroscopically, that the crack-propagation plane is parallel to the cross-sectional planes of the elongated primary-Nb particles. The toughness values for the HIP + heat-treated Nb-16Si alloy were found to be slightly lower than those for the cast Nb-10Si alloy; this may be due to a smaller volume fraction of the dendritically formed primary-Nb particles (Table I) contributing to the toughening than in the cast + heat-treated Nb-10Si alloy.

Table II. Fracture Toughness, K_Q, as a Function of Composition, Processing, and Heat Treatment

Alloy	Processing/Heat Treatment	K_Q, MPa$\sqrt{m}$
Nb-10Si	as-cast	RT-9.5, 8.9*
	as-cast + 1500 °C/100 h	RT-9.67, 9.64
		600 °C-8.3
		800 °C-9.8
	extruded	RT-16.38, 16.5
	extruded + 1500 °C/100 h	RT-20.26, 21.06
Nb-16Si	as-cast	RT-5.4
	as-cast + 1500 °C/100 h	RT-7.56, 8.1, 6.4

*RT = room temperature.

C. *Fractographic Observations*

A detailed SEM fractographic analysis was carried out on bend bars fractured at room temperature as a function of composition and thermomechanical treatments. The purpose of the fractographic analysis was to examine the fracture modes in the different microconstituents in the two-phase composites, *i.e.*, in the Nb_5Si_3 matrix and in large primary-Nb as well as small secondary-Nb phase particles.

For the Nb-10Si alloy in the as-cast + 1500 °C/100 h heat-treated condition, the Nb_5Si_3 phase fractured in a brittle cleavage mode. However, the large primary-Nb particles exhibited a number of different modes. These included (a) cleavage, (b) extensive plastic-stretching, (c) plastic-stretching plus microvoid coalescence, and (d) Nb/Nb_5Si_3 interface decohesion. The large Nb particles marked by arrows in Figures 9(a) through (c) exhibit cleavage fracture, significant plastic-stretching, and plastic-stretching plus microvoid coalescence, respectively. Energy dispersive X-ray analysis during SEM examination confirmed that these were Nb-phase particles. The microvoids could have nucleated at the interface between the small silicide precipitates and the Nb matrix. Even though a variety of fracture modes was observed, the predominant mode was the cleavage mode (~90 pct of the fracture area). The fracture behavior of the small Nb particles in the Nb_5Si_3 matrix of the eutectoid microconstituent could not be established unambiguously. As shown in Figure 9(d), it appeared that the fracture process consisted of some plastic stretching (arrow A) and interface separation indicated by the presence of holes (arrow B).

As shown in Table II, a large increase in toughness was obtained in the as-extruded and as-extruded + heat-treated Nb-10Si alloy over that in the as-cast + heat-treated alloy. Concomitant with this improvement was a significant change in the fracture modes and fracture surface topology. In the as-extruded condition, a significant fraction of large Nb particles fractured after extensive plastic-stretching and cavity coalescence (Figure 10(a)). In the as-extruded + heat-treated condition, as shown in Figure 10(b), the large Nb particles plastically stretched to almost 100 pct reduction in area without cavitation before rupturing. In many instances, the plastic-stretching of the large Nb particles was associated with extensive decohesion of silicide-Nb interfaces. In addition, Figure 10(c) shows that almost all of the small Nb particles in the eutectoid matrix exhibited high ductility before fracture.

IV. DISCUSSION

In a model system comprised of lead wires constrained by glass, Ashby *et al.*[14] have shown that the constrained ductility of the lead wires is strongly dependent upon particular failure mechanisms and the degree of local constraint, even though the lead wires are highly ductile without the constraint. Those mechanisms (*i.e.*, including interface decohesion and glass matrix cracking) which

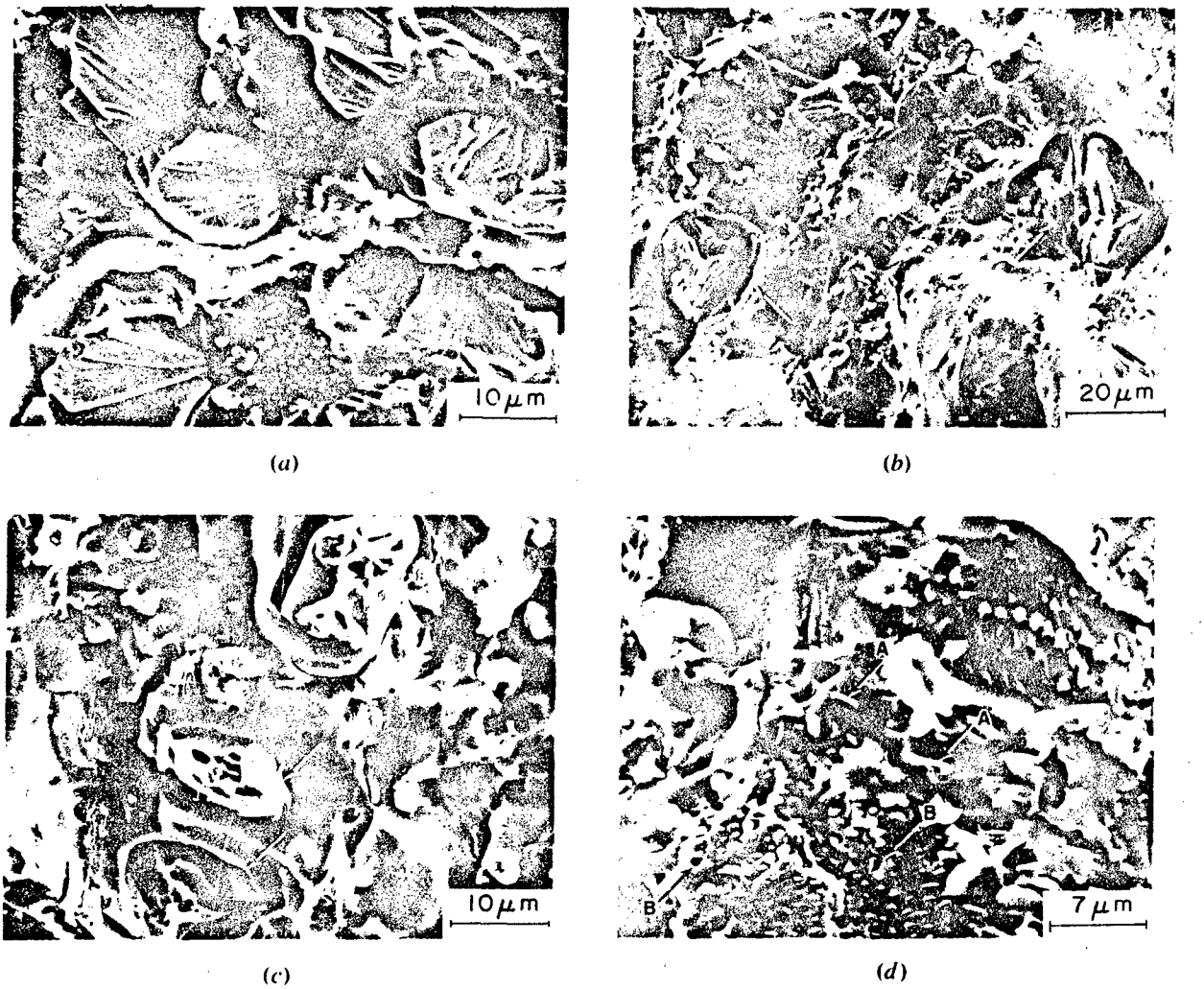

Fig. 9—Various room-temperature fracture modes of Nb phase exhibited in the as-cast + heat-treated Nb-10Si alloy: (*a*) cleavage; (*b*) plastic-stretching; and (*c*) plastic-stretching + microvoid coalescence in the primary-Nb phase. Figure 9(d) shows fracture behavior of secondary-Nb particles, including plastic-stretching and interface-debonding.

produce some magnitude of a "gage length," *i.e.*, an unconstrained volume of lead wires above and below the crack plane, lead to increased crack-opening displacement before fracture, thereby increasing the fracture toughness. Conversely, the absence of any interface decohesion or matrix cracking produces maximum constraint and results in only a small toughening increment. Thus, there are two fundamental requirements for toughness enhancement. The first is that the crack must be attracted to rather than bypass the inclusions which must be highly ductile without the constraint. Second, there must be some degree of interface decohesion (*i.e.*, constraint relaxation) between the brittle matrix and the ductile inclusions during the cracking and rupture processes. In addition, other factors also contribute to the toughness enhancement as given by the following equation:[13]

$$\Delta K_c = E\left[CV_f\frac{\sigma_0}{E}a_0\right]^{1/2} \qquad [1]$$

where ΔK_c = increment of toughness over that of matrix;
E = Young's modulus of the inclusions;
C = a parameter denoting the reciprocal of the degree of constraint (discussed above);
V_f = volume fraction of the inclusions (area fraction on metallographic samples);
σ_0 = uniaxial tensile yield strength of inclusion material; and
a_0 = radius of inclusions.

This relationship shows that the toughness increases with increasing E, V_f, σ_0, and a_0.

As mentioned earlier, the *in situ* Nb/Nb_5Si_3 composites are much more complex than the model composite described above. This complexity is, in part, due to the following factors. (a) The primary-Nb particles consist of two phases, a matrix of Nb with Si in solid solution and a dispersion of silicide precipitates. The effect of metallurgical changes, such as recovery/recrystallization

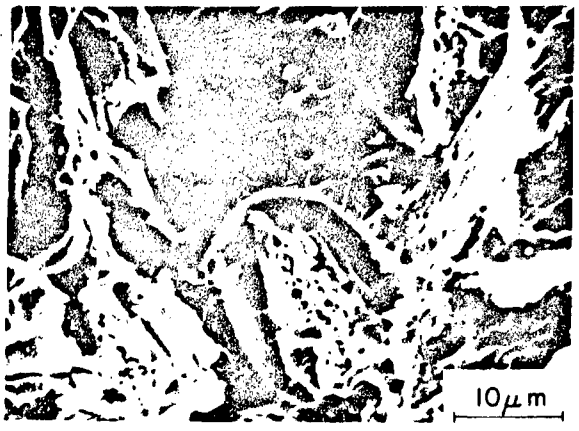

(a)

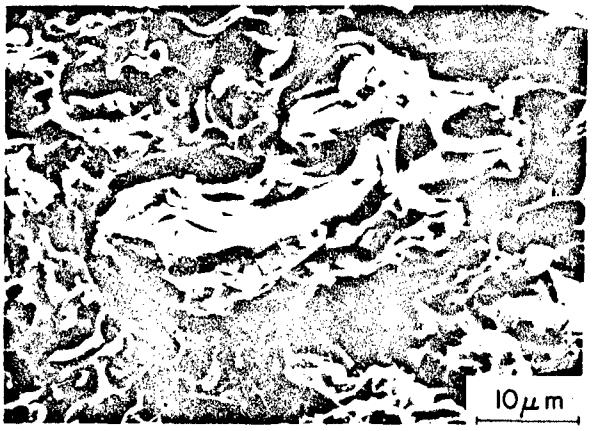

(b)

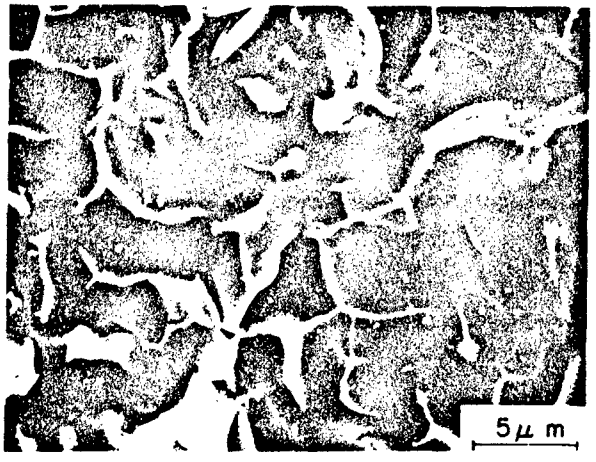

(c)

Fig. 10—(*a*) Extensive plastic-stretching and cavity coalescence of the primary-Nb contributing to the room-temperature fracture processes in the extruded Nb-10Si alloy; (*b*) extensive plastic-stretching and interface decohesion of the large primary-Nb particles of extruded + heat-treated Nb-10Si alloy; and (*c*) extensive plastic-stretching of secondary-Nb particles in the room-temperature fractured specimens of extruded + heat-treated Nb-10Si alloy.

of the matrix and volume fraction and size distribution of silicide precipitation, on the ductility and strength of primary-Nb is not known. This investigation is currently in progress.[17] (b) The geometry/morphology of the primary-Nb particles and eutectoid Nb-phase particles is quite complicated. The geometrical variations may be responsible for complex states of stress (which also include the residual stresses due to the thermal-expansion mismatch between Nb and Nb_5Si_3) in the composites which can affect the interface behavior during the crack propagation, *i.e.*, the degree of decohesion. In spite of these complexities, the fracture behavior of these composites can be discussed in terms of crack-bridging and/or ductile-phase-toughening concepts.

The major finding of the present work is that the fracture behavior of the Nb phase in the composites can be significantly altered by thermomechanical treatments. This change is accompanied by a change in fracture toughness. As compared to the as-cast + heat-treated condition, the Nb-10Si alloy in the extruded + heat-treated condition shows much lower brittle-to-ductile transition temperature (*i.e.*, room temperature *vs* 1200 °C; Figure 8), lower strength with temperature (Figure 8), and significantly higher fracture toughness (Table II). Table I shows that as expected, the volume fractions of the Nb phase in these conditions are similar, and as shown by Figure 5, the distributions of surface-to-surface distances between large Nb particles are also similar in the two conditions. This later distribution, to a first approximation, can be taken to represent the lengths of segments of a straight crack front which will move through the eutectoid microconstituent with silicide as the matrix. Therefore, these gross microstructural features are not responsible for the observed difference in the mechanical propensities in the two thermomechanical conditions. Rather, it is the changes in the behavior of primary-Nb which appear to govern the mechanical behavior.

particles in the as-cast + heat-treated Nb-10Si alloy are much harder (DPH = 338 ± 41) than nominally pure Nb (DPH ≈ 125). In addition, the bending tests on bulk solid solution Nb-0.25 Si and other Nb-Si solid-solution alloys have shown[16,18] that these alloys have very limited ductility at room temperature. It is hypothesized that fracture of the as-cast + heat-treated Nb-10Si alloy proceeds by a number of sequential events. Microcracks nucleate in the extremely brittle Nb_5Si_3 phase having a low fracture toughness.* During their extension, these microcracks interact with the small Nb particles which decohere and stretch; however, these interactions provide a negligible increment in toughness[14] due to the small size of the Nb particles. Further crack propagation involves interactions with large primary-Nb particles which are presumed to have a higher toughness than the silicide matrix. Even though a majority of Nb particles fracture in a brittle cleavage mode, formation of cleavage steps dissipates some energy of advancing cracks. Unpublished research[22] has shown that these composites exhibit a resistance curve behavior during stable crack propagation; this implies an occurrence of crack-bridging. In addition, a low, but not insignificant, number of large primary-Nb particles fracture after extensive plastic-stretching. In fact, the estimated fracture strain of the ductile particles is as high as a 75 to 100 pct reduction in area (*e.g.*, Figure 9(b)). All of the mechanisms enumerated above provide an increment of toughening, *i.e.*, 7 to 8 $MPa\sqrt{m}$, over that of the Nb_5Si_3 matrix.

*The toughness of the bulk, powder-processed Nb_5Si_3 has been determined[21] recently by the diamond hardness indentation technique. The values were between 1 and 2 $MPa\sqrt{m}$.

In contrast to the as-cast + heat-treated alloy, the extruded + heat-treated Nb-10Si alloy exhibited a high degree of ductile-phase toughening. The primary-Nb particles showed considerable softening (as determined by microhardness), and the fractographic observations indicated significant changes in the fracture modes. A very large fraction of large Nb particles fractured after extensive plastic-stretching and interface-debonding. The softness of the large Nb particles may blunt the advancing crack by local plastic flow. Further crack growth may occur by particle decohesion of the silicide/Nb interface which then provides a finite gage length for further plastic-stretching of Nb particles. The shape of the high aspect ratio Nb particles may be more conducive to interface separation (as opposed to highly irregularly shaped dendrites in the as-cast + heat-treated condition). The sequence consisting of crack-blunting, interface decohesion, and plastic-stretching can become self-sustaining, resulting in a high degree of toughening increment.

Equation [1] can be used to arrive at an estimate of the toughening increment in the case of extruded + heat-treated Nb-10Si alloy where significant ductile-phase toughening occurs. For this calculation, the value of E is taken to be ~105 GPa* for the solid solution Nb(Si) phase,[21] σ_0 is taken to be 386 MPa (calculated from the microhardness value), and volume fractions and particle toid Nb particles — are taken from data given in Table I. It is assumed that the toughening increment due to large Nb and small Nb particles is additive. The major uncertainty lies in the value of parameter C. In the experimental work on lead wires constrained by glass,[14] this parameter ranges from 1.6 (fully constrained condition) to 6 (for matrix cracking and extensive decohesion). This range may be system specific; nevertheless, it is used for the present case to obtain some idea of toughening increment. The calculated ΔK_c are 39 $MPa\sqrt{m}$ and 20 $MPa\sqrt{m}$ for C = 6 and 1.6, respectively. These values should be compared with the measured toughness of ~21 $MPa\sqrt{m}$ (Table II). Considering the number of assumptions involved in the derivation of Eq. [1] and the microstructural complexities in the alloy, the agreement between the calculated and experimentally measured toughening is reasonable (*i.e.*, within a factor of 2).

*This is an interpolated value from values for Nb-0.1 and Nb-2Si alloys measured by the dynamic ultrasonic technique.

The present fractographic data together with the toughness data are in qualitative accord with the ductile-phase toughening of brittle matrices. Quantification of the microstructural effects (*e.g.*, distribution and length of bridged ligaments in the crack wake) on the magnitude of toughening is presently continuing on specimens where fracture is being monitored *in situ*[22] using optical microscopy and SEM techniques.

V. SUMMARY AND CONCLUSIONS

This study has shown that for certain compositions and thermomechanical treatments, the Nb/Nb_5Si_3 composite system exhibits ductile-phase toughening at low temperatures and reasonable strength retention at high temperatures. Silicon has a pronounced effect on strength and ductility of these composites: strength increases and ductility decreases with increasing Si content in the Nb-10 to 16Si range. In the as-cast + heat-treated alloys, a high level of strength is retained in the temperature range of 1400 °C to 1600 °C, even though these alloys are totally brittle at temperatures below 1000 °C. Cast alloys with these compositions have a room-temperature toughness in the range of 6 to 9.6 $MPa\sqrt{m}$. Fractographic examination revealed that although the predominant fracture mode in both the silicide and Nb phases is cleavage, a number of Nb particles exhibit considerable plastic-stretching. Dramatic changes in the mechanical properties occur as a result of hot extrusion of the Nb-10Si alloy, showing a slight ductility even at room temperature and a toughness of ~21 $MPa\sqrt{m}$. The fractographic observations revealed that the dominant fracture mode of Nb particles changed from cleavage to extensive debonding and plastic-stretching. These observations are in qualitative accord with the recent theories on ductile-phase toughening of brittle matrices.

The most significant result of this study is that hot extrusion "ductilizes" the Nb phase. The reasons for this ductilizing have not yet been investigated and are the subject of continuing research.

ACKNOWLEDGMENTS

This work was supported by Air Force Contract No. F33615-89-C-5604. Partial support of this work for one

of the authors (JJL) by AFOSR-89-0508 is also acknowledged. Technical discussions with Dr. T.A. Parathasarthy of UES, Inc., are appreciated.

REFERENCES

1. R.L. Fleischer: *J. Met.*, 1985, vol. 37, pp. 16-20.
2. D.M. Dimiduk and D.B. Miracle: *Mater. Res. Symp. Proc.*, 1989, vol. 133, pp. 349-59.
3. R.L. Fleischer, D.M. Dimiduk, and H.A. Lipsitt: *Annu. Rev. Mater. Sci.*, 1989, vol. 19, pp. 231-63.
4. D.L. Anton and D.M. Shah: *Mater. Res. Symp. Proc.*, 1989, vol. 133, pp. 361-71.
5. J.D. Embury: *Strength of Metals and Alloys*, Proc. ICSMA, H. McQueen, ed., 1985.
6. D.P. DeLuca and B.A. Cowles: WRDC-TR-89-4136, Pratt & Whitney, WRDC/MLL, Wright-Patterson AFB, OH, 1989.
7. M.J. Blackburn and M.P. Smith: WRDC-TR-89-4095, United Technologies Corporation, WRDC/MLL, Wright-Patterson AFB, OH, 1989.
8. B.J. Marquardt: WRDC-TR-89-4133, General Electric Corporation, WRDC/MLL, Wright-Patterson AFB, OH, 1989.
9. M.L. Gambone: WRDC-TR-89-4145, Vol. II, Allison, WRDC/MLL, Wright-Patterson AFB, OH, 1989.
10. C.K. Elliott, G.R. Odette, G.E. Lucas, and J.W. Sheckherd: *High Temperature, High Performance Composites*, MRS Proc., Lemkey, ed., Materials Research Society, Pittsburgh, PA, 1988, vol. 120, pp. 95-101.
11. V.D. Krstic: *Phil. Mag.*, 1983, vol. 48 (5), pp. 695-708.
12. L.S. Sigl and H.E. Exner: *Metall. Trans. A*, 1987, vol. 18A, pp. 1299-1308.
13. L.S. Sigl, P.A. Mataga, B.J. Dalgleish, R.M. McMeeking, and A.G. Evans: *Acta Metall.*, 1988, vol. 36 (4), pp. 945-53.
14. M.F. Ashby, F.J. Blunt, and M. Bannister: *Acta Metall.*, 1989, vol. 7, pp. 1847-57.
15. *Binary Alloy Phase Diagrams*, T.B. Massalski, ed., ASM, Metals Park, OH, 1986, p. 1696.
16. M.G. Mendiratta and D.M. Dimiduk: *Mater. Res. Soc. Symp. Proc.*, Materials Research Society, Pittsburgh, PA, 1989, vol. 133, pp. 441-46.
17. M.G. Mendiratta: Universal Energy Systems, Inc., Dayton, OH, unpublished research, 1990.
18. J.J. Lewandowski, D. Dimiduk, W. Kerr, and M.G. Mendiratta: *Mater. Res. Soc. Symp. Proc.*, 1990, vol. 120, pp. 103-08.
19. *Quantitative Microscopy*, R.T. DeHoff and F.N. Rhines, eds., McGraw-Hill, Inc., New York, NY, 1968, pp. 45-77.
20. D. Tabor: *Hardness of Metals*, Clarenden Press, London, 1951.
21. R. Nekkanti: WRDC/MLLM, Wright-Patterson AFB, OH, unpublished research, 1990.
22. J.J. Lewandowski and J. Rigney: *Proc. 2nd Int. Ceramic Science and Technology Congress*, M.D. Sacks, ed., The American Ceramic Society, Inc., Westerville, OH, 1990, in press.